Department of Mechanical and Aerospace Engineering

PhD Mechanical Engineering

June 2022

Experimental Study of Alcohol Fuels on Engine Performance, Efficiency and Emissions

Enshen Lu
1732641

A thesis submitted for the degree of
Doctor of Philosophy by

Department of Mechanical and Aerospace Engineering
College of Engineering, Design and Physical Sciences
Brunel University London
Uxbridge
Middlesex
UB8 3PH
United Kingdom
T: +44 1895 274000

Abstract

In order to reduce emissions of carbon dioxide (CO_2) to minimize global warming and climate change, and pollutants emissions from vehicles for better air quality, it is necessary to improve the efficiency and minimize pollutant emissions from internal combustion engines by means of better engine technologies and low/zero carbon fuels, as well as the electrification of the powertrain system in vehicles.

Renewable ethanol and methanol are the two alcohol fuels which can significantly reduce CO_2 emissions. In this project, a state-of-art single cylinder spark ignition (SI) engine and testing facility were set up and used to study the combustion characteristics, fuel efficiency as well as gaseous and particle emissions from the engine operations with ethanol or methanol. The engine performance and the combustion process of ethanol and methanol were measured and compared with E10 RON95 gasoline.

The first part of the study was carried out at three engine speeds of 2000rpm, 3000rpm and 4000rpm under different load conditions with the same engine parameter settings (cam timings, injection parameters) for gasoline, ethanol and methanol to have a direct comparison between alcohol fuels and gasoline. Particular emphasis was on the high load operations at and above 16bar IMEP when gasoline engine operation was found to be prone to knocking combustion and over-fuelling was introduced to keep the exhaust gas temperature below 780°C. In comparison, engine could be operated at stoichiometric conditions without exceeding the exhaust gas temperature limit due to their higher enthalpy of evaporation and the use of MBT timings without knocking combustion for ethanol and methanol. The result shows that methanol leads to 3.6% higher brake thermal efficiency than gasoline, and ethanol by 3.3% when operated at higher load operations at around 18bar IMEP. Both ethanol and methanol fuels lead to substantial reductions in the emission of particles, with the particle numbers reduced by up to 90%.

The second series of experiments were then carried out to find the best injection strategies for ethanol and methanol. The result shows that both ethanol and methanol have larger best efficiency island than gasoline because of their greater

evaporation and charge cooling effect. In addition, there’s also a reduction in emission across the fuel matrix testing.

Finally, a low speed & load spark timing sweep was carried out to assess the performance of the engine fuelled by ethanol and methanol under catalyst light off condition. The result shows that both ethanol and methanol could operate with more retarded spark timings than gasoline to enable by faster catalyst-light-off. In addition, particulate emissions released by alcohol fuels are much less and of smaller sizes.

The novelty of the work is enabling detailed systematic analysis of alcohol fuelled combustion, fuel consumption, performance and emissions under advanced, highly boosted SI engine conditions. The load sweep part fills in the gap of high load test conditions of pure ethanol/methanol fuelled SI engine. The fuel matrix part presents the effect of injection timing and injection pressure variation on fuel efficiency, combustion characteristic and emissions which gives a deeper understanding of air-fuel mixture of ethanol and methanol benefit from their greater evaporation and charge cooling effect. The cold start spark timing sweep shows that both ethanol and methanol could operate with more retarded spark timings than gasoline to enable by faster catalyst-light-off.

Acknowledgements

First of all, I would like to express my deep gratitude to my supervisor, Professor Hua Zhao, for granting me the opportunity to study in the great engine research group at Brunel University London, and also for his invaluable guidance on my research and learning, and for all the help given to make my life easier during these years.

I would like to acknowledge MAHLE Powertrain UK for all the support provided to this work. Particularly I am grateful to Mr Anthony Harrington, Mr Jonathan Hall, Mr Adrian Cooper and Dr Mike Bassett for share of experience and knowledge and the warm help; and to Mr Tony Cains and Mr Justin Mape for their excellent technical supports on EMS system and engine rebuild.

I am thankful to my friends and colleagues in the group. Thanks to Dr Xinyan Wang for lots of valuable help on both my study and life. Thanks to Dr Reza Golzari for his teaching and company in engine testing. Thanks to Mr Andy Selway, Mr Eamon Wyse for their expertise and assistance to support the research work.

Thanks to Mr Ziyan Fu and Mr Chris Nichols for their friendship and help.

I also would like to thank all other friends met here for their company, help and encouragement. The life is much more joyful here thanks to all of you.

Finally, my most sincere gratitude goes to my family - my mother, my father and my sister for their endless and selfless love, encourage and support, which are the most important resources and powerful backing for me to pursue better life.

At the end of writing the thesis, particularly and most important, I must express my gratitude to my wife Ms Jiawen Si - without your unconditional love and support and your endeavour, it would be not possible for me to overcome the difficulties and complete the study. Also thank my new born Son Zebang Lu - you did so well and made so less trouble during my writing and your smile is the best gift spiriting me up.

List of Abbreviations

ABDC	After Bottom Dead Centre
AFR	Air Fuel Ratio
APV	Alternatively-Powered Vehicles
ATDC	After Top Dead Centre
BBDC	Before Bottom Dead Centre
BDC	Bottom Dead Centre
BLD	Borderline Detonation
BMEP	Brake Mean Effective Pressure
BSFC	Brake Specific Fuel Consumption
BTDC	Before Top Dead Centre
BTDCF	Before Top Dead Centre Firing
BTDCNF	Before Top Dead Centre Non-firing
CA	Crank Angle
CA10	Crank Angle at 10% Mass Fraction of Mixture Burned
CA50	Crank Angle at 50% Mass Fraction of Mixture Burned
CA90	Crank Angle at 90% Mass Fraction of Mixture Burned
CAD	Crank Angle Degrees
CAFE	Corporate Average Fuel Economy
CAI	Controlled Autoignition
CFD	Computational Fluid Dynamics
CI	Compression Ignition
COV	Coefficient of Variation
CR	Compression Ratio
DAQ	Data Acquisition
DI	Direct Injection
eBoost	Electrical Boosting
ECU	Electronic Control Unit
EGR	Exhaust Gas Recirculation

EMOP	Exhaust Maximum Opening Point
EMS	Engine Management System
EOI	End of Injection
EPA	Environmental Protection Agency
EVC	Exhaust Valve Closing
FID	Flame Ionization Detector
GDI	Gasoline Direct Injection
HCCI	Homogeneous Charge Compression Ignition
HEV	Hybrid Electric Vehicle
ICE	Internal Combustion Engine
IEffg	Gross Indicated Fuel Conversion Efficiency
IEffn	Net Indicated Fuel Conversion Efficiency
IEffp	Pumping Indicated Fuel Conversion Efficiency
IMEP	Indicated Mean Effective Pressure
IMOP	Intake Maximum Opening Point
ISFC	Indicated Specific Fuel Consumption
IVC	Intake Valve Closing
IVO	Intake Valve Opening
KI	Knock Intensity
LIVC	Late Intake Valve Closing
LIVO	Late Intake Valve Open
MBT	Minimum spark advance for Best Torque
MFB	Mass Fraction burn
NA	Naturally Aspirated
NI	National Instruments
NIMEP	Net Indicated Mean Effective Pressure
NISFC	Net Indicated Specific Fuel Consumption

NOx	Nitrogen Oxides
PFI	Port Fuel Injection
PID	Proportional Integral Derivative
PM	Particulate Matter
PMEP	Pumping Mean Effective Pressure
PN	Particulate Number
PRT	Platinum Resistance Thermometer
RON	Research Octane Number
rpm	revolutions per minute
SI	Spark Ignition
SOI	Start of Injection
TDC	Top Dead Centre
ULG	Unleaded Gasoline
VVA	Variable Valve Actuation
VVT	Variable Valve Timing
WOT	Wide Open Throttle

Chemical Abbreviations

CO	Carbon Monoxide
CO_2	Carbon dioxide
H	Hydrogen atom
N	Nitrogen atom
N_2	Nitrogen
NO	Nitric oxide
NO_2	Nitrogen dioxide
O	Oxygen atom
O_2	Oxygen
THC	Total hydrocarbons

List of Figures

List of Tables

Contents

1. Chapter One: Introduction

1.1 Introduction

In the modern world, the invention of the Internal Combustion Engine (ICE) represents an important development, both in terms of mobility and power generation. There is a long history of ICE engines which dates back to 1876 when Otto developed the spark ignition (SI) engine which was followed by Diesel in 1892 with the demonstration of a single cylinder compression ignition (CI) engine. The IC engines are used in a range of applications and they are the most popular powertrain for land and water vehicles all over the world [1].

In the early years, fuel economy and power output were the chief motivations for the development and optimization of these engines. To meet both the requirements of power and fuel efficiency, technologies such as turbocharging, direct injection have been developed.

In the last few decades, the rapid increase in the application of internal combustion engines in vehicles has resulted in increased concerns regarding the environmental and health effects of their exhaust emissions and their legislations. It was in the early 1960s that the United States began regulating air emissions from automobiles. Beginning in California at first, then nationwide with the United States Environmental Protection Agency (EPA), emission regulations for automobiles were developed and enacted. Emissions legislations have then been adopted by other countries, such as Europe, Japan, Australia and China.

As a result of the popularity of internal combustion engines in the automotive sector, the demand for fossil fuels has also increased significantly. To achieve a substantial reduction in fuel consumption, greater fuel efficiency must be achieved from those engines. In particular, as the main greenhouse gas, legislations on fuel economy and CO_2 emissions have been introduced for light duty vehicles in the last 10 years. These factors have led to intensive research into more environmentally friendly and fuel saving engines.

1.2 Alcohol Fuels for IC Engines

In terms of decarbonizing fleet CO_2 for internal combustion engines, renewable alcohol fuels have been increasing used as neat fuel or a mixture with gasoline. Series of research have already been conducted on ethanol and methanol blend fuels, and the idea of blending greater amounts of alcohol into fossil gasoline is not new [2,3]. The use of ethanol blended fuel is already prevalent around the world today, and it contributes to reducing embedded CO_2 with a content of up to 10% in most gasoline supplies of these countries. The Brazilian government has taken a step further and has begun making ethanol blends up to neat form available in its publicly available fuel supplies [4]. The availability of methanol as a fuel source is less prevalent. Nevertheless, it was historically used as a fuel for racing cars and more recent research has examined its use in IC engine [3,5]. It would therefore be necessary for the production of pure ethanol and pure methanol to be sourced from renewable sources from 2nd generation feedstocks in order to justify the use of such fuels.

According to previous research, both ethanol and methanol can increase the thermal efficiency of a SI engine as well as reducing particle emissions. The efficiency benefit is attributed to faster laminar flame speed and charge cooling effects of alcohol fuels [3,6]. In addition, alcohol fuels have a higher knocking resistance than gasoline fuels. Last but not the least, due to their lower boiling temperature and high oxygen content, ethanol and methanol fuels will produce less particles.

In the last few years, electric vehicles are moving rapidly into the light passenger vehicle market in the form of battery electric vehicles (BEV) and hybrid engine and electric vehicle. BEV is well suited for the customers who can have easy access to the electric charging facility and regions where electricity is produced from renewable sources. Hybrid vehicles can overcome the shortcomings of the BEV by combined use of an efficient engine preferably running on renewable or zero carbon fuels for extended range and the zero exhaust pipe emissions of an electrical powertrain. Furthermore, for countries and regions where the electricity is generated from fossil

fuels or limited electric supply infrastructure, and applications where the battery will be considered to be too bulky, expensive, taking too long charging time or of limited range, IC engines will remain the most viable powertrain system.

On 25 August 2022, California announced that the sale of new gasoline-powered cars and light trucks will be banned by 2035. Standard hybrid vehicles which have no plug and rely much more on gasoline than plug-in models are treated the same as gasoline models due to the emissions[7].

However, the current legislation only considers the emissions emitted by vehicles at the tailpipe without considering the emissions produced during production (e.g. batteries) and energy sources: hydrogen and electricity, respectively. The research done by Burton et al shows that It is unclear whether widespread adoption of BEVs in the United States will reduce greenhouse gas emissions substantially over the lifespan of the vehicle in the near term compared to FHEV and PHEV alternatives, particularly when the required infrastructure upgrades are considered [8].

Therefore, the application and optimisation of renewable ethanol and methanol fuels in IC engines provide an alternative solution to achieve low-carbon and zero-carbon transport in the future.

1.3 Project Objectives

The aim of this study is to investigate the effect of methanol and ethanol on the engine's performance, combustion and emissions by carrying out an extensive and systematic experiments on a single cylinder direct injection (DI) spark ignition engine which has been updated to operate with pure ethanol and methanol. The engine efficiency, as well as emissions data, will be analysed and compared with RON95 E10 gasoline.

The specific objectives of the study include quantification of:

(1.) The effect of methanol and ethanol on the in-cylinder heat release and combustion process and the resulting impact on the SI engine's performance, efficiency and emissions at different engine speeds and load conditions. In particular, how the high-load engine operations can be improved by the use of methanol and ethanol fuels in terms of knocking combustion and exhaust gas temperature control.

(2.) The effect of injection strategies of different fuels on the engine's performance, efficiency and emissions when gasoline, ethanol and methanol fuels, by adjusting the injection timing and rail pressure at different engine speeds and loads.

(3.) The capability and effectiveness of methanol and ethanol fuels to operate with retarded spark ignition and combustion for fast catalyst light off.

1.4 Outline of Thesis

Chapter 2 provides the literature review which includes some basic knowledge related to direct injection spark ignition engine, combustion efficiency and emissions. The advanced engine technologies are introduced and reviewed and both their advantage and disadvantage are discussed. the current and future emission regulation are shown which includes CO, CO_2, NO_x, THC as well as particulate emission.

In chapter 3, all the equipment on the engine testbed are described which include the engine itself and its conditioning system. All temperature sensor and pressure transducers used as well as all emission analysers are described, together with the engine management system (EMS) and data acquisition system. The equations of some important calculation of combustion parameters are explained such as indicated mean effective pressure (IMEP), indicated power, net indicated specific fuel consumption (NISFC). Finally, the procedures for improving the data accuracy are explained.

Chapter 4 presents of the results of load sweep at 2000, 3000 and 4000rpm load sweep between 2bar IMEP to 28 bar IMEP. The difference between alcohol fuel (ethanol& methanol) and baseline (E10 gasoline) of combustion characteristics, fuel efficiency as well as emissions are analysed.

Chapter 5 focus on the different injection timings and rail pressures on the engine performance, efficiency, combustion characteristics, gaseous and particle emissions. Two groups of fuel matrix test which are 2000rpm 4.6bar IMEP and 3000rpm 16bar IMEP were used to investigate the difference between alcohol fuel and gasoline.

Chapter 6 shows the result of 2000rpm 2bar cold start sweep in which the 50% mass fraction burn was retarded from 8 Deg ATDC to 45 Deg ATDC. This test is aimed to find the most retarded spark timing and the maximum exhaust gas temperature during the spark sweep for the catalyst light off.

The main conclusions of this experimental study on the difference between pure alcohol fuel and E10 gasoline are summarised in Chapter 7.

2. Chapter Two: Literature review

2.1 Introduction

In the last 50 years, substantial progress has been made on internal combustion engines in terms of their performance, fuel efficiency and emissions.

The history of emission legislation started in the 1960s when the air quality became worse day by day, particularly noted in California US. Ever since, government agencies were set up and legislation introduced to limit the tailpipe emission [9]. Figure 2.1 shows the toxic emissions standards in different countries and regions [10]. The development of emission regulation is mainly about decreasing the toxic component in the exhaust as well as making improvement of test cycles.

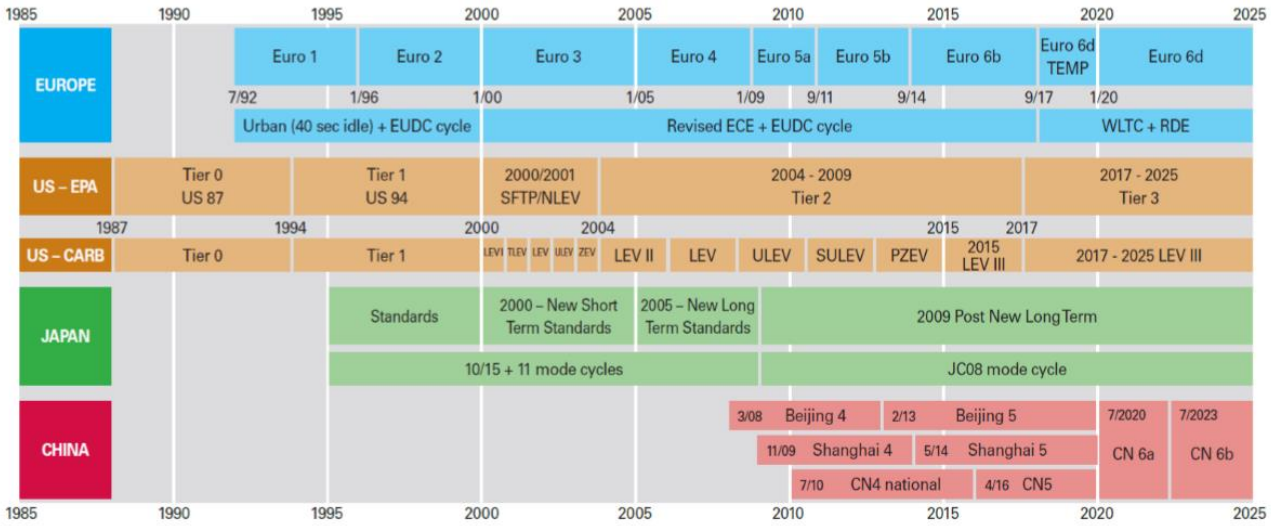

Figure 2-1 Toxic Emissions Standards for Passenger Cars *[10]*

The first stage of Europe emission regulation came out in July 1992 and it has been upgraded to 6th stage in September 2014. All the listed pollutants have been reduced substantially stage by stage which is shown in Table 2.1 [11]. It can also be found that the limit on particle mass (PM) has been applied for gasoline engine from Euro 5 and the limit of particle numbers (PN) has been added to Euro 6.

Table 2-1 EU Emission Standards for Passenger Cars (Category M1*) *[11]*

Stage	Date	CO	HC	HC+NOx	NOx	PM	PN
		g/km					*#/km*
Positive Ignition (Gasoline)							
Euro 1†	1992.07	2.72 (3.16)	-	0.97 (1.13)	-	-	-
Euro 2	1996.01	2.2	-	0.5	-	-	-
Euro 3	2000.01	2.30	0.20	-	0.15	-	-
Euro 4	2005.01	1.0	0.10	-	0.08	-	-
Euro 5	2009.09[b]	1.0	0.10[d]	-	0.06	0.005[e,f]	-
Euro 6	2014.09	1.0	0.10[d]	-	0.06	0.005[e,f]	6.0×10^{11} [e,g]
Compression Ignition (Diesel)							
Euro 1†	1992.07	2.72 (3.16)	-	0.97 (1.13)	-	0.14 (0.18)	-
Euro 2, IDI	1996.01	1.0	-	0.7	-	0.08	-
Euro 2, DI	1996.01[a]	1.0	-	0.9	-	0.10	-
Euro 3	2000.01	0.64	-	0.56	0.50	0.05	-
Euro 4	2005.01	0.50	-	0.30	0.25	0.025	-
Euro 5a	2009.09[b]	0.50	-	0.23	0.18	0.005[f]	-
Euro 5b	2011.09[c]	0.50	-	0.23	0.18	0.005[f]	6.0×10^{11}
Euro 6	2014.09	0.50	-	0.17	0.08	0.005[f]	6.0×10^{11}

* At the Euro 1..4 stages, passenger vehicles > 2,500 kg were type approved as Category N_1 vehicles
† Values in brackets are conformity of production (COP) limits
a. until 1999.09.30 (after that date DI engines must meet the IDI limits)
b. 2011.01 for all models
c. 2013.01 for all models
d. and NMHC = 0.068 g/km
e. applicable only to vehicles using DI engines
f. 0.0045 g/km using the PMP measurement procedure
g. 6.0×10^{12} 1/km within first three years from Euro 6 effective dates

Figure 2.2 shows that the limits of tailpipe emissions has been reduced significantly from Euro 0 to Euro 4 [12]. What's more, since the regulation become more and more stringent, new technologies such as electronic control, fuel injection technology, as well as aftertreatment devices have been developed to limit the tailpipe emissions.

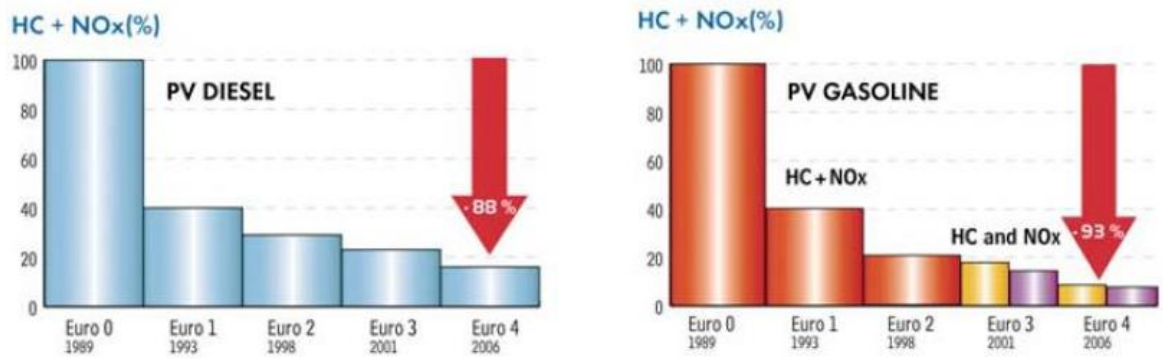

Figure 2-2 Reduction of HC+ NOx on Passenger Cars from Euro 0 to Euro 4 *[12]*

2.2 Main Component of Exhaust Gas

2.2.1 Carbon Dioxide (CO_2)

Recently, CO_2 caught more attention than other toxic component in the tailpipe emission since CO_2 is the main greenhouse gas responsible for the increase of global temperature. Figure 2.3 shows the CO_2 release proportion by sources. The CO_2 released by cars running on fossil fuels takes the second position [13]. The most effective way to reduce CO_2 release by cars is to reduce the fuel consumption by improving the engine efficiency and the use of low carbon and zero carbon fuels.

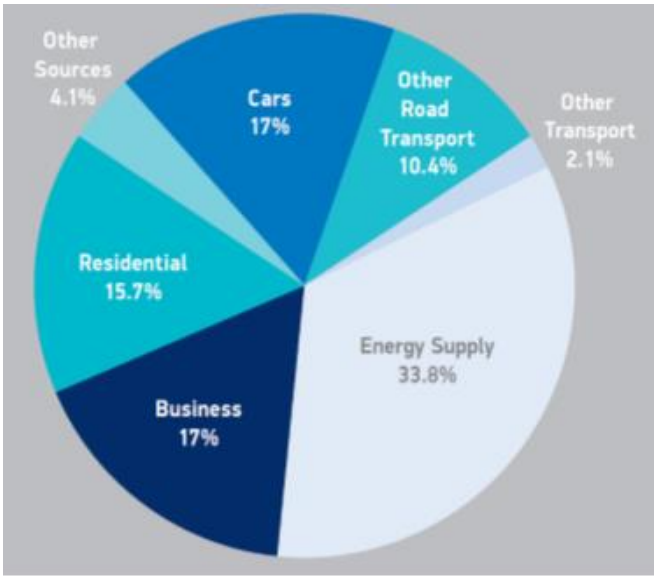

Figure 2-3 The Fraction of CO2 Emissions by Source *[13]*

Governments (China, United States, The Europe Union, Japan, India, Mexico, Canada, Saudi Arabia, Brazil, South Korea) which are the core members among the top 15 vehicle markets have set out mandatory CO_2 emission standard for light duty vehicles to reduce “greenhouse” gas emission of CO_2 [14]. Figure 2.4 shows that the standard of CO_2 emissions becomes more and more stringent so that all the car makers should apply new technology to reduce the fuel consumption also guarantee the engine efficiency of cars.

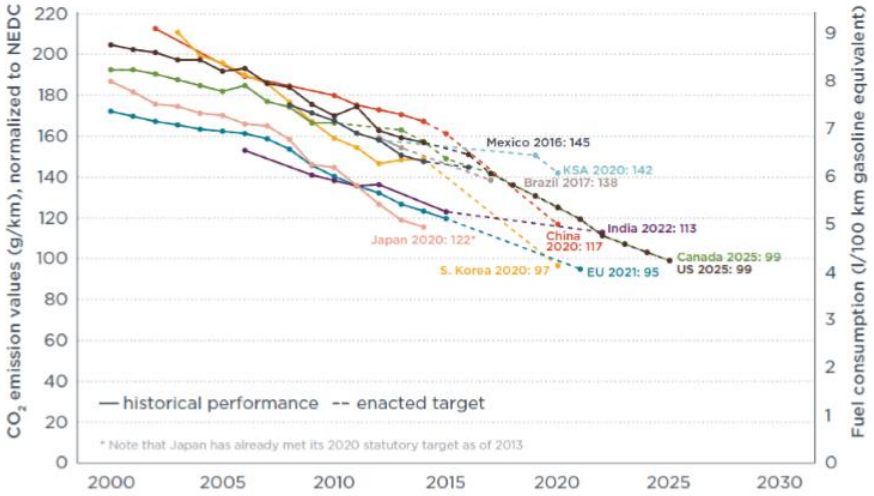

Figure 2-4 Historical Fleet CO2 Emissions Performance and Current Standards (gCO2/km normalized to NEDC) for Passenger Cars *[14]*

2.2.1.1 Technologies to Reduce CO_2 Released by Vehicle

Due to the standard of fuel economy become more stringent, advanced engine technologies and designs have been developed and applied to optimise the fuel consumption of cars, including

- Improved combustion and engine control methods
- Improved transmission efficiency and powertrain integration
- Intelligent thermal management
- Brake/ kinetic energy recovery
- Exhaust/heat energy recovery
- Alternative fuels
- Propulsion electrification
- Improved aerodynamics and rolling resistance
- Light-weighting design and materials

Recently, an annual survey done by WardsAuto shows that the important things carmaker focus on are light-weighting as well as optimising fuel consumption to meet the CO_2 standard of 2025, as shown in Figure 2.5 [15].

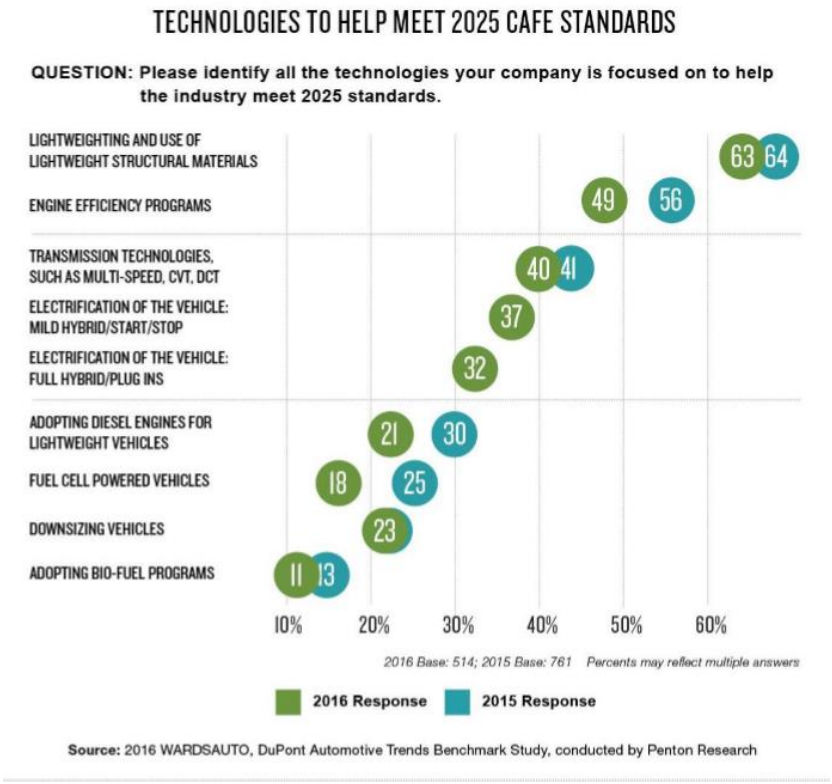

Figure 2-5 WardsAuto Annual Survey: Technologies to Help Meet 2025 CAFE Standards *[15]*

2.2.2 Carbon Monoxide (CO)

CO is a kind of toxic gas which has big effect on human's health since it can combine with haemoglobin in the blood to form CO_2 so that the capacity of oxygen carried by blood is reduced. Small quantities of CO may cause light headedness while large quantities will lead to loss of consciousness and asphyxia [16].

The amount of CO exist in the tailpipe gas is mainly affected by the Air Fuel Ratio (AFR) [17]. It was found that the production of CO increases rapidly when equivalence ratio is greater than 0.95. What's more, the production rate of CO is also influenced by the inhomogeneity of the mixture as well as the burned gas temperature and temperature gradients in the expansion and exhaust strokes [18].

The kinetic chemical formation process of CO is shown below, in which R is a hydrocarbon radical [19].

$$RH \rightarrow R \rightarrow RH_2 \rightarrow RCHO \rightarrow RCO \rightarrow CO$$

The CO is oxidised into CO_2 in the burned gas in a slow speed and the reaction process is shown below.

$$CO + OH = CO_2 + H$$

It has also been found that the concentration of CO after the exhaust valve open is lower than when in cylinder but it's still higher than at equilibrium conditions [20].

2.2.3 Unburned Hydrocarbon (THC)

Unburned Hydrocarbons are also an important component in emission and they can lead to worsening human health such as coughing, dry throat and wheezing. What's more, HC can react with NO_x to produce O_3 and photochemical smog which is quite harmful to humans as well as the environment [16].

Hydrocarbon compounds emitted from vehicles are represented with the general term of uHCs which include paraffins, olefins, acetylene and aromatics, etcall of them can be found in exhaust gas. Different kinds of HC emissions can lead cause the phenomenon call photochemical smog which is quite harmful to human as well as environment.

There are so many influencing factors which have effects on the production of HC, of which incomplete combustion is the main factor. What's more, fuel impingement on the cylinder surface in a DI gasoline engine also leads to the production of HC and it is mainly affected by the injection strategies (injection timing and rail pressure) and injector orientation relative to the cylinder axis and the piston crown [21]. It has been found that flame quenching has big effect on the production of THC on the surface of cylinder [22]. Moreover, the fuel which cannot be oxidised by the flame front propagate may cause the production of THC and lubricating oil can also be oxidised with the charge to form THC [23].

2.2.4 Nitrogen Oxides (NO_x)

There are two specific emissions referred to NO_x, which are nitrogen dioxide (NO_2) and nitric oxide (NO). Researchers have proved that the reaction between NO and haemoglobin is harmful to humans. NO_2 is a kind of irritant chemical which become harmful when it reaches a high concentration [16].

An equilibrium analysis by Stone [24,25] shows that the content of NO is greater than the content of NO_2 in the cylinder of the gasoline engine. There are two ways in which NO can be produced in the engine. The first one is because of the oxidation of the nitrogen in the fuel, while the other and most common one is the oxidation of atmospheric nitrogen [25,26]. Nitrogen is present in negligible quantities in gasoline. The process to form NO from atmospheric nitrogen when the combustion is stoichiometric is as followed.

$$O + N_2 = NO + N$$

$$N + O_2 = NO + O$$

$$N + OH = H + NO$$

The formation of NO_x is mainly affected by the temperature of burned gas. With the increase of the gas temperature, the concentration of NO_2 also increases. What's more, since spark timing also has a big effect on the temperature of burned gas so the production of NO_x can be optimised by controlling of spark timing. The peak in-cylinder pressure increases with the advanced of spark timing since more fuel is burned before top dead centre and the peak pressure moves close to top dead centre when the volume is smaller. An increase in peak in-cylinder pressure is accompanied with an increase in peak burned gas temperature, and as a consequence, there is a higher rate of NOx formation.

The burned gas fraction or exhaust gas recirculation (EGR) is another variable which would affect NO_x emission. Thanks to the presence of CO2 and water vapour in the EGR, the combustion temperature can be significantly decreased with the increase of burned gas mass fraction, because of their dilution and increased heat capacity of

the in-cylinder charge. It has been found that the production of NO_x can be decreased by more than 50% with the employment of 15-25% EGR [27].

2.2.5 Particle Matter (PM)

PM comprises carbon particles (soot) and condensates of liquid (sulphate, unburned fuel and oil). PM has a bad effect on human health and the extent of its potential danger mainly depends on the type (nucleation mode and accumulation mode) and size of PM. The very fine particles whose size is very small (≤10nm) would contaminate the lung as the lung itself cannot clear it.

Because the production of organic particles (soot) by diesel engine is far more than the gasoline engine, diesel engine requires Diesel Particulate Filters (DPFs) to reduce the quantity of PM to meet emission legislation and protect human and environment. Similar technology is also being applied to DI gasoline engines for the EU 6.0 vehicles.

2.3 Internal Combustion Engine Efficiency

As a means of reducing the fuel consumption and CO_2 emissions of automobiles, it is essential to improve the fuel conversion efficiency of the IC engine. The process that which chemical energy contained in the fuel is converted to mechanical power in an internal combustion engine is very complicated since this process involves combustion, thermodynamic, fluid dynamics, mechanic movement as well as energy losses such as friction. The fuel conversion efficiency of fuel is defined as how much chemical energy of the fuel is converted into mechanical power output by percentage. The summary of the energy conversion process and efficiency principles are shown in Figure 2-6 [24,28-33].

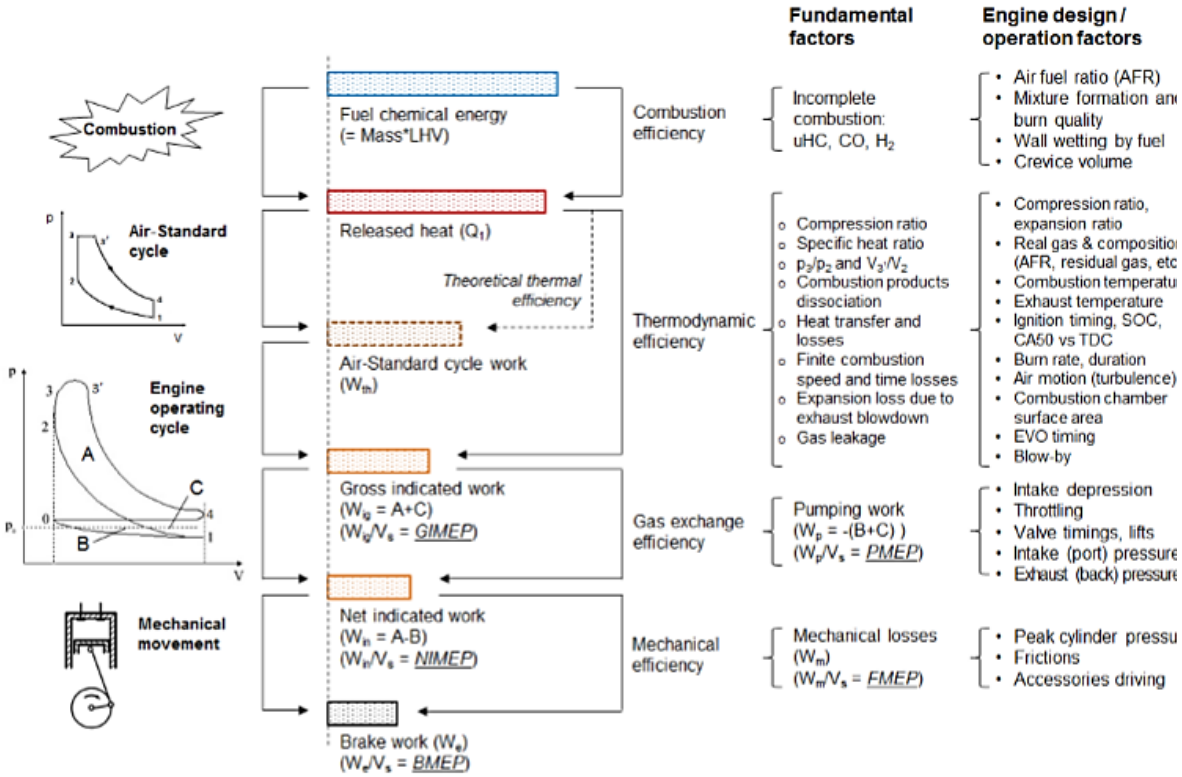

Figure 2-6 Fuel Energy Conversion Process and Efficiencies in Internal Combustion Engines *[24,28-33]*

Gasoline Spark ignition gasoline engine is still the first choice of power plant for passenger cars all over the world since nearly 80% of light-duty vehicles use gasoline engine according to the data shown by IEA. This number is a little bit lower in developed countries but still close to 70% [34]. Since the fuel consumption of the diesel engine is lower than that of the gasoline engine, diesel engine vehicles are very popular in some European countries. Diesel is produced as part of the distillation process of petroleum and can also be produced from renewable sources. The diesel CI engine operates with higher thermal efficiency and much lower fuel consumption. But they emit more gaseous and pollutant emissions and would need expensive and costly aftertreatment devices. The key points for gasoline engines are to improve its fuel consumption and fuel efficiency. Table 2.2 shows the main methods to improve the engine fuel economy and the associated technical challenges.

Table 2-2 Key points for improving Gasoline Engine Efficiency

Objectives	Limitation of gasoline engine operation
Increase compression ratio	1) Abnormal combustion: knocking, low speed pre-ignition (LSPI) 2) The design and reduction of friction result of the limit of in-cylinder peak pressure.
	1) The operation of a spark ignition (SI) engine is stoichiometric combustion (Lambda=1) which is richer than a diesel engine due to the fellow reasons: a) The air-fuel ratio (AFR) has a big effect on the spark ignition and the flame propagation of the gasoline engine. The AFR of some typical SI engines should be less than 20. b) In order to decrease the CO, HC and NO_x in the emission of exhaust, a 3-way catalyst is used on the SI engine. The fraction of the air and fuel should be stoichiometric of the combustion. 2) Because the combustion type is stoichiometric combustion which can decrease the specific heat ratio so that the combustion temperature of gasoline is higher than that of a diesel engine.

Increase specific heat ratio	3) When the engine is running at high load and high speed, enrich mixture should be used to cool down the temperature of the exhaust so that to protect the exhaust component. But this will cause a decrease in the combustion efficiency as well as the specific heat ratio.
Reduce pumping loss	At part load conditions, the throttle is used to reduce the mass of intake air so that to control the output as well as keep the AFR stoichiometric. High pumping loss and the pressure of intake decrease as a result of this.
Optimise combustion time	1) Combustion time losses are caused by the finite combustion speed in the gasoline engine. Furthermore, both the increase of residual gas fraction and EGR will decrease the speed of combustion. 2) Knocking at high load condition pushes the retarded of the spark timing as well as CA50 which causes the combustion phase away from the optimum point.

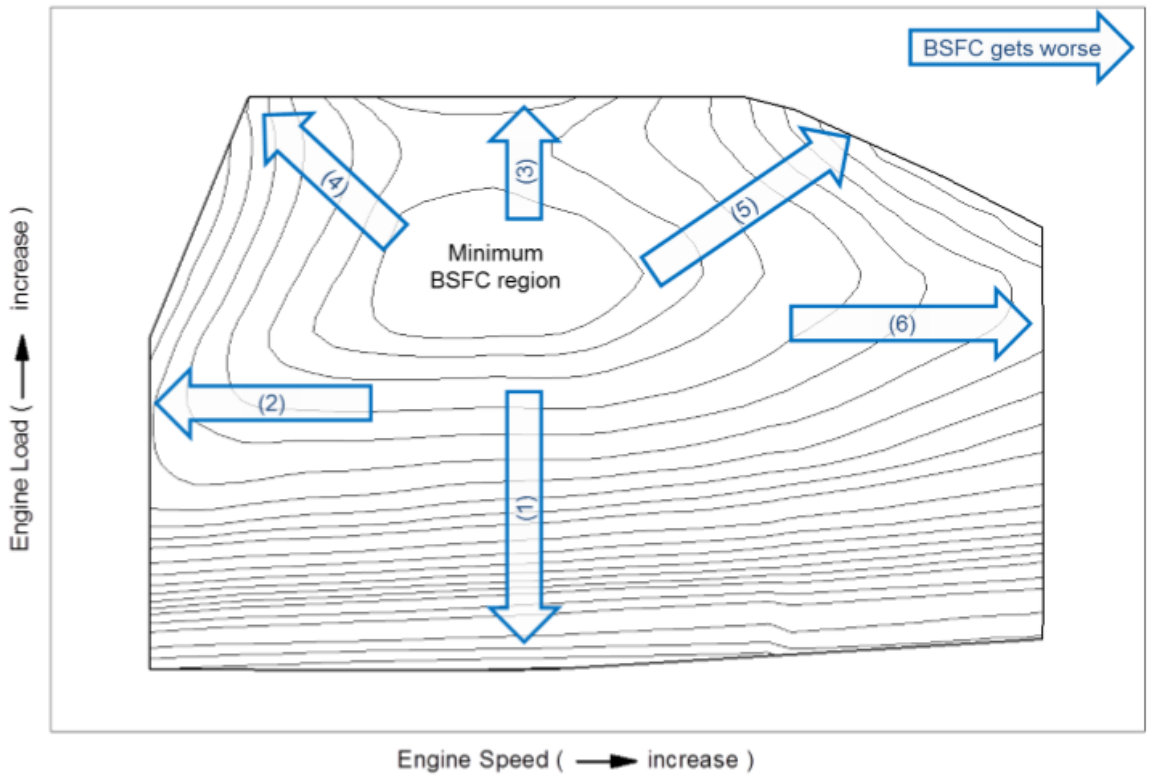

Figure 2-7 BSFC Contour Map of a Turbocharged Gasoline DI Engine

The specific fuel consumption of a gasoline engine varies with load and speed. Figure 2-7 shows that the minimum BSFC is achieved in the middle-speed high load area. As the speed and load go lower or higher from this area, the BSFC gets worst due to factors listed in Table 2.3.

Table 2-3 Reasons for BSFC Increases in a Gasoline Engine Operation Map

BSFC increase	Main reasons
(1)	i. Throttling at a lower load leads to the intake pressure decrease which would cause higher pumping loss. ii. High residual gas fraction is also caused by low intake pressure. What's more, the in-cylinder temperature is low at the condition of low load. Both of these results in combustion speed slowing down and combustion time loss increasing.

(2)	i. Heat loss and gas leakage increase as a result of the time of each cycle increase. ii. The decrease of engine speed would lead to in-cylinder charge motion and turbulence becoming weak so that the burning rate decrease and combustion duration extend.
(3) & (4)	i. For the gasoline engine, pumping loss decrease with the increase of engine load. ii. However, knocking combustion happens when the engine run at high BMEP since the thermal load is higher. The spark timing should be retarded which results in later CA50 and increase in combustion time loss to deal with knocking combustion. iii. At low speed and high load conditions, the knock tendency increase since the low combustion speed and high gas temperature. Spark timing and CA50 should be retarded to decrease the knocking tendency. • The low-speed pre-ignition (LSPI) may occur at a low-speed high load area in a highly downsized gasoline engine.
(5)	i. Knocking tendency reduces at high-speed high load. ii. Enrich AFR is adopted at high load high-speed condition to reduce the exhaust temperature so that to avoid destroying the turbine blades in a turbocharged engine. Naturally Aspirated engines employ enrich AFR is also used for improving the peak power. Combustion efficiency and heat ratio get worse as a result of over-fuelling.
(6)	The mechanical losses increase with the increase of engine speed since friction and pumping loss increase.

2.4 Technologies for Improving Gasoline Spark Ignition Engine Fuel Economy

Recently, a series of new technologies have been researched and adopted on gasoline spark ignition engines to improve the fuel economy and engine efficiency as well as reducing the emissions. Some new technologies and will be reviewed are introduced in this section.

2.4.1 Gasoline Direct Injection

In 1996, mass production of direct injection gasoline engines was introduced to the market to achieve stratified lean combustion by Mitsubishi and Toyota. There are some major advantages of the direct injection technology in the development of gasoline spark ignition engines [35].

(1.) The injector injects the fuel into the combustion chamber directly at high pressure and most of the fuel evaporates in the air which can absorb heat from the air and lead to charge cooling effect. The in-cylinder temperature decrease also causes the reduction of the heat loss, knocking tendency and improved engine volumetric efficiency so that torque and power can be increased.

(2.) Direct injection is necessary to achieve the stratified lean combustion for higher thermal efficiency at part-load operations and can be employed to improve the cold start performance and emissions.

(3.) Direct injection combined with boosting enables the engine downsizing to improve fuel economy by operating the gasoline engine in the best BSFC region at higher load.

(4.) Direct injection can be used to facilitate the fast catalyst light off during the cold-start operation by retarding injection timing to form a stratified fuel rich mixture in the central region of the combustion chamber, so that stable ignition and combustion can be achieved after TDC to enable retarded combustion and hence higher exhaust gas temperature.

2.4.2 Stratified Lean Combustion

The reason why the fuel economy of gasoline engines is worse than diesel engine is the larger pumping loss and lower specific heat ratio of a stoichiometric mixture. Research on lean combustion to reduce fuel consumption of gasoline engines has been conducted for a long time [36-38]. It is essential to improve the ignition process to ensure reliable ignition of homogenous lean combustion. In the stratified lean combustion, the reliable ignition is achieved by generating a slight rich or near stoichiometric air/fuel mixture around the spark plug at the time of spark ignition and the rest of the chamber is filled with a leaner mixture.

The first generation of the DI gasoline engine with stratified lean combustion systems [31,39], was achieved by wall-guide as well as air-guided direct injection. In 2006 and 2007, a new generation of gasoline direct injection engines with spray-guided stratified combustion systems was developed by Mercedes-Benz and BMW [31]. It is also important to note that Ford developed a spray-guided combustion system that uses a solenoid-actuated multi-hole injector but it was not as robust [40].

The stratified lean burn DI gasoline engine requires an additional NO_x after-treatment system [41,42], which is costly and sensitive to fuel sulphur since NO_x storage catalysts can be destroyed by a high concentration of sulphur in the fuel of sulphur poisoning. Particle matter emission is another problem of these stratified combustion gasoline engines. Because of these challenges, most the manufacturers gave up on the stratified lean-burn combustion. However, there are still some producers such as Mecedes-Benz still have interests in this technology since it is likely to meet future CO_2 regulations [43].

2.4.3 CAI and HCCI

Controlled Auto-ignition (CAI) which is also called Homogeneous Charge compression Ignition (HCCI) combustion is different from traditional spark ignition

combustion in a gasoline engine and compression ignition diffusion combustion in a diesel engine [44]. Premixed fuel and air mixture which in a condition of highly diluted and lean is used together with multiple auto-ignition sites in the combustion chamber. The high temperature zones can be eliminated and the production of particle matters and NO_x decreased as a result of this technology. The gasoline engine with CAI /HCCI enables unthrottled operation by using the lean mixture of air and fuel with recycled burned gas so that higher engine efficiency and better fuel economy can be obtained than traditional spark ignition engine.

According to previous research, CAI combustion can be achieved using the NVO (Negative Valve Overlap) method by closing exhaust valves well before top dead center (TDC), and retarding the opening of intake valves after TDC during the intake stroke. As a result of early closure of the exhaust valves, a large amount of hot burned gas is trapped inside the cylinder. The big amount of residual gases which controls the engine's load is determined by the exhaust valve close timing. What's more, the residual gas also plays an important role to increase the charge temperature to achieve auto-ignition point. For a longer operating range of diluted HCCI combustion, intake valve timing was considered as a potential method of controlling the distribution of residual gases and charge temperature since intake valve timing would have a direct impact on the intake flow and its interaction with trapped residual gases [45].

There are also some challenging for CAI/HCCI such as the control of combustion timing and switching between CAI/HCCI and spark ignition combustion mode, which have hampered the production of this kind of engines. However, Mazda have just recently announced that introduced the first commercial HCCI gasoline engine, Skyactive X will be used in their new vehicles in 2019 based on the so-called Spark Controlled Compression Ignition (SPCCI) [46], which is similar to what is proposed in the project.

2.4.4 Gasoline DI Engines and Boosting (Downsizing)

Gasoline direct injection engine with homogenous stoichiometric combustion process was researched and produced in order to avoid the complex exhaust aftertreatment system on the stratified combustion engine. Such engines are equipped with the standard three-way catalyst for emission control. However, there is little improvement on the fuel economy level.

Over the last decade, recently, engine downsizing has been adopted by major European OEMs to improve the fuel economy. It involves the replacement of a NA engine by a boosted engine with smaller displacement volume and the same even more power [47]. Downsized engine will run at higher BMEP more in the area of good fuel consumption with better efficiency due to less pumping loss. Moreover, engine downsizing also reduces CO_2 emission by reducing the numbers of cylinder so that the total friction and total weight of the engine decrease [48].

It is essential necessary to decrease the compression ratio of boosted downsizing spark ignition engine in order to prevent knocking combustion which has bad effect on fuel economy as well as engine performance. Because direct injection can result in charge cooling effect to reduce charge temperature and knock tendency, there is the synergy between GDI and boosting. Boost/ downsized direct injection spark ignition engine is so success that the majority of new gasoline engine would be turbocharged DI engines by 2018 in Europe as the Figure 2.8 shows [49].

Recently, the development of internal combustion engine has been changed from downsizing towards rightsizing. In this trend, the focus is not on reducing displacement, but instead on selecting the appropriate size to achieve a balance between customer expectations for operating comfort and the manufacturer's ability to reduce fuel consumption and greenhouse gas emissions [50].

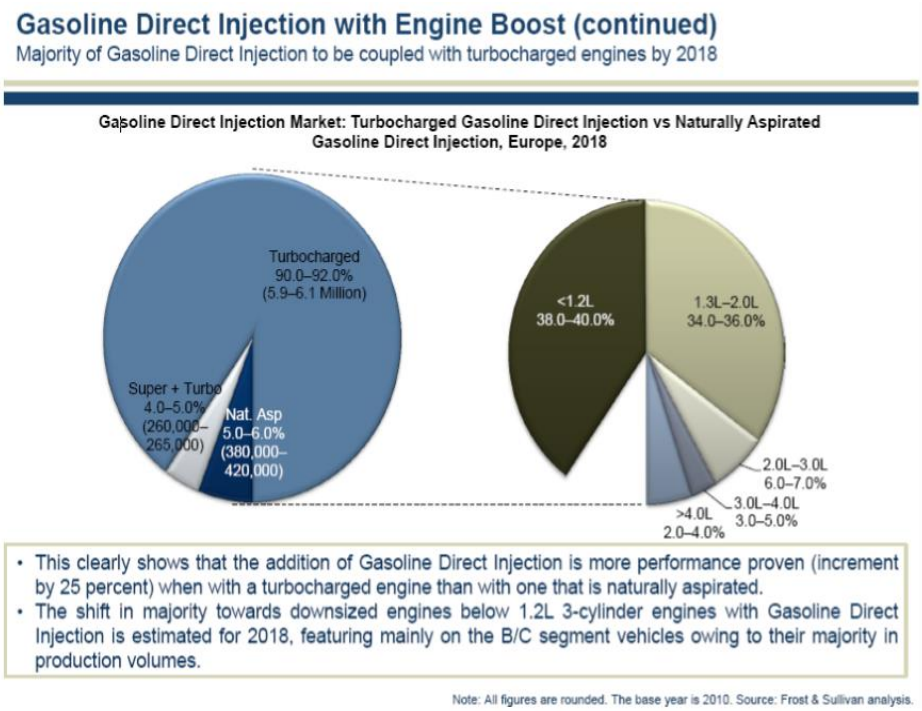

Figure 2-8 Gasoline direct injection with boosting *[49]*

2.4.5 Variable Valve Actuation and Air Intake

A lot of work has been done by researchers to improve the air intake system to optimise the gas exchange process since this process has a big effect on pumping loss as well as combustion process engine performance on gasoline engine. Different devices have been shown to make an improvement of fuel consumption between 3%-12%: Variable Intake Manifold, Variable Cam Timing / Phaser (VCT / VCP), 2-Step or 3-Step Cam Profile Switching (CPS) / Variable Valve Lift (VVL), Continuous Variable Valve Lift (CVVL), camless Valvetrain and Variable Charge Motion [51].

Variable intake manifolds can be realised by step adjusting or continuous adjusting the manifold length to optimise intake turning effect for different engine speeds. The volumetric efficiency of the engine increase as a result of variable intake manifold. Therefore, engine torque can be optimised in the whole speed range [52].

It is very common to use VCT and VCP devices on modern spark ignition engine. During the operation, the valve open and close timing can be changed by crank timing which related to camshaft timing and it can be advanced or retarded by VCT or VCP devices. Both hydraulically and electrically driven continuously adjustable VCT are widely used in gasoline engines on both intake and exhaust valves to optimise the valves open/close timings so that to reduce pumping loss as well as improve low speed peak torque through scavenging behaviour [53,54].

One limit of these devices is that both the valves opening and closing timings have to be changed simultaneously since VCT devices move the camshaft timing. The fixed valve lift profiles of intake and exhaust valves cannot be changed is are another limit of this type of systems. By switching the cam profile, some devices can provide 2-step or 3-step lift adjustment of intake and exhaust valve such as Audi Valvelift System (AVS) and Honda VTEC. CVVL systems can provide continuous valve lift adjustment in a big range such as BMW Valvetronic, Nissan VVEL, Toyota Valvematic and Mitsubishi MIVEC. VVL especially CVVL systems can reduce pumping loss significantly by reducing throttling even provide un-throttling operating on gasoline engine. These devices can be used with other technologies together, such as Miller cycle, CAI/HCCI combustion to optimise engine performance and emissions [55]. What's more, Electronic and electrohydraulic camless valvetrains can provide even more flexible control of valve actions. However, because of the limited durability, cost and complexity, these devices haven't been used on mass production engines.

There are still some other devices and systems which been developed to adjust the intake charge motion. A tumble flap fitted in the intake manifold is used by some VW / Audi gasoline DI engines which are able to increase tumble motion at part loads by blocking the bottom half of intake ports [56,57]. These systems work on enhance air charge motion and turbulence so that to beneficial air fuel mixing as well as combustion process hence improve gasoline engine fuel consumption and efficiency.

2.4.6 Variable Compression Ratio

Higher thermal efficiency can be achieved by increasing the compression ratio. The main reason why the gasoline engine has worse fuel conversion efficiency than the diesel engine is its lower CR since the detonation limit at high load operation. With a Variable Compression Ratio mechanism, fuel conversation efficiency of gasoline engine can be improved since it allows gasoline engine use high CR when it runs at low load and while reduced CR at high load operation. Different VCR systems have been shown to improve the fuel economy of the gasoline engine by 5% to 12 %. If VCR can cooperate with other technology such as lean burn, CAI/HCCI, VVL, Miller cycle, there would be more benefit [58]. Nissan has introduced the VCR technology in their premium brand vehicles. VCR hasn't been more widerly applied on mass production engine since there are still quite challenge such as durability, complexity and high cost. However, VCR technology is considered with great potential in reducing CO_2 emission. Nissan has introduced the VCR technology in their premium brand vehicles in 2016.

2.4.7 Water Injection

A big problem in the gasoline engine is the knocking combustion at high load which is normally solved by retarding spark timing resulting in poor performance and fuel economy. For boost downsized engines, this problem becomes more intensive and limits their performance.

The research on water injection can date back to the 1920s when gasoline piston engines were used in aircraft. Recently, this concept attracts the sight of researchers again since its potential to reduce knocking combustion and decrease heat transfer loss and consequently improve the fuel conversion efficiency of downsized SI engines [59]. The main challenge is the requirement of additional storage and supply of distilled water.

2.4.8 Cooled Exhaust Gas Recirculation

Exhaust Gas Recirculation (EGR) technology has traditionally been used to reduce NO_x emission and fuel consumption on gasoline engines. EGR is used to dilute the in-cylinder charge and maintain stoichiometric AFR at the same time so that to lower the pumping loss at part load and in-cylinder temperature in the combustion chamber. More recently, cooled EGR has been exploited to reduce knocking tendency at high load operation. Toyota produce their latest hybrid vehicles with Si engine which use EGR as its key measure and it achieves the highest thermal efficiency of 41% [36,60].

2.4.9 Miller Cycle

The name Miller Cycle came from an American engineer, Ralph Miller who proposed and applied the early intake valve closure as an effective means to improve the boost SI engine's performance in the 1950s. The main potential benefits are listed below:

- For a supercharged SI engine, thermal load and knocking/ pre-ignition tendency should be decreased by the earlier IVC.
- The charge temperature would decrease by reducing effective compression ratio (ECR) associated with earlier IVC while retain the thermodynamic benefit of a high expansion ratio at the same time.
- The AFR should be correct to control auto-ignition and enable operating at higher load and high expansion ratio / geometric compression ratio.
- Load control by intake valve can help to reduce the pumping loss by wider open throttle.
- Scavenging should be improved since high boost pressure and subsequent increased differential between the boost pressure and the exhaust back pressure.

- Different load operation should apply different valve lift.
- A supercharged/ turbocharged engine should be a preferred application, but the process can also be used on a NA engine as well.
- The work can apply on gases, diesel as well as gasoline engine.

Related to the Miller cycle, the Atkinson cycle should also be mentioned. It is named by the British engineer James Atkinson who was the first person to describe a four-stroke internal combustion engine process with unequal compression stroke and expansion stroke. This concept was first presented in 1886 for an opposed piston engine [61]. After that, a four-stroke engine with special crank mechanism was used to realize the Atkinson process in 1887 [62]. However, the name of Atkinson cycle engine has recently been adopted to describe the technology based on the retarded intake valve closure by means of a longer intake valve lift profile. Similar to the early intake valve close (EIVC), the late intake valve closure (LIVC)in such engines is employed to lower the effective compression ratio to enable higher geometric compression ratio (hence longer expansion stroke) being used for better engine efficiency, such as the engines used in the Toyota Prius Hybrid Vehicles.

2.5 Spark Ignition Engines with Alternative Fuels

2.5.1 Natural Gas Engine

Natural gas, whose main composition is methane, is an alternative fuel to gasoline for the spark ignition engine with a higher H/C ratio and greater research octane number (about 130). When changing the fuel from gasoline to CNG, the H/C ratio is changed from 1.85 to 3.7-4.0. Compared to the stoichiometric SI gasoline engine operation, the natural gas engine can be operated at a higher compression ratio. If operated with a lean burn mixture and a high rate of EGR, a significant reduction in pollutant emissions and an improvement in thermal efficiency can be achieved by a natural gas engine [63]. It has been shown that the natural gas engine can achieve a

CO_2 emission reduction by 20% compared with the gasoline engine at equal torque and power [64].

Moreover, since natural gas doesn't contain aromatic compounds such as benzene and contains less dissolved impurities like sulphur compounds than petroleum so that natural gas engine produces less little PM than gasoline engine particle emissions. Natural gas is also reliable when consider its safety. Natural gas has the characteristic of low density as well as high dispersal and it is difficult to form explosive mixture when there is a leak event.

With the significant increase in the production of natural gas and bio-methane from renewable sources, there is increased demand for the research and development of high-efficiency and ultra-low emission gas engines for light-duty and heavy-duty vehicles.

2.5.2 Alcohol as Alternative Fuel in Spark Ignition Engine

2.5.2.1 Overview of Alcohol Fuels

The chemical structure of alcohol can be expressed by CnH2n+1OH. When they are produced from renewable sources, alcohol fuels can lead to the reduction of fossil fuel consumption and greenhouse gas emissions as well as toxic emissions [65]. In a spark ignition engine fuelled by alcohol, the air-fuel mixture has some advantages such as reducing knock tendency and toxic emissions [66].

As a fuel for high-performance engines, methanol which is the chemically simplest alcohol was used during the 1930s as an alternative to gasoline [67]. The liquid form of methanol is toxic, tasteless, colourless, and is commonly referred to as wood alcohol and can be produced from a range of raw materials and sources [68]. What's more, methanol has a lower boiling point compared with gasoline, which allows it to evaporate more quickly, which has a positive effect on engine combustion and reduces hydrocarbon emissions. In addition, as a result of the high oxygen content of

methanol and its simple structure, its combustion can be more efficient and less polluting in spark-ignition engines [69,70].

Ethanol is derived from fermentation of biological material and is a renewable and efficient fuel [71,72]. In the United States, ethanol was first proposed for using as a fuel for internal combustion engines in the 1930s, and has been widely spread since 1970. Brazil established the national alcohol program (NAP) in response to the first oil crisis in 1973, which led to a reduction in its dependency on fossil fuels [73]. Approximately 60% of global ethanol production was produced in 2014 by the United States, while the Brazilian government produced approximately 23.47 billion litres representing 25% of global production. From 2007 to 2015, the global ethanol production by country is represented in Figure 2-9 [74]. The production rose sharply between 2007 and 2010, however, the largest production occurred in 2015, after that it went down in 2011 and 2012. With gasoline prices increasingly high and emission regulations becoming stricter, ethanol could become a more important renewable fuel. There have been extensive studies undertaken to ensure high ignition temperatures, higher research octane numbers, lower freezing points, higher heats of vaporization for ethanol in comparison with gasoline [75,76].

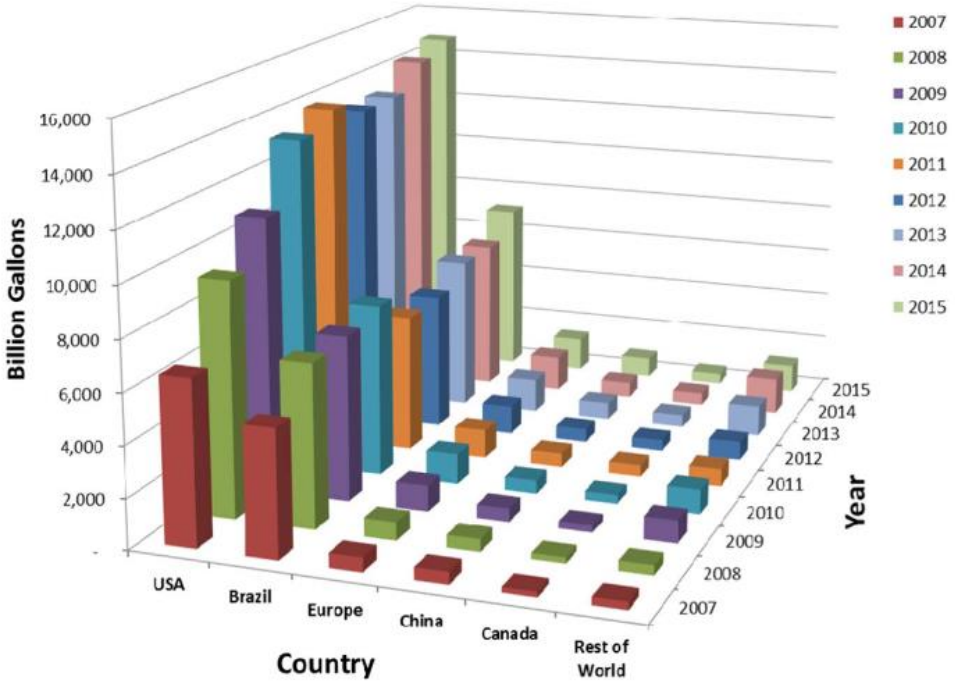

Figure 2-9 The global production of ethanol from 2007 to 2015, by country *[74]*

Regular gasoline can have an auto-ignition point ranging from 221°C to 257°C, and that of ethanol is at 329°C, and methanol is 470°C [77].

When a substance is in the process of changing from liquid to vapor, additional heat must be absorbed in order to bring about that change, and this is how heat of vaporization come from [78]. To changing from liquid state to vapor, ethanol needs to absorb 918.7KJ/Kg (25°C, 1ATM), while gasoline needs 341.9KJ/Kg. Since ethanol absorb more heat during evaporation, it can create a cooler operating condition during injection in an IC engine. Because it has a high latent heat of evaporation, ethanol contributes to the reduction of NO_x emissions [79]. It is typically thought that high latent heat of evaporation of alcohol fuels has indirectly affect on knocking by cooling the air-fuel mixture evaporating during the intake stroke while the fuel is being injected into a DISI engine and thereby postponing the ignition of the fuel under knock conditions [80]. This is also called charge cooling effect.

As alcohol fuels contain a higher percentage of oxygen compared with gasoline, their combustion could be more complete and cleaner, and the in-cylinder temperature could be reduced because of the oxygen content and high latent heat of vaporization [81]. Ethanol's oxygen content (34.8 by weight) is lower than that of methanol (49.9

by weight). Methanol will therefore function as a less diluent than other oxygenates. The engine fuelled by alcohol fuel has higher combustion efficiency compared with gasoline. According to some studies, this can be attributed to the relative oxygen content in fuel, despite the fact that oxygen limits fuel consumption performance because it does not permit any additional energy conversion. In addition, the oxygen content in alcohol fuel contributes to the completeness of combustible [82]. What's more, since alcohol fuels have higher oxygen/carbon ratios, its lower heating value is lower than gasoline which causes more fuel is consumed to achieve the same power as gasoline [83].

A higher RON (research octane number) is generally associated with alcohol than the MON (motor octane number). The RON of ethanol and methanol in this research are 107 and 108, their MON are 89.5 and 88.7. The sensitivity (RON-MON) of gasoline is lower than that of ethanol and methanol.

Similar to ethanol, butanol can be produced from corn grain and another biomass [84]. Biobutanol has the advantages of being immiscible in water, having a higher energy content, and having a lower Reid vapor pressure when compared with ethanol. What's more, butanol meets the Renewable Fuel Standard's threshold for reducing greenhouse gas emissions by 20%.

Isobutanol attracts currently the most active commercialization work among the four isomers of butanol. It is permitted to blend up to 12.5% biobutanol into gasoline under two provisions of the Clean Air Act. In addition, the U.S. Environmental Protection Agency (EPA) recently granted a waiver that allows a 16% biobutanol blend to be considered the same as E10 as a legal fuel. The EPA has approved blends containing up to 16% biobutanol in June 2018.

With the following advantages which make biobutanol an alternative to conventional transportation fuels:

- In comparison with gasoline alternatives, biobutanol has a relatively high energy content.
- The vapor pressure of biobutanol is lower than that of ethanol, which results in less volatility and evaporative emissions.

- A variety of feedstocks can be used to produce biobutanol.
- Butanol releases less greenhouse emissions compared with other fossil fuels. What's more, growing feedstocks capture carbon dioxide, which is offset by carbon dioxide released by the combustion of biobutanol, thereby reducing greenhouse gas emissions overall.
- Due to its immiscibility with water, butanol might be capable of being transported in pipelines, thereby reducing transportation costs.

2.5.2.2 Application of Alcohol Fuels in Spark Ignition Engines

Ethanol and methanol have been in used as a blended component with gasoline [85]. The most widely used one is E10 which consist of 10% ethanol and 90% gasoline. Brazilians have long used ethanol as a neat fuel. Approximately five million cars on the road are fuelled by 190-proof ethanol (95% ethanol, 5% water) and hence neat (pure) ethanol are well suited for use as a primary fuel for vehicles.

Several studies have indicated that ethanol and pure methanol increase engine thermal efficiency as a result of lower in-cylinder temperatures and peak in-cylinder pressures. What's more, pure ethanol and methanol release less NO_x and CO_2 than gasoline [86]. When change gasoline to pure methanol, the output power and CO decrease while the brake specific fuel consumption increase since the lower heating value of methanol is lower than that of gasoline [87].

Koichi et al. [88] studied the effect of pure ethanol on spark ignition engine compared with gasoline. The experiment was carried out on a 1.5L 1NZ-FE natural aspirated Toyota engine whose compression ratio has been increased from 10.5:1 to 13:1 by changing the piston. During testing, the engine's speed and load were 2800rpm, 2bar BMEP. It has been concluded that ethanol fuelled engine's thermal efficiency and torque have been increased since ethanol has the better anti-knock quality and lower cooling heat loss. What's more, the NO_x released by ethanol is lower because of the lower in-cylinder temperature. In addition, ethanol has lower THC since gasoline has components that boil at high temperatures, but ethanol does not.

Senthil et al. [89] did simulation research about the possibility of using early intake valve close (EIVC) Miller cycle to increase the efficiency of an ethanol, methanol fuelled turbocharged heavy-duty spark ignition engine by GT-Power. The test was done at 1200rpm 25bar IMEP. The result shows that even if the turbocharger efficiency is only 49%, the brake thermal efficiency could still be increased by 2-3% by increasing the geometric compression at stoichiometric combustion. At the condition of lean burn, minimal turbocharger efficiency of 55% is needed to promise the BTE increase for both ethanol and methanol with Miller cycle since the pumping loss increase.

An experimental study about compression ratio on methanol's combustion characteristic, performance and emissions was carried out on a 0.25L variable compression ratio engine. The engine speed during testing was between 1500rpm to 3500rpm. The result shows that with the compression ratio increased from 6:1 to 10:1, the engine power and brake thermal efficiency increased by up to 14% and 36%. In addition, CO, CO_2 and NO_x emissions decreased by 7%, 30% and 22% respectively. HC emissions increased by approximately 12% with an increase in CR from 6 to 10 since the surface to volume ratio increases as CR increases. As a result of this, the flame cools in the places near to surface hence misfire [90].

As a result of the better anti-knock characteristic of alcohol fuel, a higher compression ratio (CR) can be achieved (to levels of 12:1 and above) without spark retarding in order to avoid knocking. In 1981, Ford achieved a 20% increase in power and a 15% increase in efficiency for the M85 Escort model due to the increase in compression ratio [91].

Due to the faster flame speed and wide flammability ranges of alcohols, many alternative options are available for load control, particularly in the case of methanol. An investigation has been done on an experimental turbocharged lean-burn 0.61L methanol engine. The engine speed was controlled at 1200rpm. The result shows that the BTE increased by 14% compared with stoichiometrically fuelled engines with throttled load control. What's more, A reduction of over 50% CO was achieved. On the other hand, the lean burning strategy resulted in NO_x emissions increased by 150%, which brings into question the practicality of such a strategy [92].

Another research also worked on methanol fuelled spark ignition engine load control strategies. In this research, three strategies were compared including the throttled stoichiometric operation, wide open throttle (WOT) lean burn operation and WOT stoichiometric operation using EGR to control the load. Compared with the throttled operation, the other two strategies increased the BTE by up to 5% because of cooling and dissociation losses. What's more, there was also a sharp decrease of NO_x by WOT EGR since dilution caused decreasing in in-cylinder temperature. But there wasn't a significant reduction of NO_x by lean burn. EGR plays a more important role here compared with lean burn since exhaust gases have a greater heat capacity than air. Above all, WOT EGR appears to be an appropriate strategy for methanol engines [93].

There are still some challenges for using pure methanol on vehicles due to its cold start problem when the temperature is under 15°C as well as safety concern [94]. Under cold conditions, vaporizing fuel and producing a combustible mixture can be achieved in several ways, such as heating the fuel, heating the intake port, and raising the temperature of compressed air. Heating the fuel can be achieved by adding a heater to the injector. Research did by Daniel et al. [95] focused on the heated injector and fuel rail to deal with ethanol's cold start problem. With prototype systems, the E100 cold starts were robust and effective at temperatures as low as -5°C without gasoline assistance. What's more, it has been also found that the heated injector can decrease THC and CO by 40%, but there is a tiny increase in NO_x.

As an alternative to directly heating intake air, increasing the compression ratio and optimizing valve timing can be used to increase the compressed air-fuel mixture's temperature. In practical use, raising compression ratio and optimizing valve timing are thought to be most effective, since they do not require preheating the fuel as well as intake air [88].

Although the potential benefits of methanol and alcohol fuels in a spark ignition engine had been demonstrated by the previous publications, there are limited studies to quantify the improvements that could be achieved by methanol or ethanol fuel in a modern direct injection highly downsized spark ignition gasoline engine.

Therefore, the current study is aimed to fill the gap by performing a systematic experimental study of the alcohol-fuelled engine's performance, combustion and emission characteristics across the whole range of engine operations. It is also a direct comparison between E10gasoline, ethanol and methanol in the same boost high compression ratio spark ignition engine. Some high speed& load testing were also carried out with the IMEP up to 28bar. In addition, the effect of injection timing and rail pressure on the engine performance and emissions was investigated to find the best injection strategies for ethanol and methanol at different speeds & loads. Particle emission data were collected for every test condition which includes load sweep as well as injection timing & pressure sweep since there is limited research done for ethanol and methanol's particle emission. Finally, the spark sweep study was carried out to evaluate how alcohol fuels can be used to facilitate the fast catalyst light off for effective cold start emission controls.

3. Chapter Three: Experimental Facility and Methodology

3.1 Introduction

This research is based on alcohol fuel (ethanol & methanol) running in a highly downsizing, single cylinder, direct injection engine with a flexible Engine Control Unit (ECU) to improve the fuel economy and decrease all gaseous emission as well as Particulate Matter (PM). All the experiment facilities and experimental methodology which used to collect the data in this project are described in this chapter.

3.2 Experimental Set-up

In this project, the most important experimental facility is the single cylinder engine test bed which will be shown in this section. The main part of the engine test bed which includes a single cylinder engine, conditioning and supply system (external boost rig, oil, coolant, fuelling system), data acquisition system, engine control unit (ECU) as well as the emission analysers (HC, NO_x, CO_2, CO, O_2, particulate matter). The engine is coupled to a transient electrical motor dynamometer which can both control the engine speed & throttle position and measure the engine's torque output during engine testing. All the above are shown in Figure 3-1.

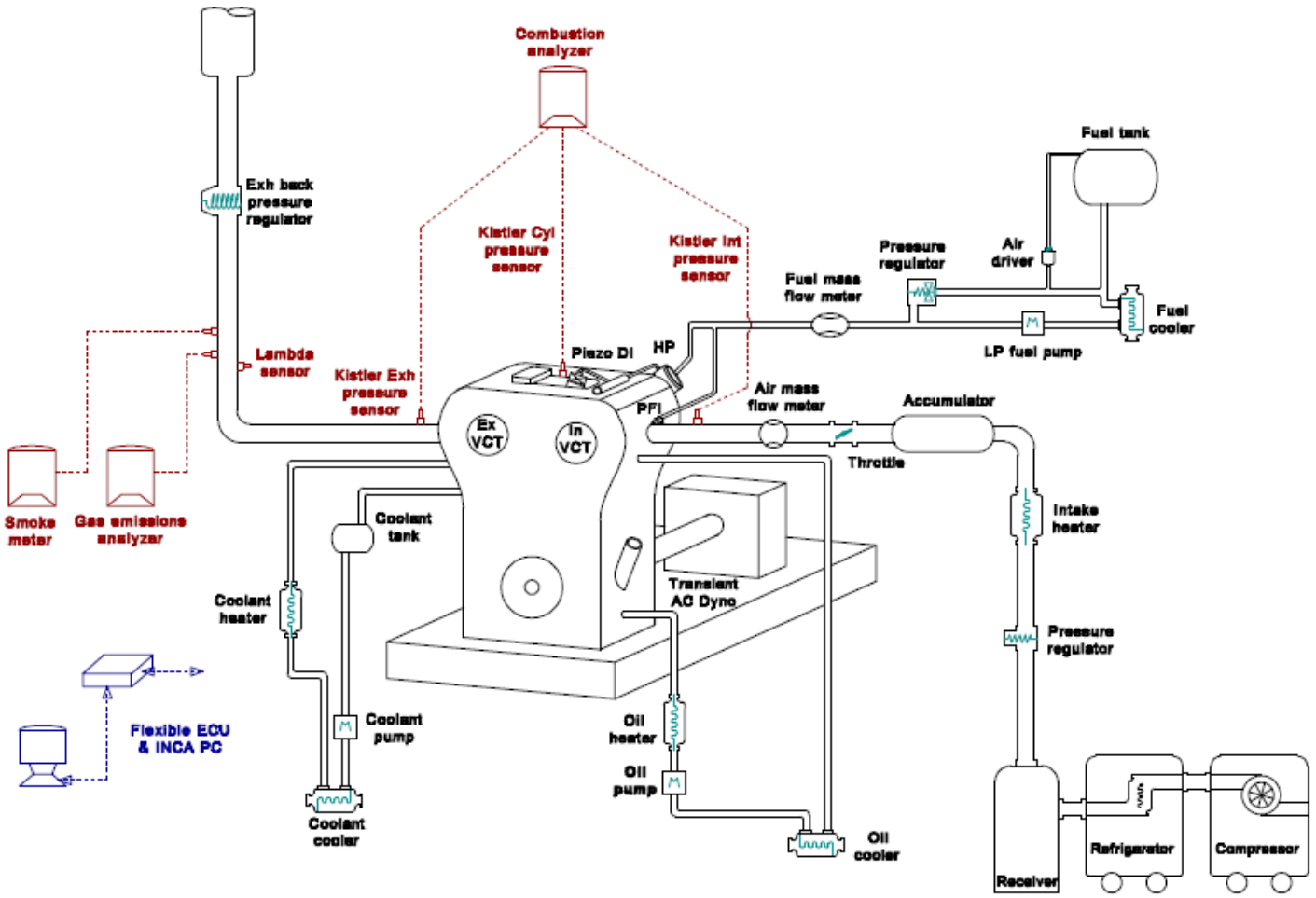

Figure 3-1 Schematic of Single Cylinder Engine Testbed

3.2.1 The Single Cylinder Engine

All the data are collected from the experiments conducted on a single-cylinder GDI engine. The GDI engine is built with a high-speed single cylinder Ricardo Hydra crankcase. The cylinder head was provided by MAHLE which is used for their 1.2L 3-cylinder downsizing demonstrator engine [96-102] and a special cylinder block was designed to match the single cylinder crankcase. All the test bed facilities, as well as the engine main specification, are shown in Figure 3-2 and Table 3.1.

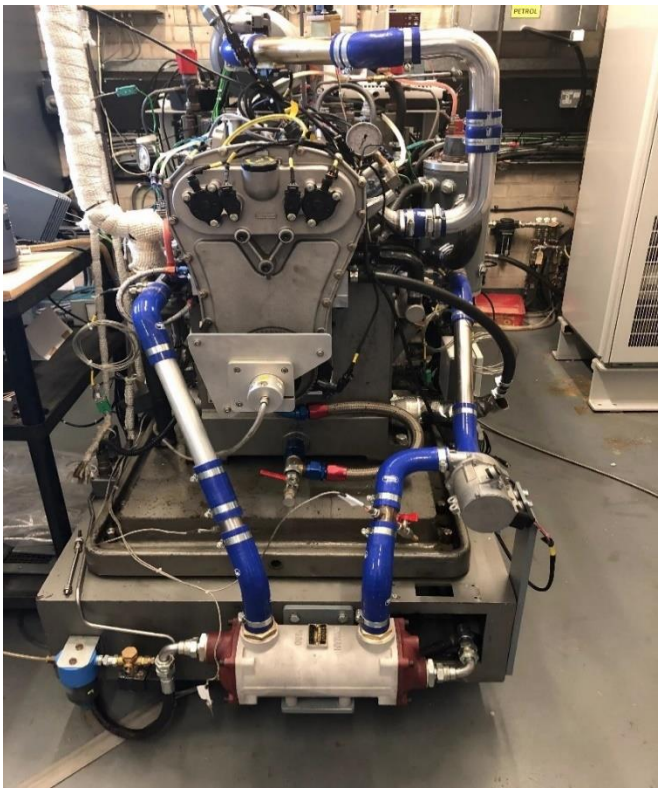

Figure 3-2 Brunel-MAHLE Single Cylinder DISI Engine on the testbed

Table 3-1 Engine Specification

Displacement Volume	400cm^3
Stroke	73.9mm
Bore	83mm
Connecting rod length	123mm
Compression ratio	11.43:1
Number of valves	4
Maximum In-cylinder pressure	120bar
Maximum pressure rise rate	6 bar/CAD
Intake cam timing (maximum open point)	80-120 CAD ATDC
Intake cam duration	240 CAD
Exhaust cam timing (maximum open point)	100-120 CAD BTDC
Exhaust cam duration	278 CAD
Direction injection system	Bosch Gasoline Direct Injector
Intake port fuel injection system	Bosch EV 12 with 4 narrow conical sprays and maximum injection pressure of 8 bar

The engine is built with a pent- proof combustion chamber which has two intake valves and two exhaust valves. The Bosch direct injector is fitted on the middle of the cylinder head and the spark plug is mounted next to the direct (Figure3-3) injector to achieve the spray charge stratification. For this direct injector, three times of injection which include one early injection (main injection) and two late injection could be

achieved in one cycle. The injection timing and pressure for the main injection as well as the injection timing and duration for the late injection could be adjusted on ECU (INCA software). The maximum injection pressure for this injector is 200bar and it was adjusted in line with the engine speed and load. For each injection event, the minimum injection duration is 0.15ms and the minimum gap between the end of one injection and the start of the next is 0.2ms.

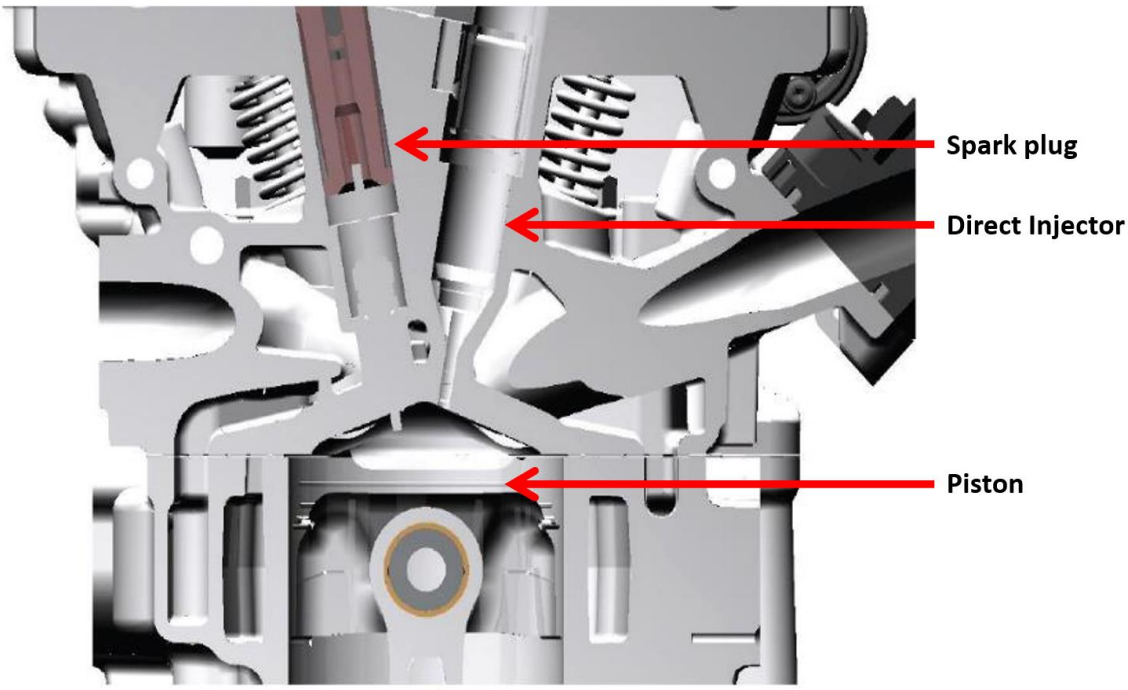

Figure 3-3 Combustion chamber with the injector and the sparkplug *[97]*

3.2.2 Details of Cam Profiles and Valve Timing

There are two hydraulic variable cam phasers situated in the cylinder head, one of them is for the intake cam and the other one is for exhaust cam. As a result of this, the intake and exhaust cam timings can be adjusted up to 40crank angle degrees (CAD). The design details and phasing of the three intake cams and the exhaust cam for the testing engine are shown in Table 3.2 and Figure 3-4. In this research, the testing engine is fitted with the standard intake camshaft with 240CAD opening

duration and an exhaust camshaft with 278CAD opening duration, both of the intake and exhaust valves have a maximum 11mm lift.

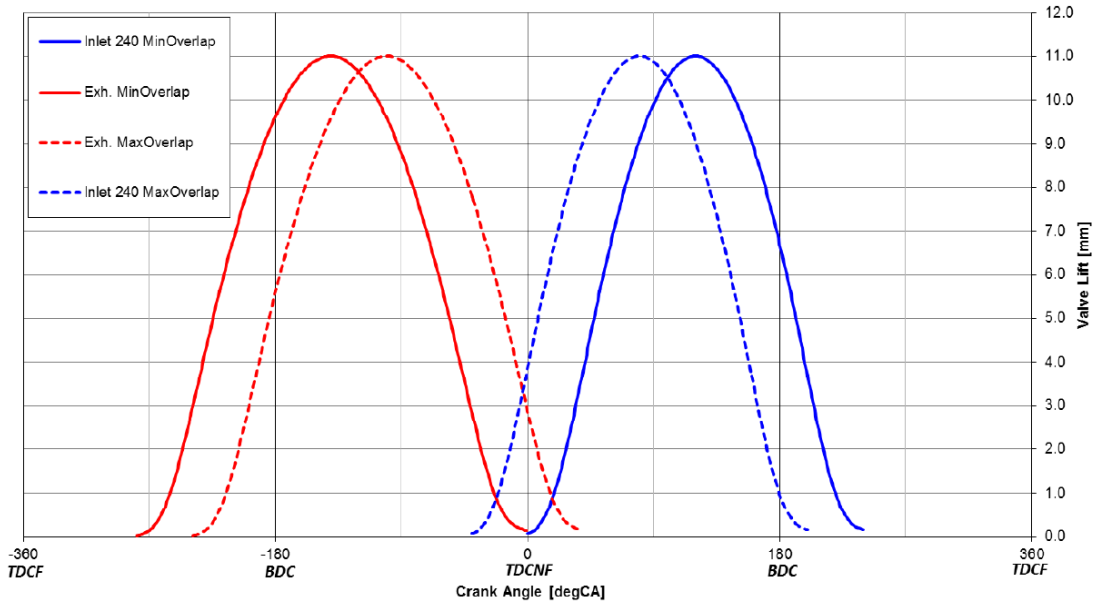

Figure 3-4 Intake and exhaust cam profile and phasing

Table 3-2 Intake and Exhaust Cam Specification and Phasing

Cam	Opening Duration (TOR)[dCA]	Minimum Overlap Phasing [dCA ATDCNF]			Maximum Overlap Phasing [dCA ATDCNF]		
		MOP	IVO/EVO (0.5mm lift)	IVC/EVC (0.5mmlift)	MOP	IVO/EVO (0.5mm lift)	IVC/EVC (0.5mmlift)
EIVC Intake	152	75	16	134	35	-24	94
Standard Intake	240	120	13	227	80	-27	187
LIVC Intake	292	144	16	272	104	-24	232
Exhaust	278	-140	-262	-17	-100	-222	23

3.2.3 Engine Oil System

The engine oil system is responsible for supplying the engine with lubrication oil at sufficient pressure and maintaining the specific oil temperature. For this testbed, the oil system consists of an oil tank, oil filter, oil heater, oil pump and an oil heat exchanger.

A wet sump lubrication system which stores the standard Mobil 1 0W-40 oil is featured in this single cylinder engine for all testing work. The oil pump in this system is an externally located single speed three-phase electronic oil pump which can circulate the oil at a nominal flow rate of 9.1L/min. In order to pre-heat the oil before running the engine or heat the oil to the requested temperature at low speed& load, two 1kW electronic oil heaters are immersed in the oil sump. An oil heat exchanger which is used to cooling the oil with the maximum heat rejection rate of 4kW situated upstream of crankcase oil gallery. The flow rate of raw cooling water run through the heat exchanger is controlled by a Spirax Sarco capillary actuator. The oil temperature is controlled by switching on/off the oil heater as well as adjusting the cooling capacity of the heat exchanger which is achieved by turning on/off tap of cooling water. For low load testing, the oil temperature can be controlled by switching on/off directly but for high load, the oil heater is off all the time and the oil temperature is controlled by adjusting the cooling capacity of the heat exchanger. An AC Delco X19 equivalent oil filter which is mounted next to the oil heat exchanger is used to filter the oil.

In order to keep the oil temperature and pressure at a safe range (especially high speed& load test point) during testing, a set of sensors are fitted in the oil circuit. There are three pressure sensors situated upstream of the crankcase oil gallery and the minimum oil pressure is set to 4.2bar at this point. A pressure gauge for quick reading during the start-up is located after the crankcase oil gallery. A pressure switch for the testbed emergency shutdown mechanism and a Druck PTX1400 (0-10bar, 4.2mA) pressure transducer provides oil pressure information to the low-speed data acquisition system. The oil temperature inside the crankcase oil gallery is measured by two Platinum Resistance Thermometers (PRT), one of them is for testbed high oil temperature emergency stop which is set to 100°C and connected to the engine

dynamometer controller, the other one is connected to the low-speed data acquisition system. The last PRT is located at the outlet of the oil sump which is used for oil temperature acquisition.

3.2.4 Coolant system

The coolant system is responsible for supplying coolant to the engine with a desired flow rate and temperature. The main part of the coolant system includes a coolant tank, coolant pump, ball valves, coolant flow meters and coolant heat exchanger.

The coolant which is used for all testing work is a mixture of half de-ionised water and half of the ethylene glycol. The coolant tank which is used to store the additional coolant in the circuit is situated 120mm higher than the top of the engine cylinder head coolant jacket so that the cooling jacket is fully submerged in coolant. What's more, the coolant tank can also allow the expansion of coolant when it starts to become hot. An internal Pierburg 12V DC Coolant pump which speed is controlled by engine control system (ECU) is used to circulate the coolant in the circuit with different flow rate depends on engine speed and load (30L/min at low load, 50L/min at high load). The entire coolant flow rate into the engine is varied by a bypass ball valve which is installed upstream of the engine inlet, and the flow rate is set to 13L/min so that the delta coolant temperature can be controlled within 6°C between engine inlet and outlet. The coolant run through the cylinder head and cylinder block was split by two ball valves situated outlets of cylinder head and blocks so that both of their coolant flow rates can be controlled independently.

During testing, the way to control coolant temperature is similar to oil temperature. A 3kW immersion heater is connected to the coolant system in order to heat up the coolant at the warm up stage or the load is low. What's more, a Bowman heat exchanger whose maximum heat rejection rate is 53kW is located after the Pierburg pump, and it works as the oil heater. When the engine is running, the coolant temperature is controlled to 90°C by adjusting the effect of coolant heating and cooling.

The coolant flow rate, temperature as well as pressure are measured by a few sensors situated in the coolant circuit. Two Apollo turbine type flow meters are used to measure the cylinder block and total engine coolant flow rate, one is located between the outlet of the cylinder block, and another one is located before the Pierburg pump. The coolant pressure is measured by a Druck PTX1400 0-4bar 4.2mA pressure transducer which is before the engine coolant inlet where a PRT is at the same location to measure the coolant temperature into the engine and another PRT is used to measure the coolant outlet temperature. Another PRT which located into the coolant tank and connected to the dynamometer is for the testbed emergency shutdown. What's more, an automotive type coolant temperature sensor which fitted at the cylinder block outlet side provides the input to ECU.

3.2.5 Fuelling System

A low-pressure loop and a high-pressure system are the main parts of the fuel conditioning and supply system. The low-pressure part is to supply the fuel with a specific temperature (30°C ±3) and pressure. A fuel flow meter is also included for fuel consumption measurement. The high-pressure fuel system consists of a high-pressure fuel pump, high-pressure rail and direct injector.

The fuel used for baseline testing is EURO 6 E10 with a Research Octane Number (RON) of 95, pure Ethanol and Methanol. Two 50L stainless steel fuel tanks located higher than all other components are used to store fuel, one is for normal gasoline, and the other is for alcohol fuel. Two Bosch automotive 12V low-pressure fuel pumps are installed under the fuel tanks. Each one is used for its matched fuel tank, and the low-pressure pumps are controlled by the fuel circuit of the testbed depending on the test fuel. Two groups of fuel systems run independently and cannot run at the same time. The fuel runs through a heater exchanger (fuel cooler), which controls the fuel temperature by adjusting the flow rate of raw cooling water run through it as a result of sucking by the fuel pump. After that, the fuel is running through a filter, then a mechanical pressure regulator which can promise the fuel supply pressure is 5bar, and it is shown on a gauge and should be checked every time before running the

engine. This loop is connected with the entrance of the fuel tank at atmospheric pressure by a pipe that goes upwards, and its top ends are higher than the rest of the system so that the air bubbles can be removed from the low-pressure fuel system.

After the regulator, a Druck PTX 1400(1-10bar, 4.2mA) pressure sensor and a PRT temperature sensor aim to measure the pressure and temperature of the supply fuel, both of them are connected to the low-speed data acquisition system. During all engine testing, the fuel consumption is measured by a Coriolis type mass flow meter which is manufactured by Endress+Hauser. It has a DN01 1/24'' sensor size, which is more suitable for very small mass flow rate measurement. For this project, the range of the fuel flow meter is 0-20kg/h, which is determined by considering the lower heating value (LHV) of ethanol and methanol.

Figure 3-5 Coriolis mass flow meter by Endress+Hauser

The fuel line is split into two lines after the fuel flow meter. One of them connects to the low-pressure fuel rail which supplies fuel to the PFI injector directly (not used in this project). The other fuel line supplies fuel to the high-pressure cam-driven type

fuel pump which is driven by the intake camshaft. The required amount of fuel is supplied to the high-pressure common rail, and the fuel pressure can be increased up to 200bar by the high-pressure fuel pump. The rail pressure is controlled by the ECU through a proportional–integral–derivative (PID) control. To achieve this, a high-pressure automotive type pressure sensor is put on the common rail. The physical rail pressure is detected by the pressure sensor which gives feedback to ECU, after that it compare the actual rail pressure with the set pressure and change the rail pressure by increasing or decreasing the fuel quantity fed into the common rail. The high-pressure fuel is supplied from the common rail to the injector through a short stainless-steel pipe.

3.2.6 Intake System

The boosted downsized GDI engine requires the supply of compressed air above ambient pressure. This is achieved by an external boost rig.

The dried compressed air with pre-set pressure and temperature is supplied to the engine by the external boost rig. The boost rig includes a compressor (CompAir HV22RS AERD hydrovane type compressor) which is driven by a 22kW electric motor, a refrigerator (dryer unit), a five mivron oil filter and a 272 litres receiver.

The minimum pressure which provided by the compressor is 6bar, the air has a nominal flow rate of 3.53m^3/min at this pressure. After the compressor, there is a refrigerator which can provide air with humidity less than 3% (according to the manufacturer manual) and it can also cool down the air to approximately to 3°C. A receiver which volume is 272 litres situates downstream of the refrigerator, it can store and keep the compressed dried air’s pressure stable. The rig controller turns the compressor on/off in order to maintain the pressure of the air in receiver between 6.5 to 7bar. After that, two Parker Hannifin EPDN4 type pressure regulators are used to regulator the intake pressure to the required pressure for engine air consumption and has a precision of ±0.15bar. The first is only used when the load is low and is controlled manually. It will be bypassed or fully opened when the engine load is high

since more compressed air is required. The second Parker regulator is close-loop controlled by the ECU and is fitted after the first Parker pressure regulator.

The intake temperature is set to 40°C for all experiment in this thesis. In order to increase the dried compressed air temperature which cooled by the dryer from 3°C to 40°C, an electrical 3 kW Secomark 632 type heater is used after the second Parker pressure regulator. This intake heater is closed- loop controlled by ECU with the precision of ±1°C.

A large volume plenum(accumulator) with a k-type thermocouple which volume is 40L and made of stainless steel is included in the intake system. The thermocouple is used to measure the air temperature inside the plenum and then as a feedback to a Eurotherm PID controller to control the intake heater. Another function of the large plenum is to minimize pressure fluctuations. A Bosch DV-E5 40mm automotive type electronic throttle is situated downstream of the plenum which is controlled by dyno. The temperature and pressure between the plenum and throttle body are measured by a Bosch automotive type boost pressure and temperature sensor and gives feedback to ECU. After receiving the feedbacks, the ECU will increase or decrease the boost pressure before the throttle body by adjusting the second pressure regulator. A large diameter and long intake pipe are used between the throttle body and the engine intake port which is for achieving the desired and stable intake port pressure required at different speeds and loads. The pressure wave after the throttle body could be more stable as a result of this. The air mass flow after the throttle body is measured by a Bosch 1-way hot wire automotive type mass air flow meter which gives signal to ECU. The pressure and temperature are also measured after the throttle has been applied using pressure and temperature sensors which communicate with the ECU.

There is also a Kistler 4005B piezoresistive absolute pressure sensor (Figure 3-7) installed in the intake port just before the intake valves for the purpose of measuring the transient intake port pressure for the combustion analyser software and for subsequent analysis. The intake port air temperature is also measured by a PRT in the same location.

3.2.7 Exhaust System

The main component of the exhaust system is made of austenitic stainless steel pipes that have no sudden changes in diameter, thereby ensuring that the exhaust gas flow is as smooth as possible. The pipe is designed to withstand temperatures of up to 780°C and pressures of up to 4 bars in the exhaust gas. In order to minimize the back pressure associated with exhaust, a large automotive-type exhaust muffler is installed at the exit of the exhaust system. Additionally, the exhaust back pressure is controlled by a servo motor actuated butterfly valve fitted upstream of the muffler. When the dynamometer computer is required to adjust the valve, the valve can be remotely adjusted to achieve the required back pressure on the testbed so that the presence of the turbocharger turbine can be simulated.

It is necessary to install a K-type thermocouple close to the exhaust valves in order to measure the exhaust port temperature. In spite of its higher accuracy than thermocouples, PRT is not used as a measurement point for exhaust port temperatures because it cannot withstand high exhaust temperatures. Two different kinds of pressure sensors are used in the exhaust system. The first one is fitted 100mm after the exhaust port which is Kistler 4005B type piezoresistive absolute pressure sensor (Figure3-6) with a cooling water adaptor, the cooling water is controlled by a valve and should be on before running the engine. The transient exhaust pressure is measured by the Kistler pressure sensor which is necessary for gas exchange analysis. Kistler pressure sensor is connected to the high-speed NI card. The specification of the Kistler sensor is also included in Figure3-6.

Kistler 4005BA10FA0

Range	0 - 10 bar abs
Pressure range	0 - 10 bar abs
Temperature range	-20 - 125 degC (1100deg C w/cooling adapter)
Linearity	± 0.2%
Size	M5 (M10 w/cooling adapter)
Construction	316 Stainless Steel
Warm up	30 mins
Output	0 - 10V

Figure 3-6 Kistler 4005B type Piezoresistive Absolute Pressure Sensor

A Druck PTX 1400 (0-10bar) type low-speed pressure sensor is used to measure the mean exhaust pressure. This pressure sensor is located downstream from the first and is connected to the low-speed NI card. What's more, two automotive-type Universal Exhaust Gas Oxygen (UEGO) Lambda sensors are installed on the exhaust pipe. The lambda is controlled by ECU while the signal is from the first lambda sensor, the second lambda sensor is only used for confirming the reading of the first sensor is right. What's more, there are also some emission analysers such as gaseous and particulate analyser connect to the exhaust pipe. The NO_x is measured by a Signal Ambitech Model 443 Chemiluminescent Analyser, the HC is measured by a Signal Rotork Model 523 FID HC analyser, and the CO, CO_2 and O2 are measured by a Horiba MEXA-554JE. In addition, a fast response DMS 500 particle analyser is used for measuring particle size and particle numbers.

3.2.8 Dynamometer

The engine's torque and load are controlled by an electrical motor dynamometer which model is CPEngineering 48kW AC motor with a 4 quadrant AC regenerative inverter derive. For this dynamometer, the maximum speed is limited to 6000rpm

and the maximum operating torque is 140 Nm. The dynamometer is controlled by the CP CADET V14 dynamometer control system in order to adjust the engine's speed, load as well as exhaust back pressure valve position when the test is required. The operating envelope of the dynamometer is shown in Figure 3-7. The highly downsized boosted GDI engine used in this experimental study was capable of 120 kW/litre. This is equal to 48 kW of power for the single cylinder engine which has the capacity of 0.4 litres.

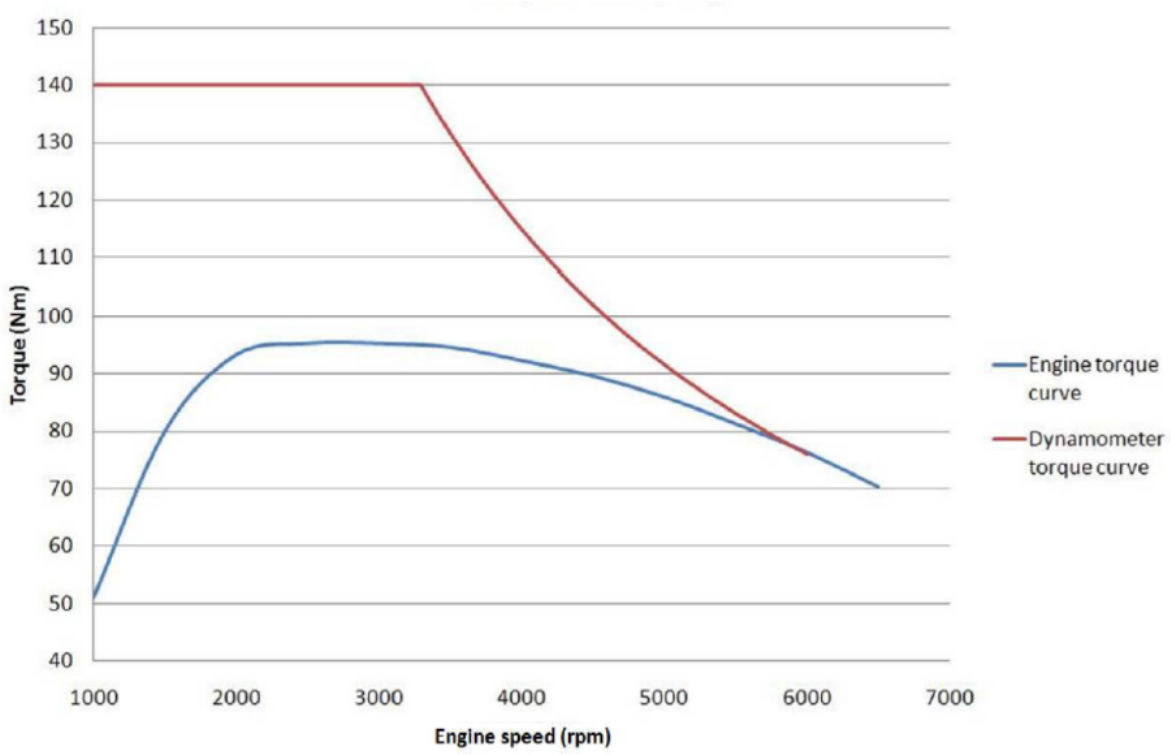

Figure 3-7 Comparison of the dynamometer torque curve and the engine torque curve

3.3 Engine Control Unit and Management System

An advanced engine management system (EMS) is used in order to control the engine more flexible and smoother. This system is consisting of the engine control unit (ECU), some sensors, actuators, a wiring harness which includes two looms as

well as a computer used to control the ETAS INCA V7.0 software for the ECU communication.

The ECU (shown in Figure 3-9) which is the main part of the engine management system is provided by MAHLE Powertrain. (the ECU is based on the AFT PROtroniC platform). In order to control the engine running, ECU needs to deliver enough processing power and supports sufficient input and output channels. What's more, this ECU has all the functions to operate a modern engine. Also, it has the ability of programming extra code for additional control if needed.

Figure 3-8 MAHLE Flexible engine control unit

The main channels of ECU to control the main engine parameter is shown in Table 3.3. All these data are also logged by ETAS INCA software for further data processing and analysis.

Table 3-3 The Main ECU inputs and outputs used during the experiments

Inputs(sensors)	Outputs(actuators)
Throttle position	Electronic Throttle body
Manifold pressure and temperature	

Intake cam position	Intake cam phaser
Exhaust cam position	Exhaust cam phaser
Exhaust lambda	PFI Injector
Boost pressure and temperature	Boost pressure regulator
Air mass flow meter	DI injector
High pressure fuel rail pressure	High pressure fuel pump
Crank angle sensor	
Knock sensor	Ignition coil
Coolant temperature	
Battery voltage	

The gasoline direct injection (GDI) injector is controlled by a Vemac driver which is also coupled to the ECU so that to control different injection strategies (rail pressure & injection timing). The ECU is controlled remotely by a Controller Area Network (CAN). The CAN is connected with an ETAS 571.3 interface card and the card is connected to the testbed PC. ETAS INCA V7.0 is used to communicate between the testbed computer and the ECU. Some important inputs are controlled by the dynamometer not ECU in order to prevent at the time testbed PC or ECU not working properly, the engine could still be controlled. These inputs consist of ignition, throttle position pedal, engine speed as well as the low-pressure fuel pump.

In this project, the exhaust lambda is close-loop controlled by MAHLE's flexible ECU. Boost pressure and exhaust back pressure (EBP) can also set to close loop control. A map of intake manifold pressure (MAP) and engine speed dictate the spark timing of the engine. The knocking indication is given by a knocking sensor which is couple with an oscilloscope and the knocking indication has no effect on the

control of spark timing. Moreover, the knocking sensor is situated at the end of the cylinder head so that its feedback cannot be accurate all the time.

3.4 Data Acquisition (DAQ) System and Instrumentation

A data acquisition system was built in order to display and record the important parameter received from several sensors and devices on the engine testbed. In a DAQ system there are two major components - DAQ hardware that collects information from the sensors, actuators, and devices on the testbed, and DAQ software that processes the signal, performs combustion analysis in real time, and also logs the raw combustion data as necessary.

3.4.1 Data Acquisition Hardware

The in-cylinder pressure, intake absolute pressure, exhaust absolute pressure, fuel flow rate, encoder clock, reference and torque channels are logged by a National Instruments (NI) USB-6353 card. This card is used for high-speed data logging, it has a maximum sampling speed of 1MS/s and can record up to 32 channels. The DAQ hardware is shown in Figure 3-10.

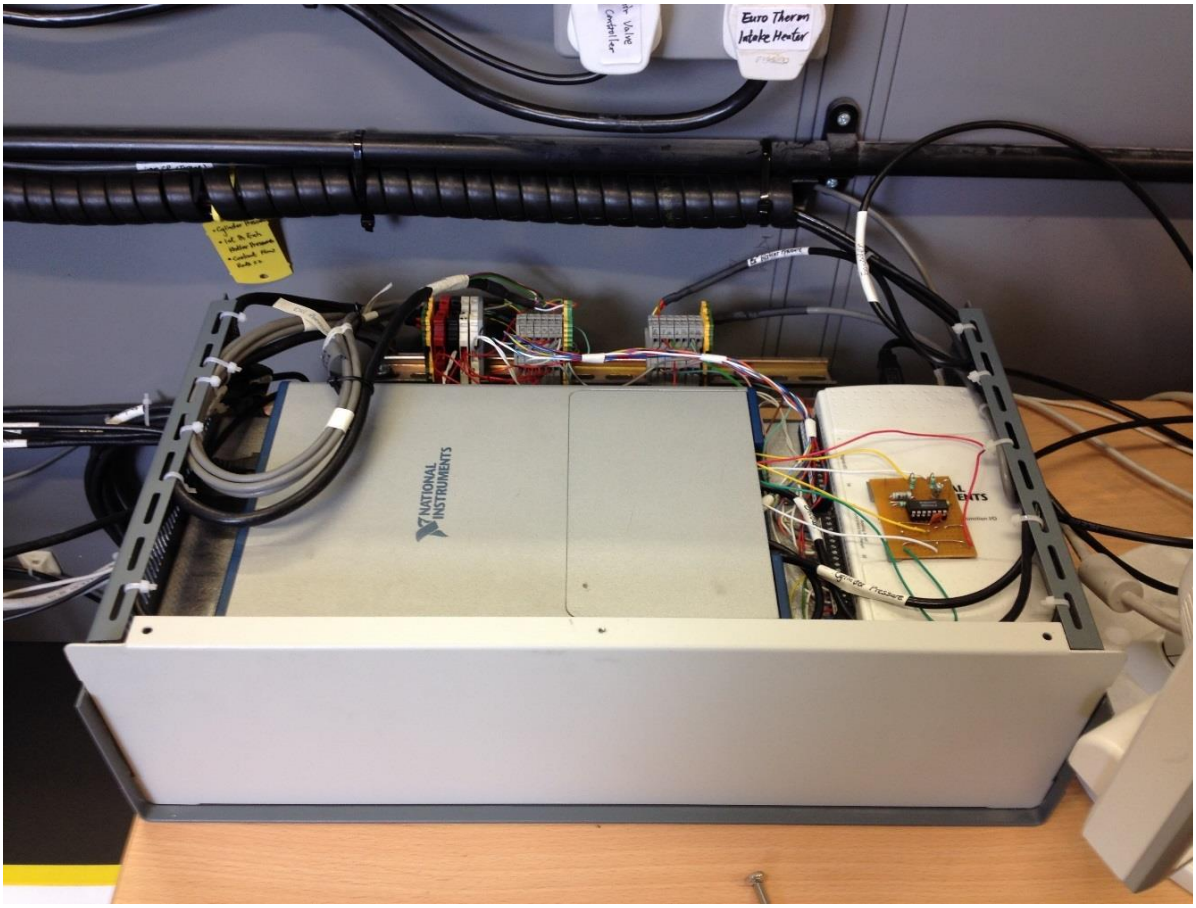

Figure 3-9 High and low-speed DAQ cards

An Encoder Technology EB58204040 shaft encoder with a 0.25 CAD resolution is used for the in-cylinder pressure analysis.

The signal from thermocouples, low-speed pressure sensors, coolant flow meters, coolant pressure, exhaust port temperature, exhaust manifold temperature, oil pressure, low-pressure fuel pump and average exhaust pressure are logged by another NI USB 6210 card for low-speed data recording. This card's sampling frequency is 0.5 Hz and it has 16 channels for data recording in this project.

All the PRT's data are recorded by an eDam-0915 acquisition card which can support maximum of 7 PRT inputs. A serial connection is used between this acquisition card and the testbed computer.

3.4.2 Data Acquisition Software (Combustion Analysis)

A Bespoke software called “Transient Combustion Analyser” receive all the data transferred from the DAQ cards, this software was developed at Brunel University by Dr. Yan Zhang [103]. The interface of this software is shown in Figure 3-11. All the signal received from the DAQ cards are processed by this software and it also shows information such as the temperature, pressure, flow rates, torque and engine speed. What’s more, a lot of real-time calculations are also done and displayed by this software such as engine power output, specific fuel consumption, combustion characteristics and heat release rate are performed based on the engine specifications. These data could also be recorded for hundreds of cycles for further analysis. In this project, 300 consecutive cycles’ raw data was recorded for combustion analysis. Heat release and combustion characteristics are analysed by one-zone heat release analysis. In the one-zone model the cylinder contents are considered as a single fluid - burned and unburned regions of gas in the combustion chamber were treated as one and modelled as homogeneous mixture, and in-cylinder pressure variations were related to energy released from the combustion of the fuel. This model allows to include heat transfer and gas flow phenomena in a simplified way [29,104].

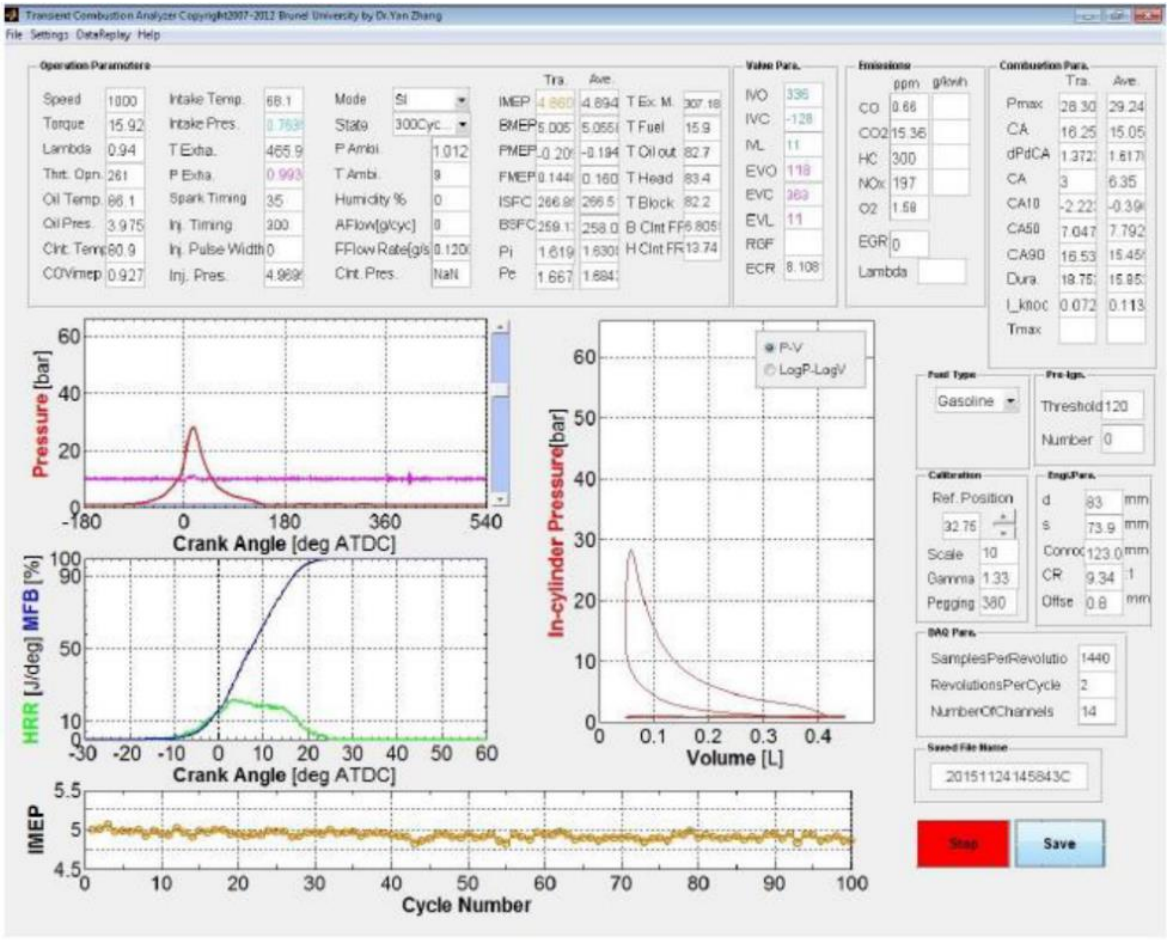

Figure 3-10 Transient Combustion Analyser user interface *[103]*

The P-V diagram of a four-stroke spark ignition engine at both fully open throttle and the part open throttle is shown in Figure 3-11. Equation 3-1 is used to calculate Net Indicated Mean Effective Pressure (NIMEP) which is the work received by the piston over one four-stroke cycle. (IMEP= area A- area B in Figure 3-11).

$$NIMEP = \int_{-180}^{540} \frac{P}{Vs} V(\dot{\varphi}) d\varphi \ \ (4-stroke)$$

Equation 3-1

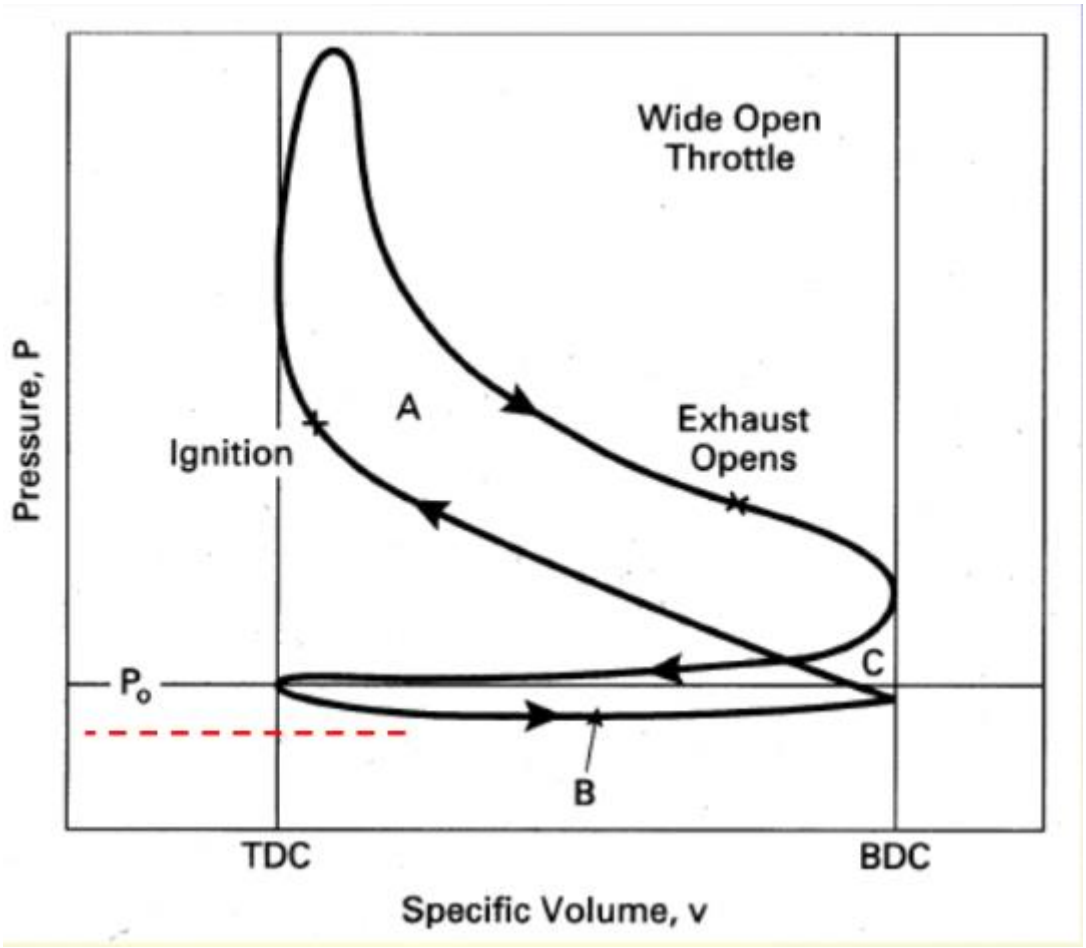

Figure 3-11 P-V diagrams of a four-stroke SI engine at full load *[104]*

What's more, Gross Indicated Mean Effective Pressure (GIMEP) is calculated by equation 3-2. The GIMEP correlates to the work delivered to the piston over the compression and combustion strokes only (area A + area C in Figure 3-16).

$$GIMEP = \int_{-180}^{180} \frac{P}{Vs} V(\dot{\varphi}) d\varphi$$

Equation 3-2

In those two equations, Vs is the displacement volume of the engine, P is real-time in-cylinder pressure, φ is the crank angle degree and $\dot{V}(\varphi)$ is the cylinder volume correspond to that crank angle degree.

The calculation of Pumping Mean Effective Pressure is shown in equation 3-3. In Figure 3-11, this parameter equal to the area of – (area B + area C).

$$PMEP = NIMEP - GIMEP$$

Equation 3-3

Net Indicated Fuel Conversion efficiency (IEffn), Gross Indicated Fuel Conversion Efficiency (IEffg) and Pumping Indicated Fuel Conversion Efficiency (IEffp) are calculated from NIMEP, GIMEP, PMEP and fuel mass flow (measured by fuel flow meter). The calculation processes are shown in Figure 3-12.

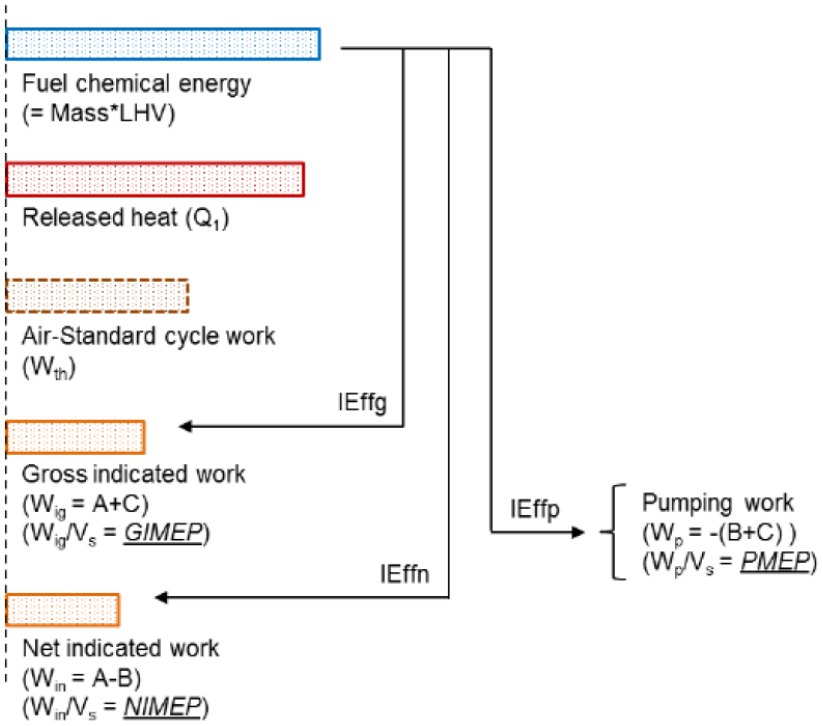

Figure 3-12 Indicated work and fuel conversion efficiencies

According to equation 3-3 and Figure 3-12, the relationship between IE_{ffn}, IE_{ffg} and IE_{ffp} can be written as equation 3-4, and it can be used for efficiency breakdown analysis.

$$IE_{ffn} = IE_{ffg} + IE_{ffp}$$

Equation 3-4

The in-cylinder pressure and knocking intensity which are updated on a cycle-to-cycle basis are also shown on the Yantech software. The high-speed DAQ card receives the in-cylinder pressure signal from the cylinder pressure transducer and then transfers it to Yantech directly. The definition of Knocking intensity (KI) is the difference between the real-time pressure measured by the in-cylinder pressure transducer and the predicted pressure. Equation 3-5 shows the way how predicted pressure is calculated. The predicted pressure of one point is the average pressure of the 10 points before and 10 points after this point.

$$Pn = \frac{\sum_{n-2.5}^{n+2.5} P}{21}$$

Equation 3-5

Figure 3-13 shows how the predicted pressure is calculated. The predicted pressure Pn at crank angle n is calculated by averaging the pressure from crank angle n-2.5 to n+2.5 with a gap of 0.25 CAD.

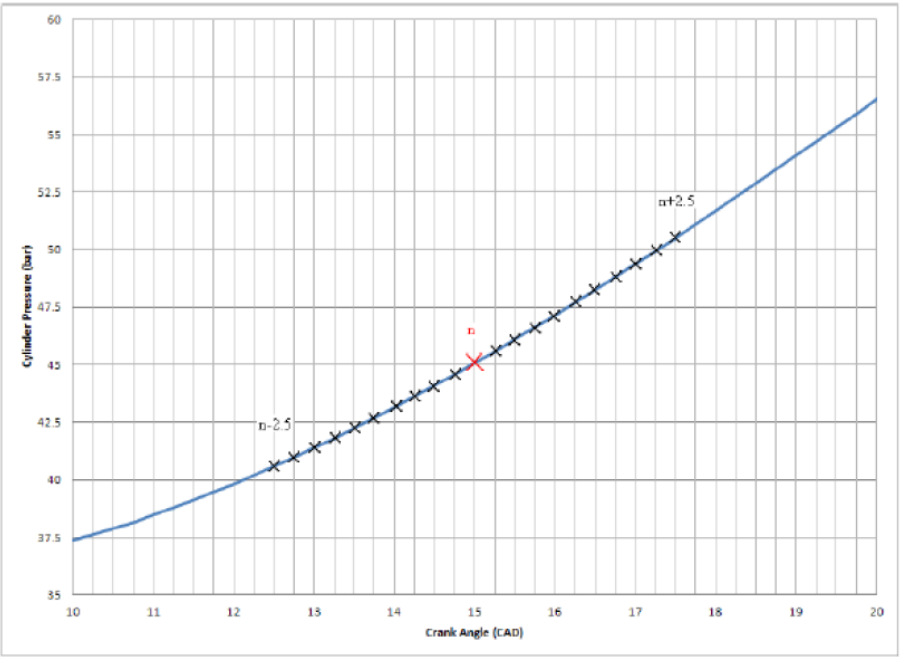

Figure 3-13 Band-Pass filtering calculation *[105]*

The knocking intensity can be calculated from the difference between real-time actual pressure (Pf, pressure feedback from the in-cylinder pressure transducer) and the predicted pressure (Pn), this process is shown in equation 3-6.

$$KI = Pf - Pn$$

Equation 3-6

3.4.3 Finding the Top Dead Centre

In this project, a lot of work has been done in order to increase the accuracy of the data. Since the in-cylinder pressure raw data is used for the calculation of indicated efficiency and combustion analysis, precise determination of the Top Dead centre (TDC) is required to achieve the accurate combustion analysis. A Kistler 2629C capacitive type TDC sensor is used to find the correct TDC position. This sensor's accuracy is 0.1 CAD but because the crank encoder's resolution is 0.25 CAD, the actual accuracy of the TDC sensor is 0.125 CAD. The toolbox of the TDC sensor is shown in Figure 3-15.

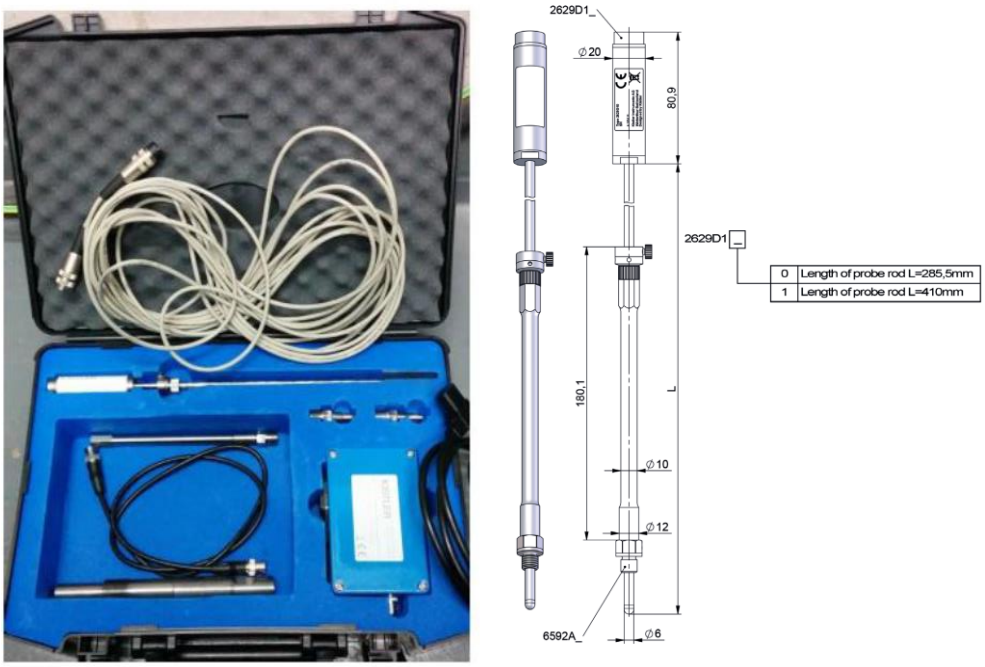

Figure 3-14 Kistler TDC sensor toolkit

Figure 3-17 shows the graphs generated by the TDC sensor. The mechanical TDC position is identified by the peak signal output in the figure. In Figure 3-16 a, there's a 20.1 CAD offset between the peak signal (TDC position) and zero crank angle degree. Figure 3-16 b shows that after inputting 20 CAD offset into the combustion analyser, the 0 CAD is now matched to the mechanical TDC position.

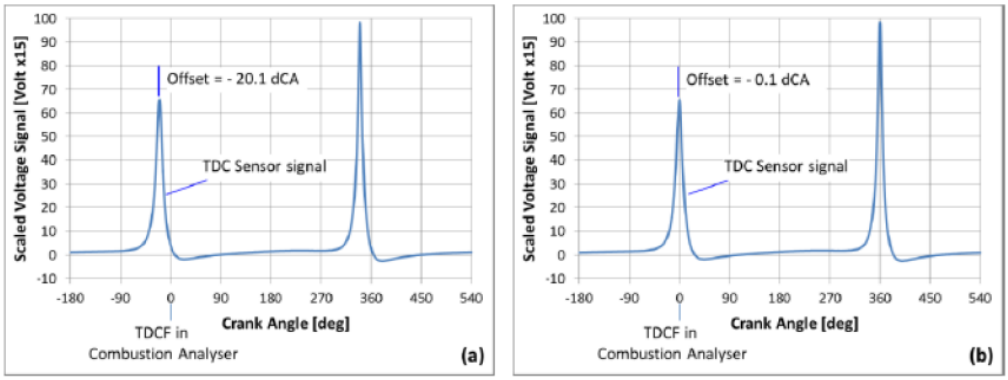

Figure 3-15 TDC determination in the combustion analyser

A motoring test is done after finding the correct mechanical TDC position. The engine speed is 1200 rpm and the log P- log V diagram is shown in Figure 3-17 a. From Figure 3-1 b, it is shown that there's a less than1 CAD offset between the peak in-cylinder pressure and the TDC points due to the heat loss [106].

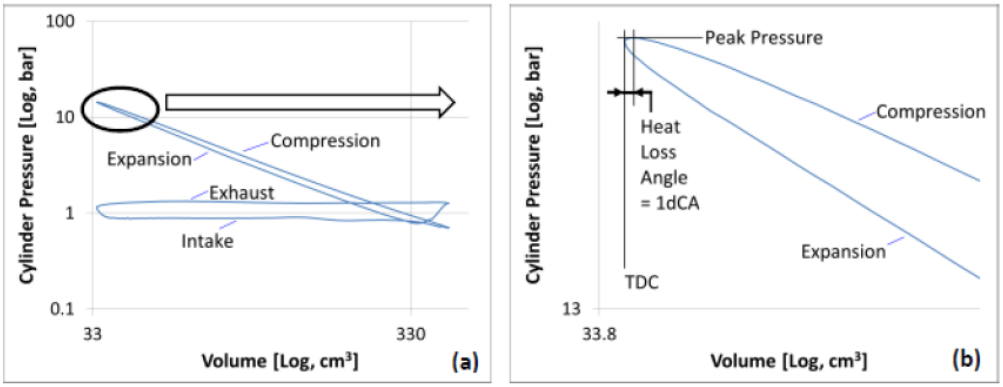

Figure 3-16 Log P-Log V diagram of engine motoring at 1200 RPM

3.4.4 In-cylinder Pressure Pegging

The piezoelectric pressure sensor is used to measure the in-cylinder pressure cannot provide absolute pressure. This sensor outputs a charge proportional to the pressure change. As a result of this, the transducer's output in the cycle needs to be referenced or pegged to a known pressure to calculate absolute pressure [106]. Cylinder pressure pegging can be achieved by several methods and are summarized by Randolph [107].

In this project, a revised method is used to pegging the in-cylinder pressure. The intake and exhaust pressure measured by piezoresistive absolute pressure sensors are used as reference pressure and it is shown in Figure 3-18.

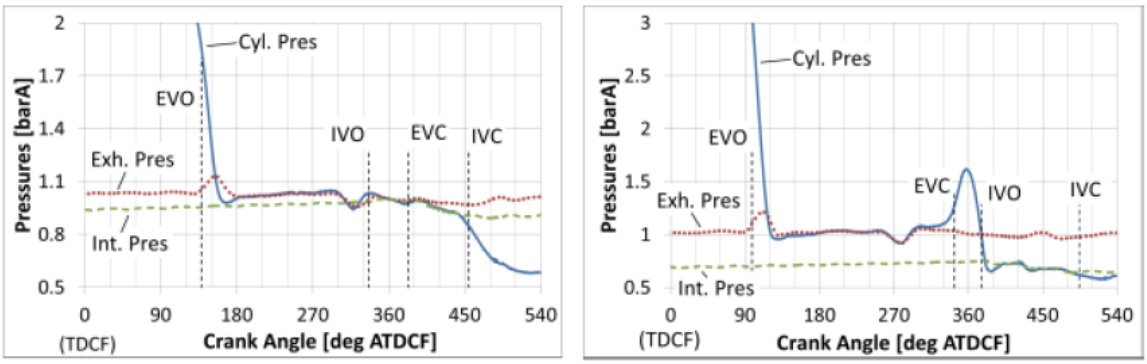

Figure 3-17 In-cylinder pressure pegging example

The Yantech combustion analyser allows the user to input the “pegging” value which means manually selecting a point on the exhaust pressure curve for in-cylinder pressure to be pegged to. By changing the “pegging” value, the in-cylinder pressure’s curve is moved upwards or downwards. After changing the pegging value at each test point, the in-cylinder pressure should match the exhaust pressure after exhaust valve close (EVC) and also match intake pressure before intake valve close (IVC). If the in-cylinder pressure cannot match either the intake pressure or exhaust pressure, intake pressure has a higher priority than exhaust.

3.5 Exhaust Emission Measurements

3.5.1 Emission Analysers

Several emission analysers are used to measure gaseous emissions in this project. A Horiba MEXA-554JE analyser is used to measure CO, CO_2 and O_2, a Signal Ambitech model 443 Chemiluminescent analyser is used to measure the NO_x and another Signal Rotork Analysis model 523 FID analyser is used to measure the HC. A combustion DMS 500 fast response particulate analyser is used to measure the particulate number and spectral size density. All the emission analysers are shown in Figure 3-19, Figure 3-20 and Figure 3-21. The specification of those emission analysers are shown in Tables 3.4, 3.5 and 3.6.

Figure 3-18 Horiba MEXA-554JE for CO, CO2, and O2 measurements

Figure 3-19 Signal Rotork Analysis model 523 FID analyser used for HC measurements (first unit at the top) and Signal Ambitech model 443 Chemiluminescent analysers used for NO/NOx measurements (bottom 3 units)

Table 3-4 Rotork Analysis model 523 FID analyser (HC) specifications

Range	0 - 10000 ppm
Pressure range	N/A, 3l/min sample fow
Temperature range	10 - 30 degC
Linearity	± 1%
Repeatability	± 1%
Size	19" rack mount
Construction	316 Stainless Steel
Warm up	40 mins
Output	Analogue display

Table 3-5 Signal Ambitech model 443 Chemiluminescent analyser (NO_x) specifications

Range	0 - 10000 ppm
Pressure range	N/A, 1.5l/min sample fow
Temperature range	10 - 30 degC
Linearity	± 1%
Repeatability	± 1%
Size	3 x 19" rack mount
Construction	316 Stainless Steel
Warm up	40 mins
Output	Analogue display

Figure 3-20 Cambustion DMS 500 fast response particulate analyzer

Table 3-6 Specifications of the Emission analysers

Device	Repeatability	Linearity	Sensitivity	Min detectable concentration/ range
NO_x analyser	±1% FS	±1% FS		0.2 ppm
HC analyser	±1% FS	±1% FS		0.1 ppm
DMS 500			1.0 ×103 (dN/dlogDp/cc)	5 nm- 1µm

3.5.2 Calculation of specific emission

The CO, HC and NO_x are recorded from the analyser as volume concentration in parts per million(ppm) and they should be converted to indicate specific emissions following the UN regulation number 49. The air humidity and water-in-fuel content are taken into account in order to obtain wet basis. But the NO_x's humidity and temperature correction are not applied in this project.

The main toxic exhaust gases CO, NO_x and HC are transferred from ppm to g/kWh by Equations 3-7, 3-8 and 3-9.

$$ISCO = \frac{u_{co}[CO]k_w\dot{m}_{exh}}{P_i}$$

Equation 3-7

$$ISNO_x = \frac{u_{NO_x}[NO_x]k_w\dot{m}_{exh}}{P_i}$$

Equation 3-8

$$SHC = \frac{u_{HC}[HC]k_w\dot{m}_{exh}}{P_i}$$

Equation 3-9

Where u_i is the molar mass fraction of each gas, $[i]$ is the gas concentration in ppm, k_w is the dry-to-wet correction factor, $\dot{m}_{exh}$ is the exhaust mass flow rate and P_i is the indicated power. These three parameters can be written as follows

$$\dot{m}_{exh} = \dot{m}_{air} + \dot{m}_{fuel}$$

Equation 3-10

$$\dot{m}_{air} = \dot{m}_{dry\ air} + \dot{m}_{humidity}$$

Equation 3-11

$$\dot{m}_{fuel} = \dot{m}_{actual\ fuel} + \dot{m}_{water}$$

Equation 3-12

The water saturation pressure polynomial estimation proposed by [108] is used to calculate the dry air and water (present in air)

$$SP = 604.8346 + 45.9058(T_a - 273.15) + 1.2444(T_a - 273.15)^2 + 0.03522481(T_a - 273.15)^3 + 0.0009322091(T_a - 273.15)^4 + 0.000004181281(T_a - 273.15)^5$$

Equation 3-13

In which T_a is the ambient temperature. Air humidity H_a can be calculated with RH (relative humidity) and p_a(ambient pressure).

$$H_a = \frac{6.211\ RH\ SP}{p_a - \frac{(RH\ SP)}{100}}$$

Equation 3-14

$$\dot{m}_{dry\ air} = \frac{\dot{m}_{air}}{1 + H_a}$$

Equation 3-15

$$\dot{m}_{humidity} = \dot{m}_{dry\ air} H_a$$

Equation 3-16

The term u_i is the tabulated ratio between the component and exhaust gas density, which varies according to the fuel used as depicted in Table 3.7.

Table 3-7 Raw gas molar mass fraction of the exhaust gases for gasoline

Exhaust Gas	μ_i(Gasoline)
CO	0.000966
NO_x	0.001587
THC	0.000499

The ambient condition, as well as the added water content from the fuel, may affect the dry-to-wet correction factor k_w which applied to CO and NO_x, the calculation is shown in equation 3-17.

$$k_w = 1.008\left(1 - \frac{1.2442H_t + 111.19W_{ALF}\left(\frac{\dot{m}_{fuel}}{\dot{m}_{dry\ air}}\right)}{773.4 + 1.2442H_t + 1000\left(\frac{\dot{m}_{fuel}}{\dot{m}_{dry\ air}}\right)k_f}\right)$$

Equation3-17

$$k_f = 0.05559W_{ALF} + 0.0070046W_{EPS}$$

Equation3-18

W_{ALF} stands for the hydrogen content in the fuel while W_{EPS} stands for the oxygen content. The total humidity factor H_t is used to replace the original air humidity factor to take into account the water-in-fuel added additional content.

$$H_t = H_a + H_f$$

Equation3-19

$$H_f = \dot{m}_{water}/\dot{m}_{dry\ air}$$

Equation3-20

Table 3-8 Properties of the fuels used for engine experiment

	Eu6 Gasoline RON95 E10	**Ethanol**	**Methanol**
Chemical Formula	$C_{5\text{-}10}H_{12\text{-}22}$	C_2H_5OH	CH_3OH
R.O.N	95.7	107	108
M.ON	86	89.5	88.7
Purity [%]	n/a	99.7	99.8
LHV (MJ/kg)	41.25	26.8	19.8
Hydrogen/Carbon Ratio	1.9	3	4
Oxygen/Carbon Ratio	0.0317	0.5	1
Stoichiometric AFR	13.9	9	6.5
Density [kg/L]	0.75	0.79	0.79

3.6 Testing and Data accuracy

The operating parameters and boundary conditions of the engine test are shown in Table 3.9.

Table 3-9 Engine operation parameters and boundary conditions

Variables	Control criteria
Engine load (NIMEP)	Controlled by throttle position (dynamometer) and boost pressure (ECU)
Engine speed	Controlled by the dynamometer (0-5400 rpm)
Intake cam timing (MOP)	Controlled by ECU
Exhaust cam timing (MOP)	Controlled by ECU
Exhaust lambda	Controlled by ECU (set as 1 unless lambda sweep or over-fuelling)
High pressure fuel rail	Controlled by ECU
Low pressure fuel rail	5 bar, controlled by pressure regulator
Injection strategy	Controlled by ECU
Spark timing	Controlled by ECU (Optimized by heat release rate at low and mid load, optimized by knock limited at high load)
Air humidity	Dry air, humidity<3%
Boost air temperature	40± 3°C

Coolant temperature	90± 3°C
Oil Temperature	90± 3°C
Low pressure fuel temperature	20± 3°C
Combustion stability	NIMEP_COV ≤ 3% (Except for cold spark sweep, NIMEP_COV ≤ 15%)
Fuel type	E10 Gasoline(baseline), Ethanol, Methanol
Exhaust back pressure	A butterfly valve is used for adjustment, Full opening represents the ambient back pressure

The quality of the recorded data has been carefully scrutinized in order to obtain the most accurate and consistent results possible. Before each testing, the following steps were taken to ensure accuracy and consistency. Before beginning the experimental work, the sensors, analysers, and other measurement devices were calibrated thoroughly, including flow meters, pressure sensors, temperature sensors, shaft encoders, and emission analysers. The calibration of these devices was also checked regularly so that adjustments could be made as necessary.

3.6.1 Cam Timings Validation

According to Figure 3-17, the pressure curves are used to validate the cam timings and valve timings as the precise control of cam timings are important for the experiments. Following the identification of valve timing on intake, exhaust and cylinder pressure curves, the controls are validated. Every time after the engine was rebuilt, this validation was performed.

3.6.2 In-Cylinder Pressure and Fuel Flow Measurements Validation

Since precise measurements of fuel flow and in-cylinder pressure are critical to the success of this project, this section describes the steps taken to ensure high levels of accuracy. DN01 1/24" sensor size was carefully selected for the Coriolis mass flow meter on this single cylinder engine. It measures a maximum flow rate of 20 kg/h and has a very small error of less than 0.1% in the range of flow rates of 1 kg/h to 20 kg/h (Figure 3-22). Generally, the error increases as the flow rate decrease especially when the flow rate is lower than 1kg/h, for example, when the flow rate is as low as 0.2 kg/h, the error might be less than 0.5 %. Before starting the engine testing, the flow meter was calibrated in the factory with the manufacturer and checked again in the university's laboratory.

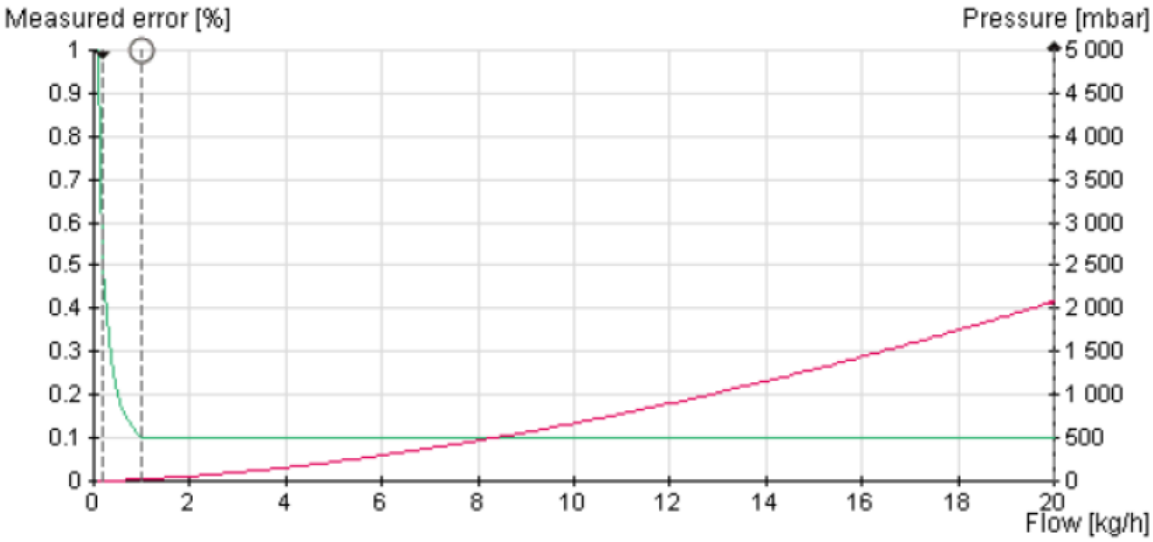

Figure 3-21 Measured error of Endress+Hauser Promass 83A01 flow meter

The Kistler pressure transducers were checked and calibrated, as necessary, on a dead weight tester in the laboratory, in order to minimize the error in measuring the indicated pressure. What's more, the Kistler intake and exhaust absolute pressure transducers and their amplifiers are checked and do zero adjustment every time before testing according to each day's local ambient pressure. In order to ensure

accurate readings, the exhaust pressure transducer was cleaned regularly in an ultrasonic bath in order to prevent the accumulation of carbon deposits. In addition, a motoring test is also conducted every time before starting the main experiments in order to check the health of both the engine and the measurement system (Table 3.10). With this test, the peak in-cylinder pressure (Pmax) and crank angle of Pmax (heat loss angle) can be determined in order to check the consistency. Besides the above measurements, the accuracy and consistency of all the other measurements are examined as well. Prior to each test, the emissions analysers were calibrated using pure air as the zero gas and the specific span gas.

3.6.3 Daily Engine Check Points

Daily motoring and firing tests were conducted and the results were recorded for further analysis before the experimental data were taken. As a first step, a zero log is recorded after daily calibrations are completed to ensure the baseline measurements in the correct range. After that, a daily motoring test is conducted and the results are recorded. Motoring tests are conducted after the engine has warmed up to the desired temperature before an analysis of the indicated measurements is undertaken. Finally, a firing test is conducted under a fixed operating condition for checking the engine's health and ensuring that the overall testing system is consistent. Table 3.10 shows the operating details for the motoring check and daily firing check.

Table 3-10 Motoring and firing daily checks settings

Variables	Motoring Check	Daily Firing Check
Engine Speed	1200 rpm	2000 rpm
Engine Load	Throttle fully open	NIMEP=4.6 bar
Intake and exhaust cam timing (MOP)	Minimum valve overlap	Minimum valve overlap
Exhaust Lambda		1
Rail pressure		100 bar
Injection Timing		Single early injection 320 CAD BTDCf
Spark timing		CA50= 8 CAD ATDCf
Air humidity	Dried air (humidity≤ 3%)	Dried air (humidity≤ 3%)
Boost air temperature	40±3°C (pre-throttle)	40±3°C (pre-throttle)
Coolant temperature	90±3°C	90±3°C
Oil temperature	90±3°C	90±3°C
Low pressure fuel temperature		20±3°C
Exhaust back pressure		Ambient EBP (0%)

Figure3-23 illustrates an example of the results of a daily motoring test. In preparation for the main tests, the peak in-cylinder pressure during engine operation as well as the angle of peak in-cylinder pressure are monitored every time.

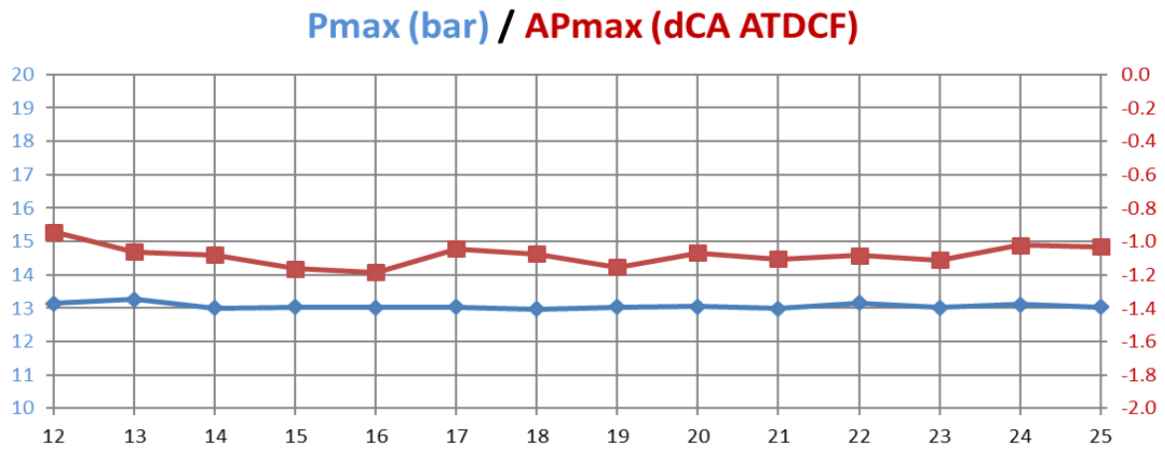

Figure 3-22 Peak cylinder pressure and its angle recorded for daily motoring checks (the x-axis shows the test days)

3.7 Summary

The single cylinder engine and all other testbed facilities which include DI fuelling system, intake/ exhaust system, coolant system, oil system, conditioning system as well as emission analysers are presented in this chapter. Also, the research methodology and the main equations used for combustion analyser software and emission are shown and discussed. What's more, the way how to increase the accuracy and consistency of the data are also discussed in this chapter.

4. Chapter Four: Spark Ignition Engine Operations with Ethanol and Methanol

4.1 Introduction

This chapter presents the spark ignition engine operations with ethanol and methanol and explains the difference between alcohol fuel (ethanol& methanol) and baseline (E10 gasoline) on the combustion performance, fuel efficiency and emissions. The test was carried out on a single-cylinder direct injection spark ignition engine at selected load points at 2000rpm, 3000rpm and 4000rpm. The overall air/ fuel ratio was maintained at the stoichiometric condition with the help of closed-loop exhaust lambda control at low and medium loads. At high loads, over-fuelling was used to keep the exhaust gas temperature under the maximum limit and avoid knocking combustion.

4.2 Results and Discussion

4.2.1 2000rpm Load Sweep

At 2000rpm, the engine load was varied from 2bar to 11bar IMEPs in order to explore the difference between these three fuels at low speed. For these three fuels, the same injection timing (i.e. the start of injection) was used for each load. It was fixed at 320 Deg $BTDC_f$ from 2bar to 6.9bar, then it was retarded to 318 Deg $BTDC_f$ at 8.9bar and 312 Deg $BTDC_f$ at 11bar. The rail pressure was also kept the same for these fuels and the rail pressure increase from 55bar to 145bar with the increase of load. With the load increase, more fuel was injected into the combustion chamber since the combustion is stoichiometric. Gasoline's fuel flow rate was increased from 0.44kg/h to 1.75kg/h, the flow rate of ethanol was increased from 0.62kg/h to 2.49kg/h and that of methanol was increased from 0.82kg/h to 3.26kg/h. The gasoline baseline boundary conditions (injection timing, rail pressure) were kept the same with the data from MAHLE's DI3 engine. Due to the lower heating value of

methanol is lower than ethanol than gasoline, that's the reason the fuel flow rate is the highest of them.

The spark timing, brake thermal efficiency, CA50, combustion duration as well as knocking intensity are shown in Figure 4-1.

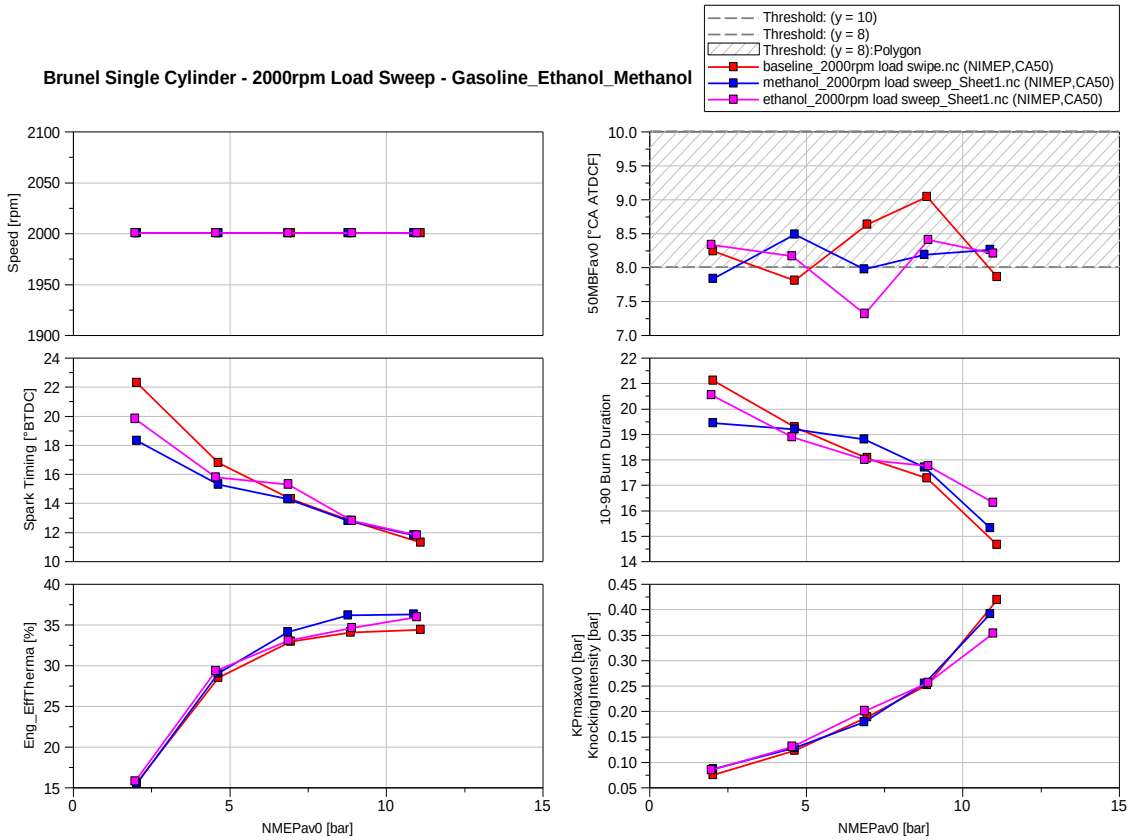

Figure 4-1 Combustion characteristics of 2000rpm load sweep

For all three fuels, the MBT (Minimum ignition advance for Best Torque) spark timings were achieved and retarded with increasing load. As shown in Figure 4-1, all test point's CA 50s are around 8 Deg $ATDC_f$ at MBT timing. Since the CA50 is controlled at 8 Deg, the burn duration becomes shorter with the increasing load as the flame speed increases. The spark timing of these fuels advanced from 18.2 Deg BTDC (methanol), 19.7 Deg BTDC (ethanol), 22.3 Deg BTDC (gasoline) to 11.8 Deg BTDC as a result of this. The laminar flame speed of methanol is faster than ethanol and gasoline and the CA50 is controlled at 8 Deg so that the spark timing of

methanol is more advanced than ethanol and gasoline at 2bar and 4bar. This phenomenon can also be found in CA10, and CA10-50 (shown in Figure 4-2). The brake thermal efficiency (BTE) of the three fuels increases with the load. The maximum BTE of them are all at 11bar (gasoline 34.33%, ethanol 35.86%, methanol 36.17%). The BTE of methanol and ethanol was increased by 4.5% and 5.5% compared to gasoline. The knocking intensity becomes higher with load increase since the in-cylinder pressure increases result in bigger difference between real time in-cylinder pressure and the predicted in-cylinder pressure, but there wasn't any knocking happen during the 2000rpm load sweep. The highest KI for these three fuels are at 11bar IMEP but all of them are lower than 1 which is the KI limit.

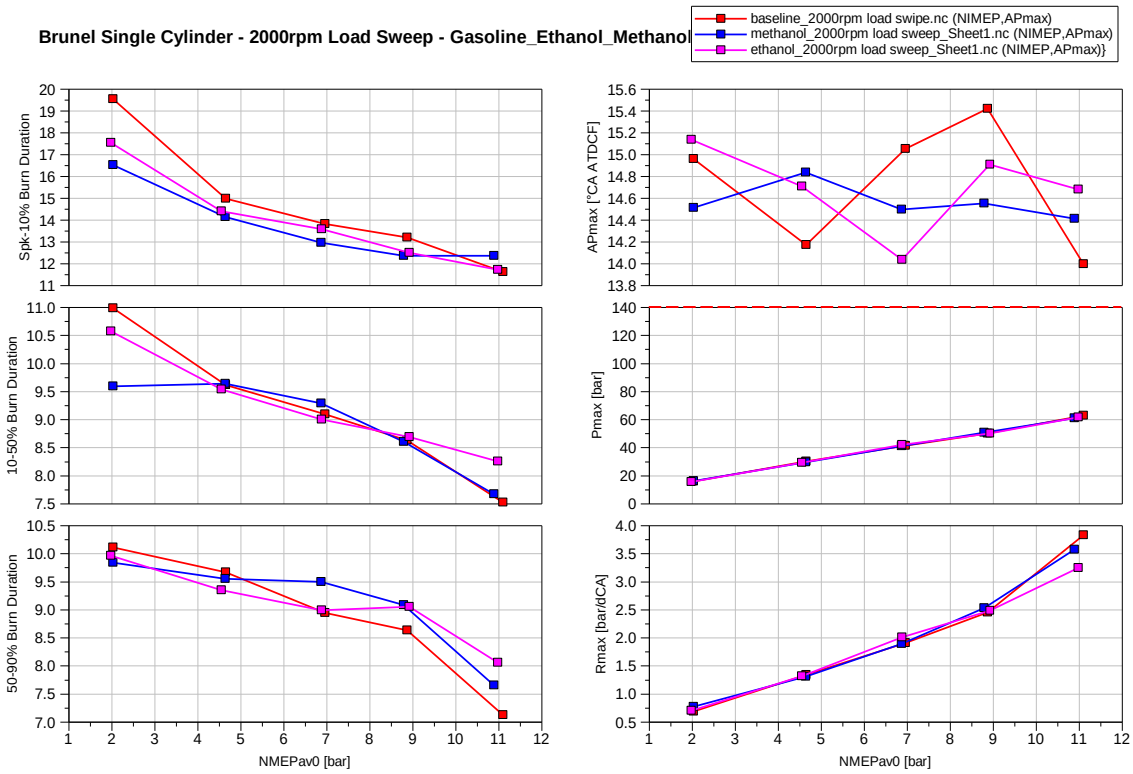

Figure 4-2 Combustion phasing, Pmax and Rmax

The combustion phasing results are shown in Figure 4-2. CA10, CA10-50, and CA50-90 all decrease with the increase of load because of the faster flame speed at elevated temperature. The higher laminar flame speed of methanol causes shorter CA10 and CA10-50 than methanol and gasoline. At 11bar IMEP, the CA10-50 of

gasoline is shorter as a result of the CA50 of gasoline is more advanced than methanol and ethanol. The peak in-cylinder pressure crank angle (Pmax) for these fuels are around 14.6 Deg $ATDC_f$. The peak cylinder pressure of gasoline, methanol and ethanol increases from 15bar to 60 bar linearly with the load. The maximum rate of pressure rise (Rmax) of these fuels increase similarly from 0.76bar/dCA to 2.5bar/dCA with the load increase from 2bar to 8.9bar. At 11.2bar, the Rmax of gasoline is 3.82bar/dCA which is higher than methanol's Rmax (3.56bar/dCA) and ethanol's (3.23bar/dCA) because the burn duration of gasoline at 11.2bar is shorter than methanol and ethanol, with the same in-cylinder peak pressure.

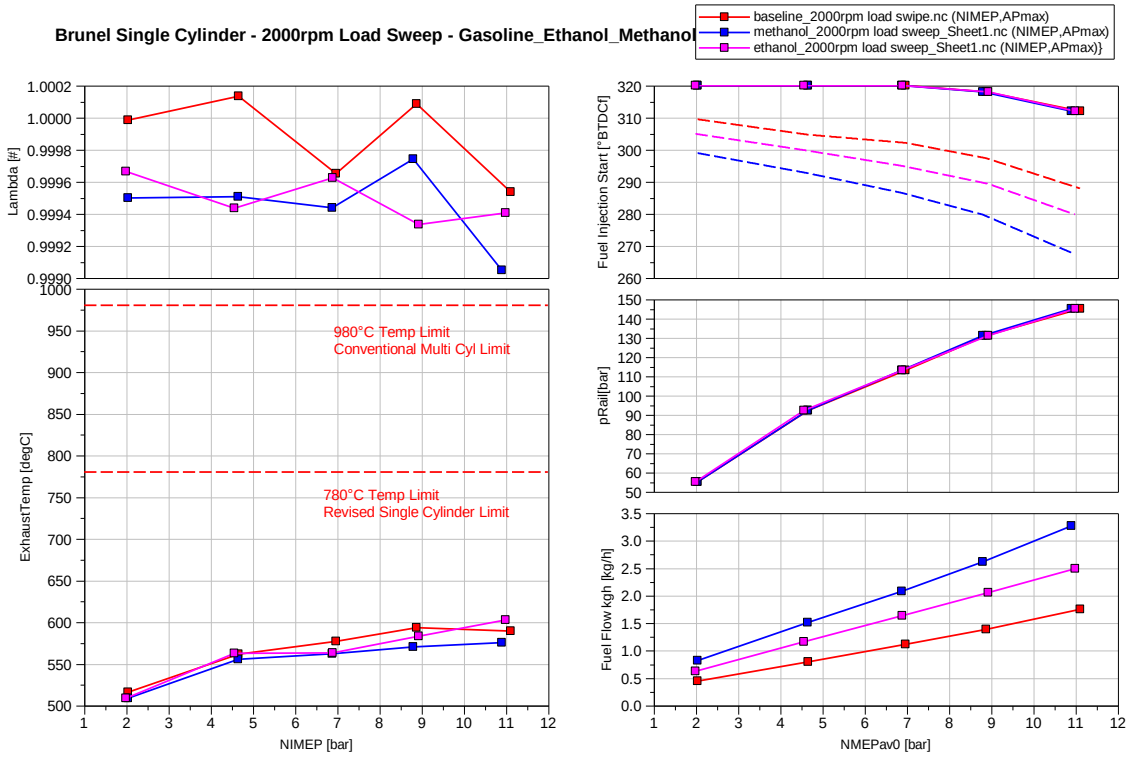

Figure 4-3 Lambda, TExh and injection parameters

From Figure 4-3, it's easy to find that all the test points' lambda which was controlled by the engine's ECU is kept very close to 1. The exhaust temperature increases with load from 515°C (gasoline), 508°C (methanol), 508°C (ethanol) to 589°C (gasoline), 575°C (methanol) 602°C (ethanol), respectively. Since all these test points knocking intensity is under 1 so spark retarded is not applied. From 2bar to 8.9bar, the

exhaust gas temperature of ethanol and methanol is lower than gasoline since their evaporation enthalpy is higher than gasoline, charge cooling effect causes the in-cylinder temperature decrease thus the exhaust gas temperature of ethanol and methanol are lower than gasoline. At 11.2bar, the exhaust gas temperature of ethanol is higher than the other two fuels since its burn duration is longer than gasoline and methanol. The injection start, rail pressure and fuel flow rate of gasoline, ethanol and methanol are also shown in Figure 4-3. Since Methanol's lower heating value is lower than ethanol and gasoline, methanol has the most retarded injection end timing and the highest fuel flow rate. The dashed line shown in Figure 4-3 shows the injection end timing of gasoline, ethanol and methanol.

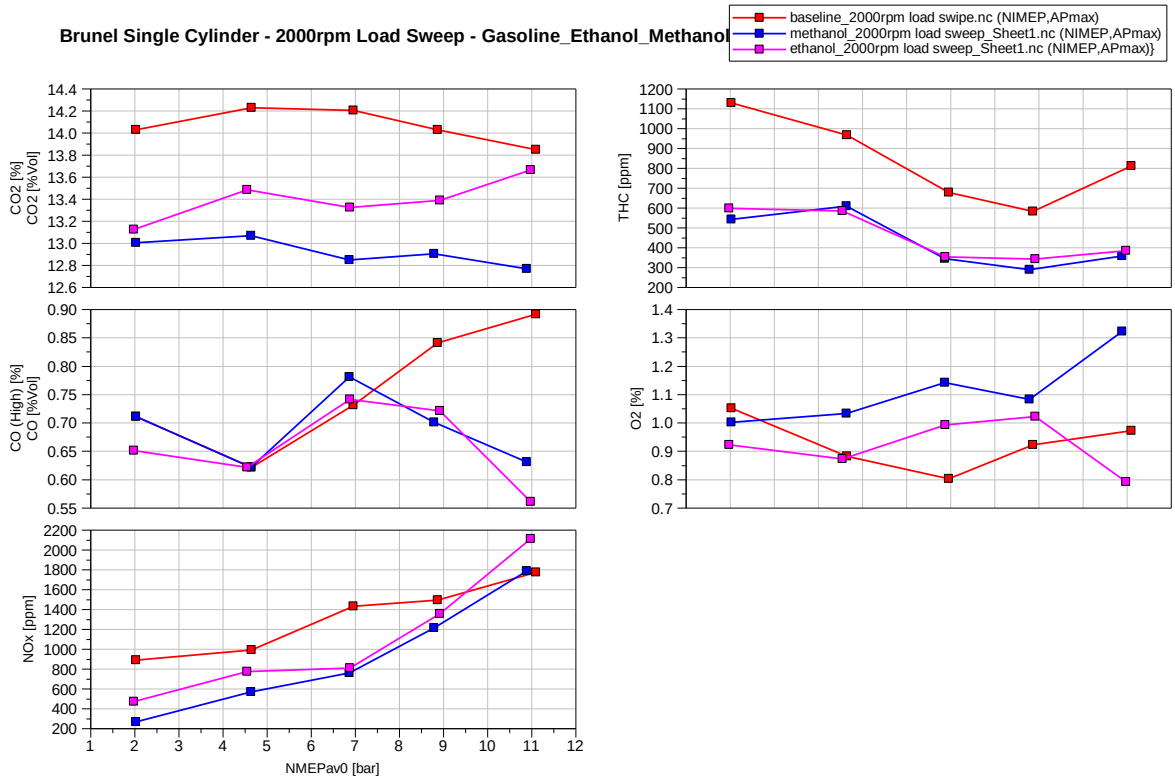

Figure 4-4 Emissions of 2000rpm load sweep

The exhaust data are shown in Figure 4-4. The CO_2 released by gasoline increases from 14.02%Vol to 14.22%vol with the load increase from 2bar to 4.6bar then keep the same at 6.9bar. It drops from 14.2%vol to 13.84%vol with the load increase to 11bar. The CO_2 released by ethanol increases from 13.12%vol to 13.48% from 2bar to 4.6bar then decreases to 13.32%vol at 6bar and increases to 13.66%vol from 6.9bar to 11bar. There is a slight drop of the CO_2 from methanol, it drops from

13%vol to 12.76%vol from 2bar to 11bar. When converted to energy-specific emissions in (gCO_2/MJ), methanol leads to 7% lower specific CO_2 emissions than gasoline.

The amount of CO varies only slightly since the lambda of all these test points was kept at 1. The CO emission by gasoline decreases from 0.71%vol to 0.62%vol firstly, then it increases to 0.89%vol from 4.6bar to 11bar. For ethanol, its CO drops from 0.65%vol to 0.62%vol from 2bar to 4bar, then it increases to 0.74%vol at 6.9bar then continue drops to 0.56%vol from 6.9bar to 11bar. The CO released by methanol has the same trends as ethanol. It drops from 0.71%vol to 0.62%vol then increase to 0.78%vol from 2bar to 6.9bar. After that, it decreases to 0.63%vol from 6.9bar to 11bar. The amount of CO in the exhaust gas is mainly affected by Lambda (shown in Figure 4-3).

The NO_x released by gasoline, ethanol and methanol increases with the increase of load as the combustion temperature increases. For the NO_x released by gasoline, it increases from 882ppm to 1768ppm with the increase in load. The NO_x from ethanol increases from 463ppm to 2103ppm and that of methanol increase from 262ppm to 1780ppm.

THC decreased slightly with the load as further oxidation can take place in the hotter exhaust gas and the THC released by methanol and ethanol is lower than gasoline.

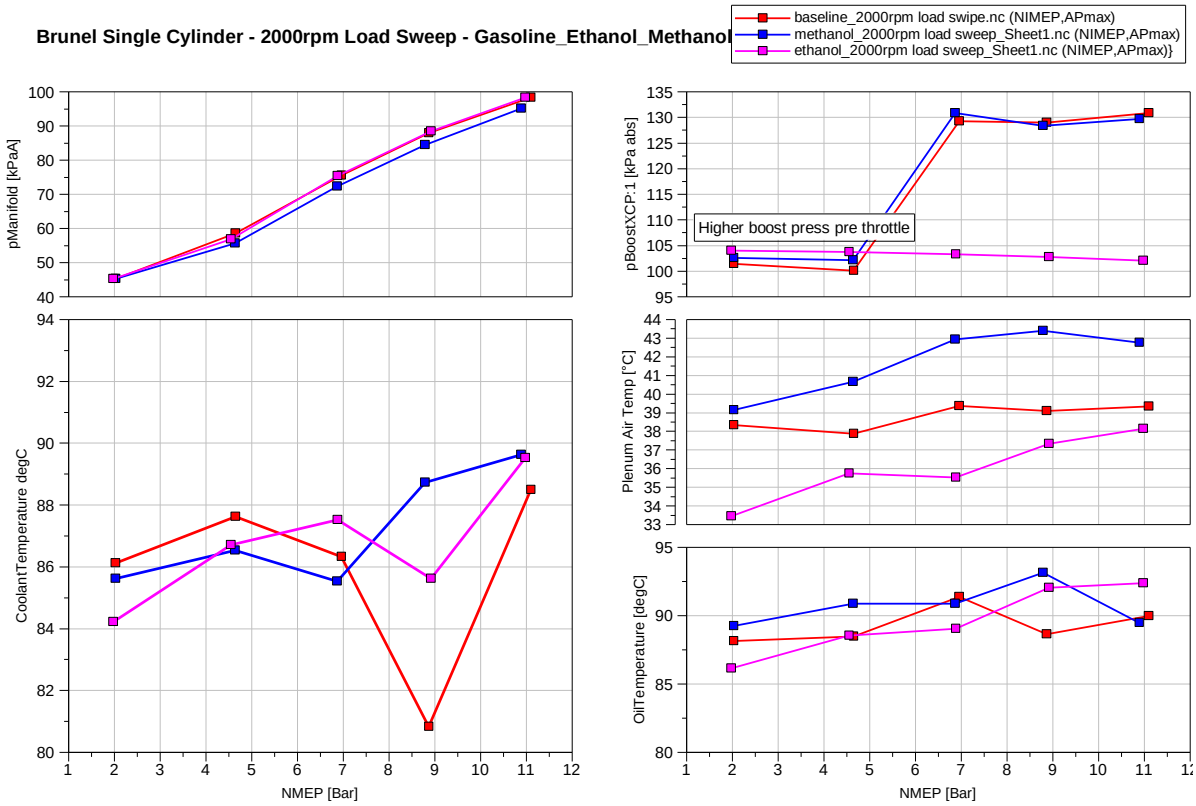

Figure 4-5 Engine conditioning pressure and temperature

Most boundary conditions of this test are shown in Figure 4-5. The manifold pressure of different fuels has small difference with each other, it increases from 46kPa to 97kPa as the load is increased. The coolant and oil temperature are kept around 90°C. The Intake air temperature are kept around 40°C.

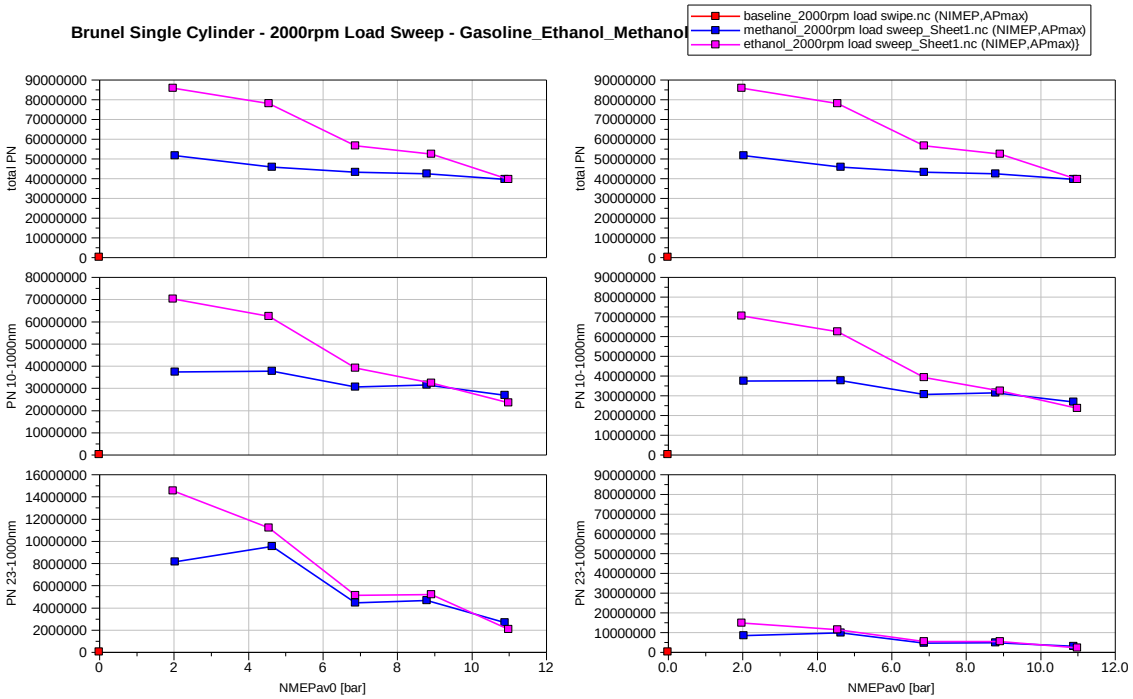

Figure 4-6 Particle numbers of methanol and Ethanol

Due to the equipment breakdown, the particle number's data of gasoline was not collected. Figure 4-6 shows the total particle numbers, PN 23-1000nm (Euro 5 regulation) and PN 10-1000nm (Euro 6 regulation) for ethanol and methanol operations. The total particle number of ethanol drops from 8.6e7 to 5e7 with the increase of load while the total PN of methanol decreases slower than ethanol, dropping from 5.2e7 to 5e7. The number of particles from 10-1000nm of ethanol drops from 7e7 to 2.4e7 and methanol drops from 3.8e7 to 2.7e7.

The particle number is mainly affected by injection timing and rail pressure which are shown in Figure 4-3. From 2bar to 11bar IMEP, the start of injection is retarded from 320 Deg $BTDC_f$ to 310 Deg $BTDC_f$. Early injection could lead to fuel impingement on combustion chamber surfaces and hence pool fires—a source of high levels of PM emissions [109]. The rail pressure was increased from 55 bar to 90 bar and increased fuel injection pressure enhances the air-fuel mixing; at higher injection pressures, fuel droplets become smaller which leads to better evaporation. The boiling point of methanol (64.7°C) is lower than that of ethanol (78.4°C) so that methanol could lead to less liquid impingement on the piston, and that's why the particle numbers of methanol is lower than ethanol at the same injection timing and rail pressure. [109]

Ethanol's PN drops quickly at 6.9bar since the spark timing is slightly advanced at this point.

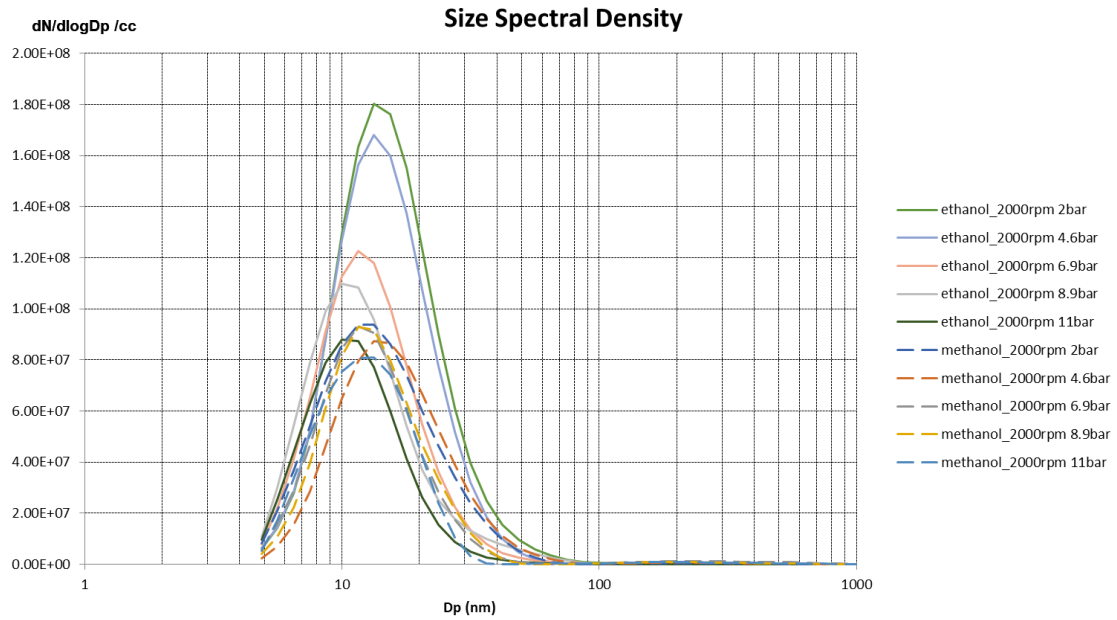

Figure 4-7 2000rpm load sweep particle size spectral size density

Figure 4-7 shows the particle size spectral density distribution. It can be seen that the size spectral density curve of each test point is peaked around 10-20nm, which means that most particles are in nucleation mode and there are limited soot emissions in accumulation mode. The particle released by ethanol and methanol's size is around 5nm to 60 nm.

4.2.2 3000rpm Load Sweep

3000rpm load sweep for gasoline, ethanol and methanol were done from 2bar to 28bar IMEP in order to explore the difference between these three fuels at a medium speed and higher load condition. The maximum load of 28bar was imposed by the severe knocking combustion of gasoline. For ethanol and methanol, longer combustion duration caused misfire after 28bar which also couldn't be controlled.

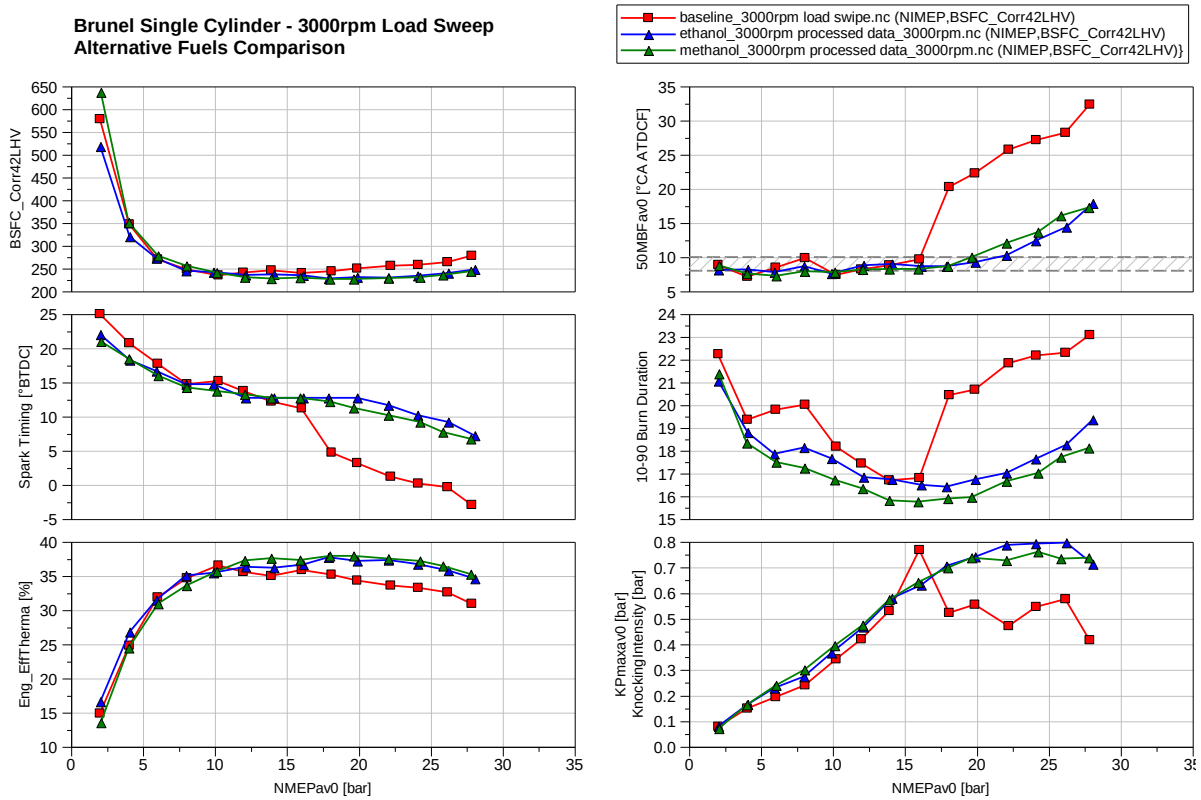

Figure 4-8 Combustion characteristic of 3000rpm load sweep

For 3000 rpm load sweep, most test points were opearated with the MBT timing set by means of CA50 at 8 Deg $ATDC_f$. For the test points where knocking intensity was greater than 1, the spark timing was retarded. The highest BSFC of gasoline is 577.7g/kWh at 2bar then it decreases to 234g/kWh at 10bar IMEP. after that, gasoline's BSFC increases to 277 g/kWh at 28bar IMEP. The BSFC trends of ethanol and methanol are similar to the gasoline one. The BSFC of ethanol

decreases from 517 g/kWh at 2bar IMEP to 227 g/kWh at 18bar IMEP then increase to 247 g/kWh at 28bar IMEP. For methanol, its BSFC drops from 636 g/kWh at 2bar IMEP to 226 g/kWh at 18bar IMEP and 20bar IMEP then increase to 243 g/kWh at 28bar IMEP. The spark timing of gasoline is retarded slowly from 24.9Deg BTDC to 11.1 Deg BTDC at 16bar IMEP. But after 16bar, the spark timing of gasoline was retarded from 11.1 Deg BTDC to -2.5 Deg BTDC quickly because of knocking intensity was too high which is also shown in Figure 4-8. For methanol and ethanol, their spark timings are also retarded with load from 2bar to 16bar IMEP. After 16bar IMEP, the spark timing is delayed to keep the Pmax below 120 bar limit and the Rmax (pressure rise rate) at 6. The knocking intensities for ethanol and methanol are always under limit even at higher load because their anti-knock characteristic is far better than gasoline. The brake thermal efficiency (BTE) for these fuels could also be found in Figure 4-8. The BTE of gasoline increase from 14.83% to 36.5% at 10bar IMEP then decreases to 30.9% from 10bar IMEP to 28bar because combustion duration increases. The BTE of ethanol increases from 16.5% to 37.7% at 18bar IMEP then decrease to 34.6% at 28bar IMEP because of the engine's limit. The BTE of methanol has the same trends as ethanol, it increases from 13.46% to 37.9% at 18bar IMEP and 20bar IMEP then decrease to 35.3%. The maximum BTE of ethanol and methanol increase by 3.2% and 3.8% compared with gasoline. The CA50 is also shown in Figure 4-8. Before 16bar IMEP, the CA50 for gasoline, ethanol and methanol are kept at 8 Deg ATDC. After 16bar, the CA50 of gasoline is retarded to 32 Deg ATDC at 28bar IMEP due to knocking, and the CA50 of ethanol and methanol are retarded to 17.3 Deg ATDC and 17.8 Deg ATDC because of engine limit. The combustion duration of gasoline, ethanol and methanol are shown in Figure 4-8. The combustion duration of gasoline decreases from 22.2 crank angle degree (CAD) to 16.8 CAD at 16bar IMEP then increase to 23.1 CAD at 28bar IMEP. At 6bar IMEP and 8bar IMEP, their CA50 are slightly retarded which cause their combustion duration longer. The combustion duration of ethanol decreases from 21 CAD to 16.4 CAD then increases to 19.3 CAD while that of methanol decreases from 21.4 CAD to 15.7 CAD then increases to 18.1 CAD.

Overall, the combustion duration of methanol is shorter than ethanol and gasoline. Below 16bar IMEP, gasoline has the longest combustion duration. After 16bar IMEP, gasoline's combustion duration increases fast as a result of knocking. The

combustion duration of ethanol and methanol also increase because of the retarded spark timing to keep the peak in-cylinder pressure and maximum pressure rise rate limits of this engine. The knocking intensity (KI) is shown in the last diagram of Figure 4-8. The knocking intensity of gasoline increase from 0.08 to 0.76 with the load increase from 2 to 16bar IMEP, then KI keeps stable at around 0.55. Ethanol's KI increase from 0.08 to 0.79 at 22, 24, and 26bar then drops to 0.71. In addition, methanol's KI increases from 0.07 to 0.76 at 24bar IMEP then decreases to 0.74.

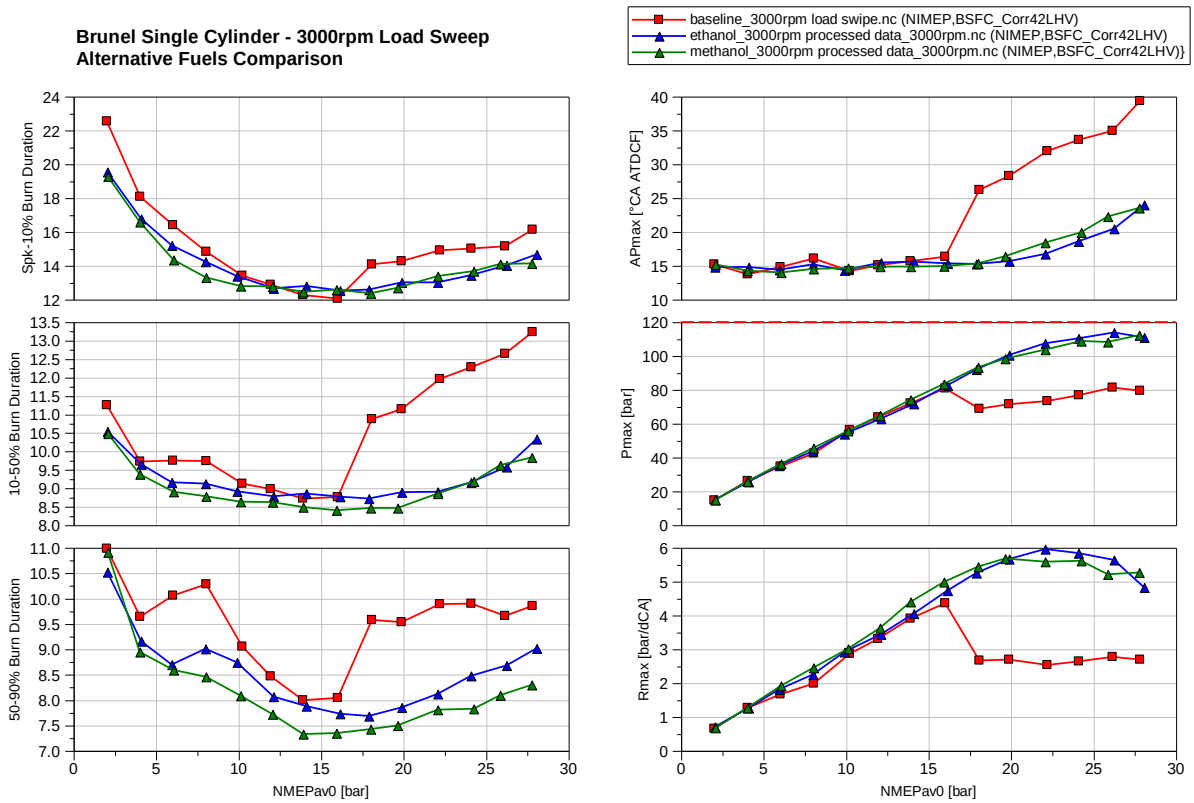

Figure 4-9 Combustion phasing, Pmax and Rmax

The different combustion phasings are shown in Figure 4-9. From 2bar to 16bar IMEP, the duration between the spark timing and CA10 of gasoline decreases from 22.5 CAD to 12 CAD as the flame speed increases with higher temperature at higher load. After that, the CA10 increases from 12CAD to 16.1 CAD because the spark timing is retarded to avoid knocking. Ethanol and methanol's CA10 decrease from 19.5CAD to 12.5 CAD then increase to 14.7 CAD. The CA10-50 of gasoline decreases from 11.2CAD to 8.7CAD at 14bar and 16bar IMEP, then increase to

13.2CAD between 16bar and 28bar IMEP. The CA10-50 of ethanol drops from 10.5CAD to 8.7CAD from 2bar to 16bar IMEP, then it increases to 10.3CAD with the load increase to 28bar IMEP. Methanol's CA10-50 has similar trends with ethanol, it decreases from 10.5CAD to 8.5CAD then increases to 9.8CAD. CA50-90 is also shown in Figure 4-9. Gasoline's CA50-90 drops from 11CAD to 9.6CAD at 4bar IMEP then increase to 10.3CAD from 4-8bar IMEP. After that, it decreases from 10.3CAD to 8CAD from 8bar to 16bar IMEP. In addition, it keeps around 9.7CAD during the load from 18bar to 28bar IMEP. Between 2 to 6bar IMEP, the CA50-90 of ethanol decreases from 10.5CAD to 8.7CAD and then slightly increases to 9.0CAD. After that, it drops to 7.9CAD at 18bar IMEP then increases to 9.0CAD at 28bar IMEP. Methanol's 50%-90% burn duration decreases from 10.9CAD to 12.4CAD at 14bar then increases to 8.3CAD at 28bar. Before 16bar, the CA10, CA10-50, and CA50-90 of ethanol and methanol are faster than gasoline since alcohol fuel's burn speed is faster than gasoline. After 16bar, as a result of knocking, gasoline needs to retard the spark timing more than alcohol fuel and got longer combustion duration. The maximum in-cylinder pressure correspond to crank angle (APmax) is shown in figure 4-9. Before 16bar, APmax of gasoline, ethanol and methanol are similar to each other around 15CAD $ATDC_f$. After 16bar, the APmax of gasoline increases to 29.3 CAD $ATDC_f$. The APmax of ethanol and methanol increases from 15 CAD $ATDC_f$ to 23.9 CAD $ATDC_f$. Between 18bar and 26bar, the APmax of methanol is more retarded than that of ethanol since the spark timing of ethanol is more advanced than methanol. The peak cylinder pressure (P_{max}) and peak pressure rise rate (R_{max}) are also shown in Figure 4-9. The P_{max} of gasoline increases from 14.4bar to 80.7bar which happens at 16bar, then it keeps around 75bar because the spark timing is retarded very close even after the engine's top dead centre. The P_{max} of ethanol and methanol increases from 14.7bar to 113.6bar from the load 2bar to 26bar then it drops to 110.7bar. The limit of P_{max} is 120bar and the maximum R_{max} is 6bar/dCA so that even the knock intensity of ethanol and methanol is under the limit, their spark timing also needed to be retarded after 16bar. That's the reason why the combustion duration of ethanol and methanol are increasing after 16bar. Since the spark timing of gasoline is retarded more than ethanol and methanol, no attention was paid to P_{max} and R_{max} of gasoline.

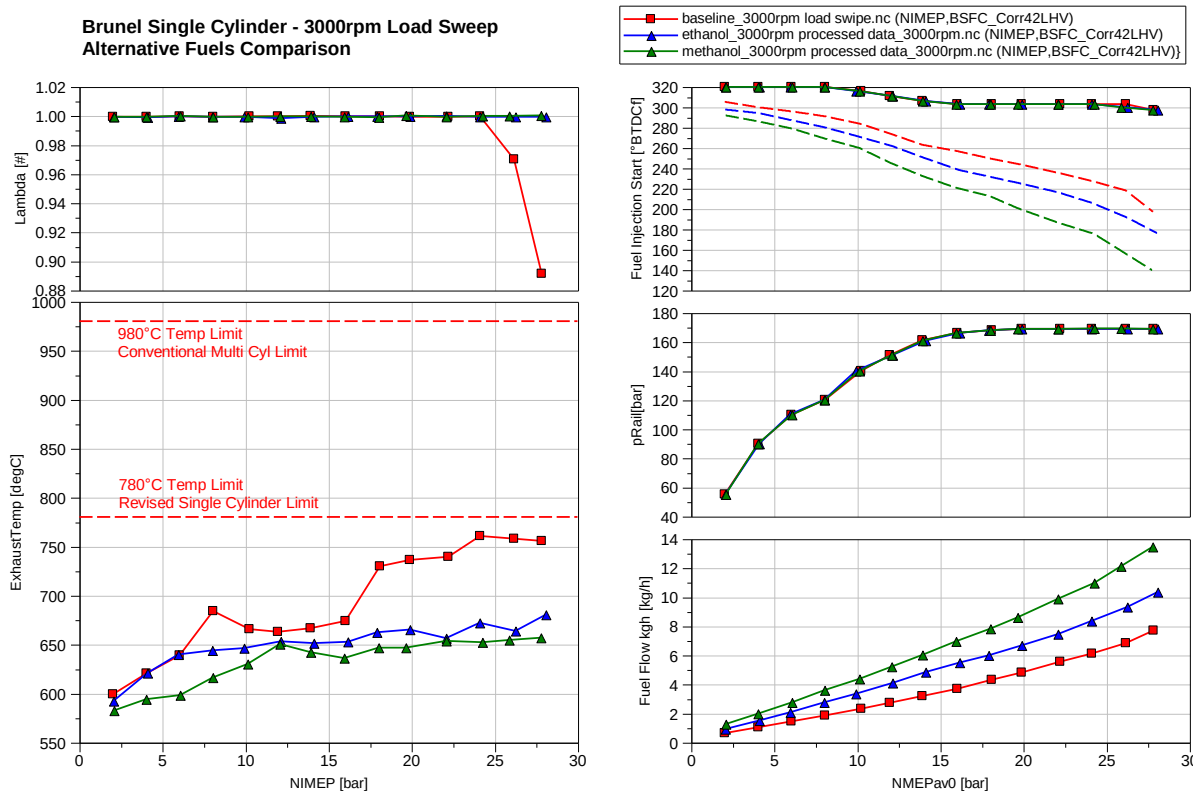

Figure 4-10 Lambda, TExh and injection parameters

The lambda values of all test points are shown in Figure 4-10. The lambda of gasoline was kept at 1 before 26bar IMEP. It is decreased to 0.97 at 26bar IMEP and 0.89 at 28bar IMEP to reduce the exhaust gas temperature. For ethanol and methanol, their lambda is kept at 1 even their combustion duration increases after 16bar IMEP, their exhaust temperature (shown in figure 4-10) is still under the limit of 780°C so that no over-fuelling is needed. The exhaust gas temperature of gasoline increases from 599°C to 684°C from 2 bar to 8bar IMEP, then it drops to around 670°C from 10bar to 16bar IMEP. The reason why exhaust gas temperature at 8bar is higher is because the spark timing at 8bar IMEP is slightly retarded which increases the combustion duration. After that, it increases fast because its spark timing is retarded which causes the combustion duration longer. It almost reaches the limit 780°C at 24bar IMEP. At 26bar and 28bar IMEP, over-fuelling is introduced because of charge cooling effect can reduce the in-cylinder temperature. During testing, over-fuelling is achieved by decreasing lambda slowly as well as increasing the load step by step, at the same time, the exhaust gas temperature is controlled to be lower than 780°C. The exhaust gas temperature of ethanol increases from 592°C

to 680°C with the load increase from 2 bar to 28bar while that of methanol increases from 582°C to 657°C. Overall, the exhaust gas temperature is lower than ethanol and gasoline. That's because methanol has the lowest lower heating value (LHV) so that more fuel is injected into the cylinder, charge cooling effect can decrease the in-cylinder temperature. Ethanol's LHV is between methanol and gasoline so its exhaust gas temperature is between methanol and gasoline.

The injection timings (i.e. the start of injection) are kept the same for different fuel as boundary condition which is shown in Figure 4-10. From 2bar to 8bar IMEP, the injection starts at 320 CAD BTDC. After that, injection timing is retarded from 316 CAD BTDC to 303 CAD BTDC and is kept at 303 CAD BTDC from 16bar to 24bar IMEP. It's advanced more to 297 CAD BTDC at 28bar. The injection pressure of these fuels is increased from 55bar to 169bar. The fuel flow rates are also shown in Figure 4-10. With the load increases from 2bar to 28bar IMEP, the fuel flow rate of gasoline increases from 0.65kg/h to 7.71kg/h, that of ethanol increase from 0.91kg/h to 10.3kg/h, and methanol's fuel flow rate increases from 1.25kg/h to 13.4kg/h. Since the lower heating value of methanol is the lowest, so the injection duration of methanol is the longest. As a result of this, the fuel consumption and fuel flow rate of methanol and ethanol are higher than gasoline at the same load. After 24bar IMEP, the gasoline's injection end timing is retarded because of increased fuelling so that the fuel flow rate increases after 24bar IMEP.

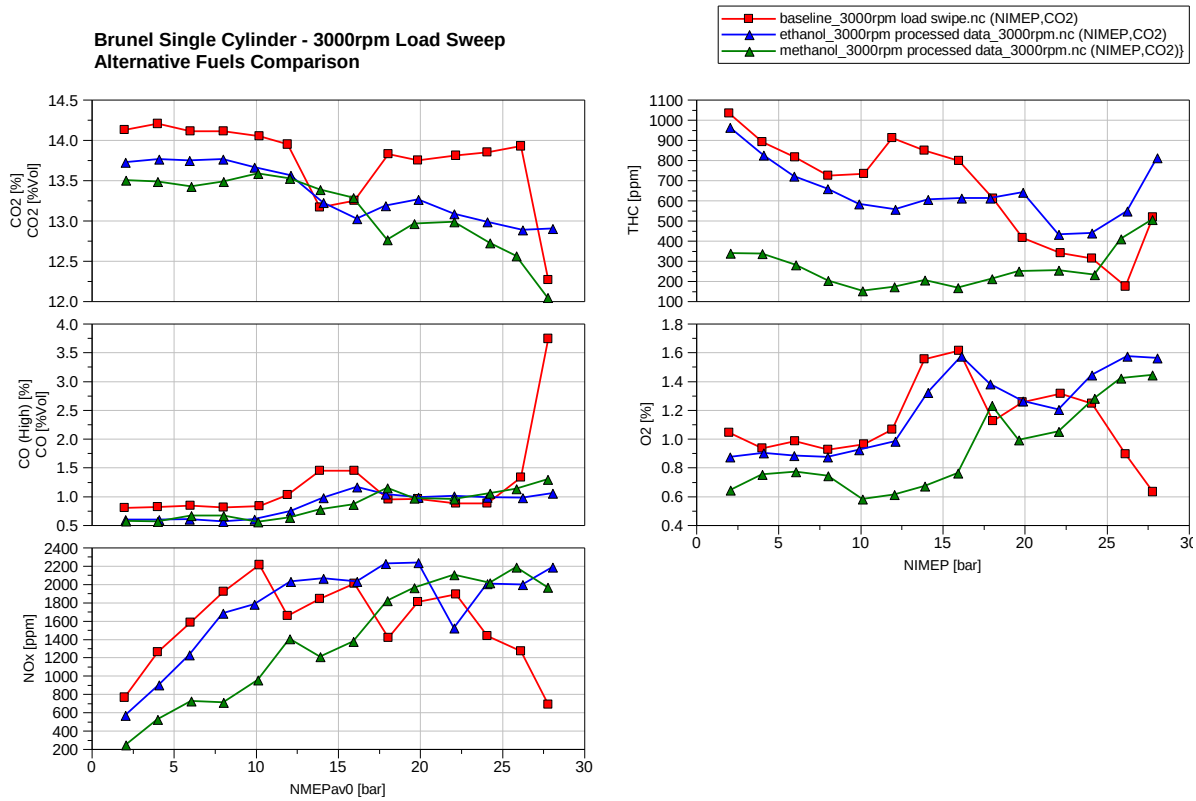

Figure 4-11 Emissions of 3000rpm load sweep

Most of the emissions data are shown in Figure 4-11. The CO_2 produced by gasoline decreases from 14.12%vol to 13.16%vol, then it increases to 13.92%vol and drops to 12.26%vol quickly because of over-fuelling. The CO_2 of ethanol reduced from 13.72%vol to 12.9%vol with the load increase and the CO_2 of methanol has the same trends as ethanol, it decreases from 13.5%vol to 12.04%vol. The CO_2 produced by ethanol and methanol is lower than gasoline since alcohol fuel leads to lower specific CO_2 because of CO_2's energy-specific basis (g CO_2/MJ). The CO produced by gasoline increases from 0.79%vol to 3.73%vol.

The CO produced by ethanol increases from 0.59%vol to 1.05%vol and that of methanol increases from 0.57%vol to 1.29%vol. The amount of CO in the exhaust gas has the opposite trend with CO_2 and it's mainly affected by Lambda (shown in Figure 4-10). The amount of CO keeps stable for methanol and ethanol since all the combustion are stoichiometric. In comparison to gasoline, methanol contains only about 44% carbon, which is directly transformed into CO during combustion, thereby reducing the formation and emission of CO. For gasoline, the content of CO is also

at a low level before 24bar IMEP. After 24bar, the CO increase because over-fuelling is introduced to decrease the in-cylinder temperature.

The NO_x released by gasoline increases from 762ppm to 2208ppm at 10bar IMEP. After that, it decreases to around 1800ppm between 12bar and 24bar IMEP, and it decreases quickly to 680ppm from 24bar to 28bar IMEP. The NO_x produced by ethanol increases from 566ppm to 2184 ppm with load increase, and methanol's NO_x also increases from 244ppm to 2181ppm. The production of NO_x is affected by the peak in-cylinder pressure (shown in figure 4-9) because higher peak cylinder pressure results in higher peak burned gas temperature then causes higher NO_x. The NO_x of methanol and ethanol increase with the increase of peak cylinder pressure before 16 bar IMEP. After that, the spark timing of them were retarded because the maximum in-cylinder pressure 120bar IMEP has achieved and the peak in-cylinder pressure was kept at 120bar so that the NO_x release by methanol and ethanol keeps stable after 16bar IMEP. For gasoline, the NO_x increases from 2bar to 16bar IMEP with the increase of peak in-cylinder pressure. Afterwards, to keep the knocking intensity under the limit, the spark timing was retarded, and the peak in-cylinder pressure is around 80bar so that the NO_x keeps stable between 16bar and 24bar IMEP. When operating at 26bar IMEP, the lambda decreases, more fuel was injected and less oxygen is available therefore NO_x decreases fast. Methanol releases the lowest NO_x since it has the highest evaporation enthalpy with the same fuel quantity. Furthermore, methanol has the lowest LHV so that more methanol was injected result in the lowest in-cylinder temperature (charge cooling effect) which cause methanol produces the lowest NO_x. THC released by methanol and ethanol are lower than gasoline. The THC released by gasoline drops from 1031ppm to 172ppm at 26bar IMEP, then increases to 515ppm at 28bar IMEP. The THC produced by ethanol reduced from 960ppm to 431ppm at 22bar IMEP, then increases to 810ppm at 28bar IMEP. Methanol's THC also drops from 336ppm to 166ppm at 16bar IMEP, then it increases to 503ppm at 28bar IMEP. Before 24bar IMEP, alcohol fuels' THC drops because their injection timing was retarded, and the injection pressure were increased which cause less fuel impingement on the piston and cylinder wall. After 24bar, ethanol and methanol's THC increase since their injection end timing are so retarded with the load increase which result in wall wetting and their THC increases. Methanol has the lowest THC since it has the

lowest boiling point so that methanol evaporates very fast in the combustion chamber which result in the air-methanol mixture quality is the best of the three fuels. As a result of this, less fuel impingement on the cylinder wall and piston which leads to less THC. The O_2 released by these fuels have the same trend which increase firstly then decrease and increase again after that. O_2 released by gasoline increases from 1.04%vol to 1.61%vol at 16bar IMEP, then keeps around 1.25%vol from 18 to 24bar, and it decreases from 1.24%vol to 0.63%vol from 24bar to 28bar because of over-fuelling. O_2 produced by ethanol increases from 0.87%vol to 1.57%vol at 16bar, then it decreases to 1.2%vol at 22bar, and increases again to 1.56%vol at 28bar. The O_2 released by methanol increases keeps around 0.7%vol from 2bar to 16bar IMEP, then it increases to 1.23%vol at 18bar IMEP. After that, it drops to 0.99%vol at 20bar then it increases to 1.44%vol at 28bar IMEP.

it should be pointed out that the flame ionization detector (FID) is less sensitive to the alcohol and their partially oxidized products, the measured value of THC from alcohol fuels is less than the true values [110].

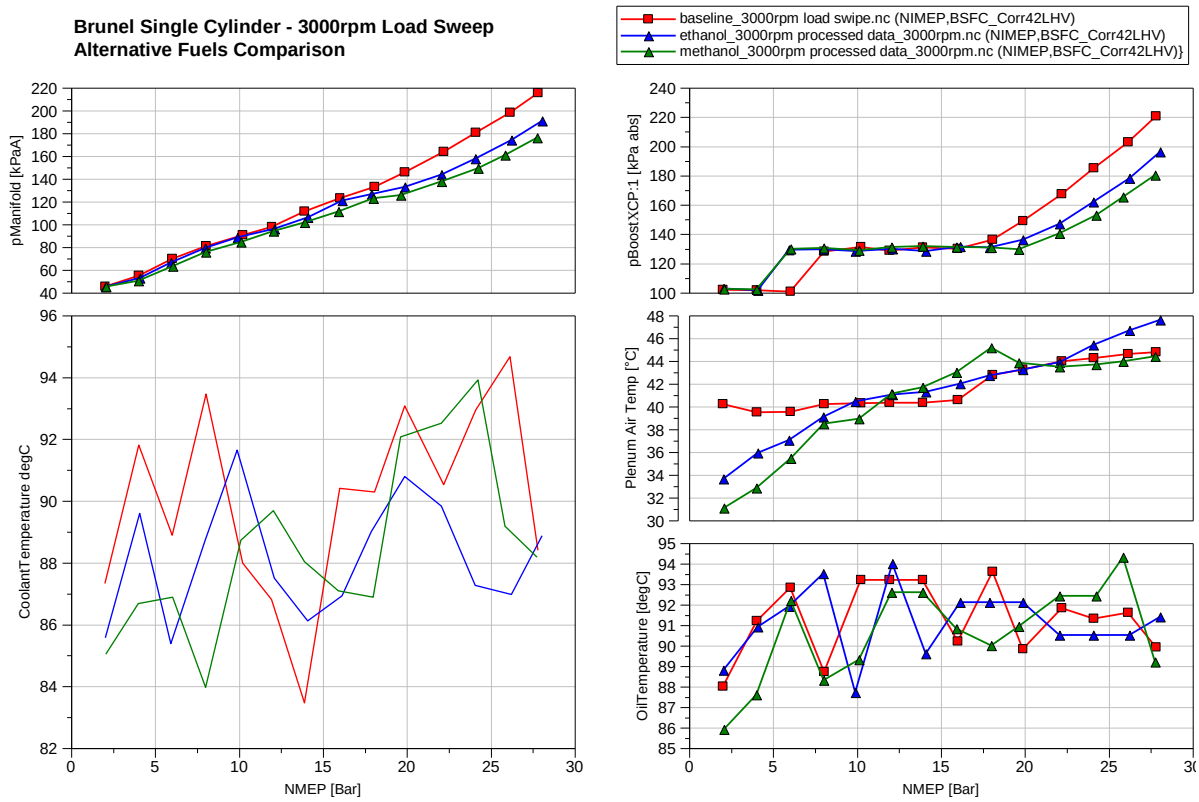

Figure 4-12 Engine conditioning temperature and pressure

Most boundary conditions of this test are shown in Figure 4-12. The intake manifold pressure of three different fuels are increased with the load increase. The intake manifold pressure of gasoline increases from 45kPa to 215kPa, while that of ethanol increases from 45kPa to 190.7kPa. The intake manifold pressure of methanol increases from 45kPa to 175.8kPa. Above 16bar IMEP, the intake manifold pressure of gasoline is higher than alcohol fuels because of its higher stoichiometric air-fuel ratio. The coolant and oil temperature are kept around 90°C. The Intake air temperature is kept around 40°C by the intake heater. The boost pressure is also shown in Figure 4-12. The P_{boost} of gasoline is kept at 101kPa by means of natural aspirate from 2 to 6bar IMEP. Because of the test bed's issue since the boost system is not stable with wide open throttle and low boost pressure. From 8 to 16bar IMEP, the P_{boost} is kept at 130kPa, the load is controlled by the throttle. After 16bar IMEP, the throttle is 100% open, the load increases with the increase of P_{boost}, the P_{boost} achieves at 220kPa for the load to achieve 28bar IMEP. The boost pressure of ethanol increases from 100kPa to 196kPa, while that of methanol increases from 100kPa to 180kPa.

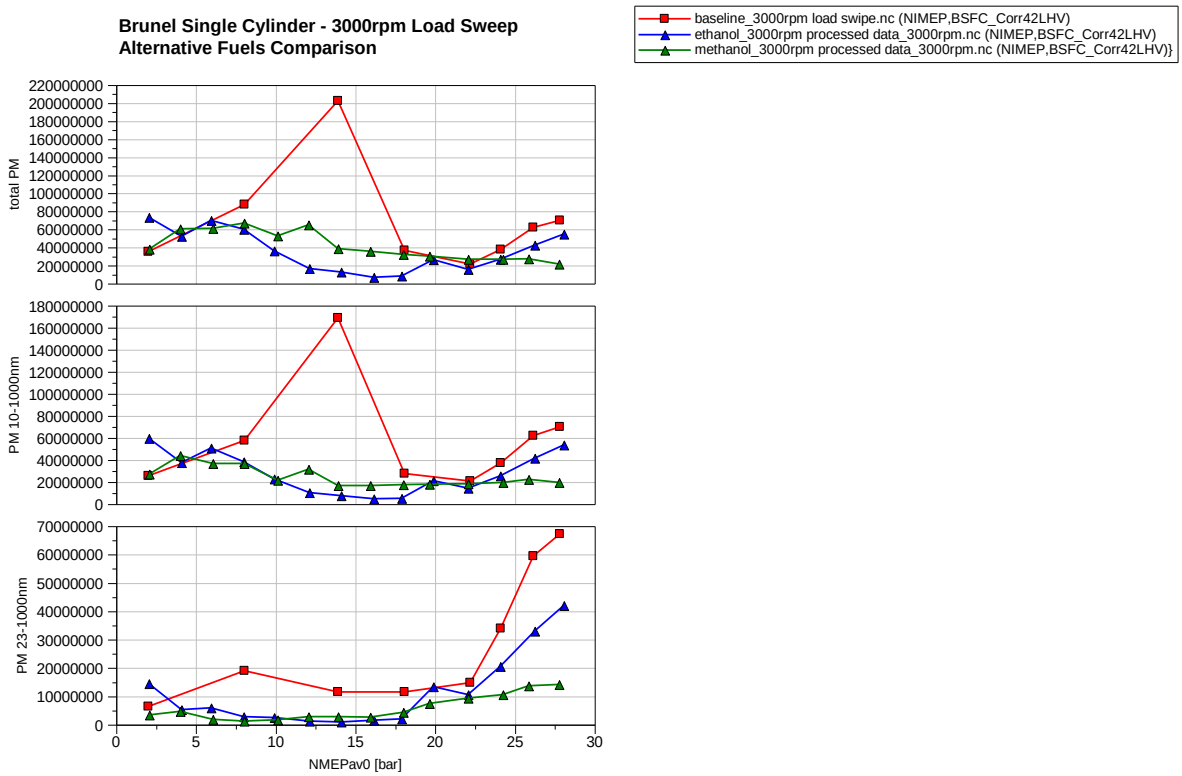

Figure 4-13 Particle numbers of gasoline, ethanol and methanol

Figure 4-13 shows the total particle numbers of all three fuels at 3000rpm, 23nm-1000nm particle numbers and the 10nm-1000nm particle numbers. Due to equipment's issue, only some gasoline points' PN data are collected. The total PN of gasoline increases from 3.47e7 to 2.02e8 at 14bar then drops to 2.13e7 at 22bar IMEP and increases again to 6.98e7 at 28bar IMEP. The total PN of ethanol reduces from 7.3e7 to 6.7e6 at 16bar then increases to 5.46e7 at 28bar. The total particle number of methanol increases from 3.77e7 to 6.48e7 at 12bar IMEP then reduces to 2.14e7 at 28bar IMEP slowly. The PN 10nm-1000nm of gasoline increases from 2.54e7 to 1.69e8 at 14bar then drops to 2.06e7 and increases to 6.97e7 at 28bar IMEP. That of ethanol decreases from 5.94e7 to 4.47e6 at 16bar IMEP then increases to 5.35e7 at 28bar IMEP. Ethanol's 10-1000 PN keeps around 2.5e7 from 2bar to 12bar IMEP, then it drops to 2e7 from 14bar to 28bar. The 23-1000nm PN of gasoline increases from 6.34e6 to 1.89e7 at 8bar then drops to 1.14e7 at 14 and 18bar IMEP. After that, the 23-1000nm PN of gasoline increases from 1.47e7 to 6.7e7 from 22bar to 28bar IMEP. That of ethanol reduces from 1.44e7 to 8.43e5 at

14bar then increases to 4.19e7 at 28bar IMEP. The 23-1000nm PN of methanol increases slowly from 3.41e6 to 1.41e7 with the load increasing from 2bar to 28bar IMEP. There are two reasons to explain why ethanol's total PN drops from 8 bar to 18bar IMEP. The first one is that injection timing (Figure 4-10) is retarded from 320 CAD BTDC to 303 CAD BTDC which could reduce fuel impingement on the cylinder wall and piston. The second one is that the rail pressure is increased from 120bar to 168bar which can improve the liquid atomization process [109]. The lower total PN of ethanol than methanol is likely caused by the longer injection duration of methanol and hence there is less time for atomisation and mixing to take place after the end of the injection. After 16bar IMEP, gasoline and ethanol's PN increase as more liquid fuel is injected.

The explanation for the lower PN of methanol than gasoline is that methanol has a 34.8% gravimetric oxygen content. Since methanol formula, "CH4O" contains only one carbon atom, and atomic mass of oxygen accounted for 50% of the relative molecular mass of methanol. Since methanol is a typical fuel which contains a small amount of carbon and a large amount of oxygen. Based on this reason, there are few PM emissions when the engine is fuelled with pure methanol [111].

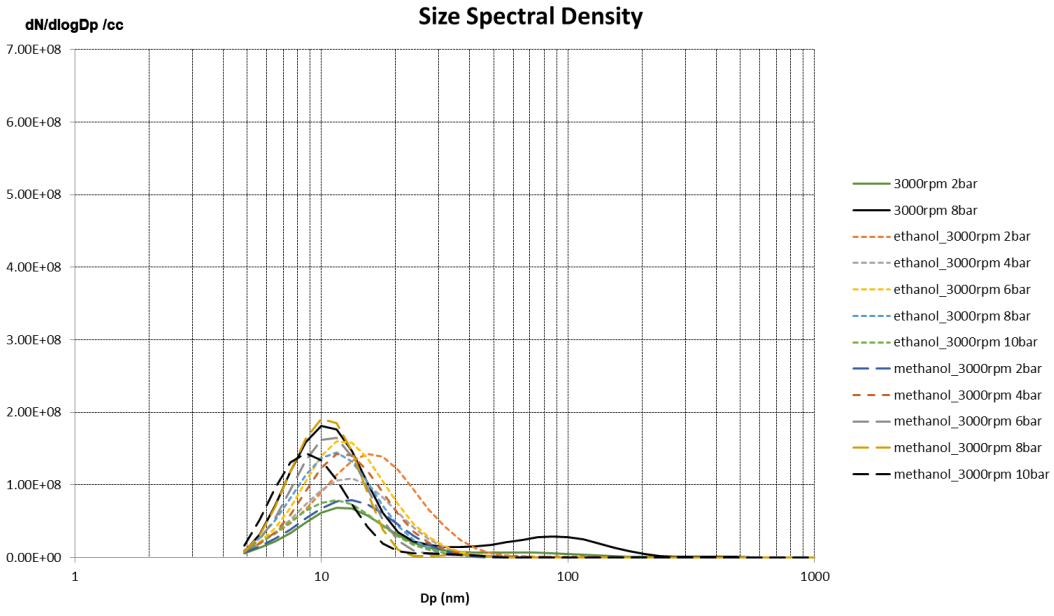

Figure 4-14 2-10bar IMEP Size spectral density

The size spectral density of gasoline, ethanol and methanol from the load 2-10bar IMEP are shown in Figure 4-14. It's clear that at the lowest load of 2 bar IMEP the particle size distributions are mano-peak shapes with most particles between 5nm to 20nm by means of nucleation mode. Only gasoline's 8bar IMEP gets dual-peaks in which the left first peak is by the particle size belong to nucleation mode caused by the oxidation of THC and the right peak is the particle size distribution from the accumulation mode. What's more, the particle number in accumulation mode is less than nucleation mode.

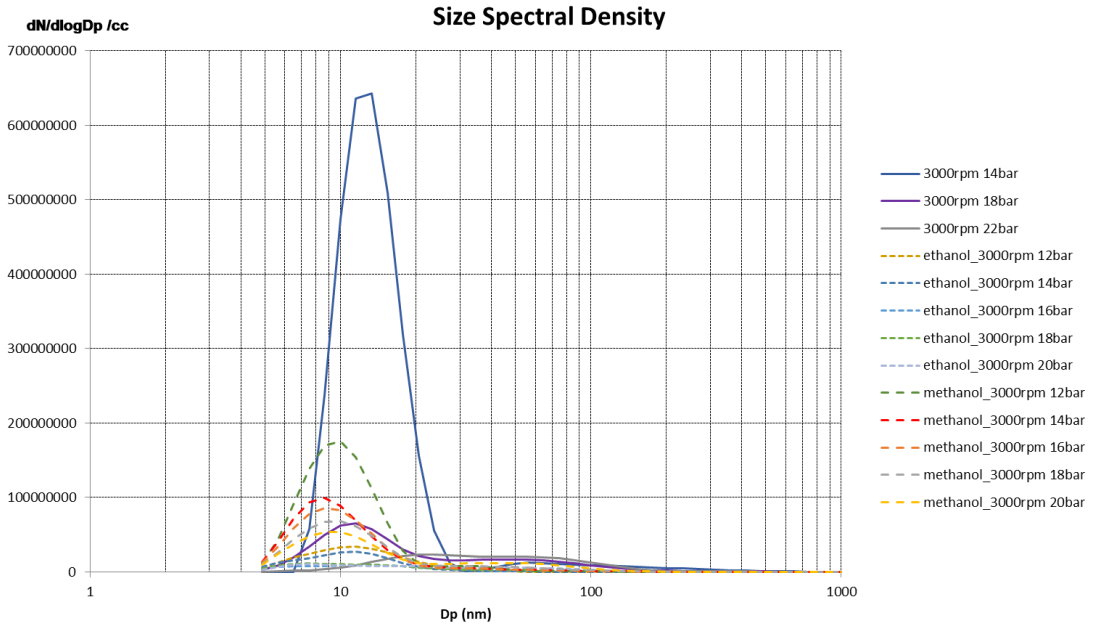

Figure 4-15 10-20bar IMEP size spectral density

The size spectral density of gasoline, ethanol and methanol from the load 12-20bar IMEP are shown in Figure 4-15. All the Gasoline's curves are dual-peaks curves. At 14bar and 18bar IMEP operations, most particles released by gasoline belong to the nucleation mode but for 22bar IMEP, the numbers of particulate in nucleation mode and accumulation mode are almost equal to each other which means some small particles stick to each other and form particles with the bigger size. Except at 20bar IMEP, all other curves of methanol are mano-peak and most particle size is in nucleation mode. Methanol's 22bar's size distribution mode is also a dual-peaks curve but only limited particle size is in accumulation mode.

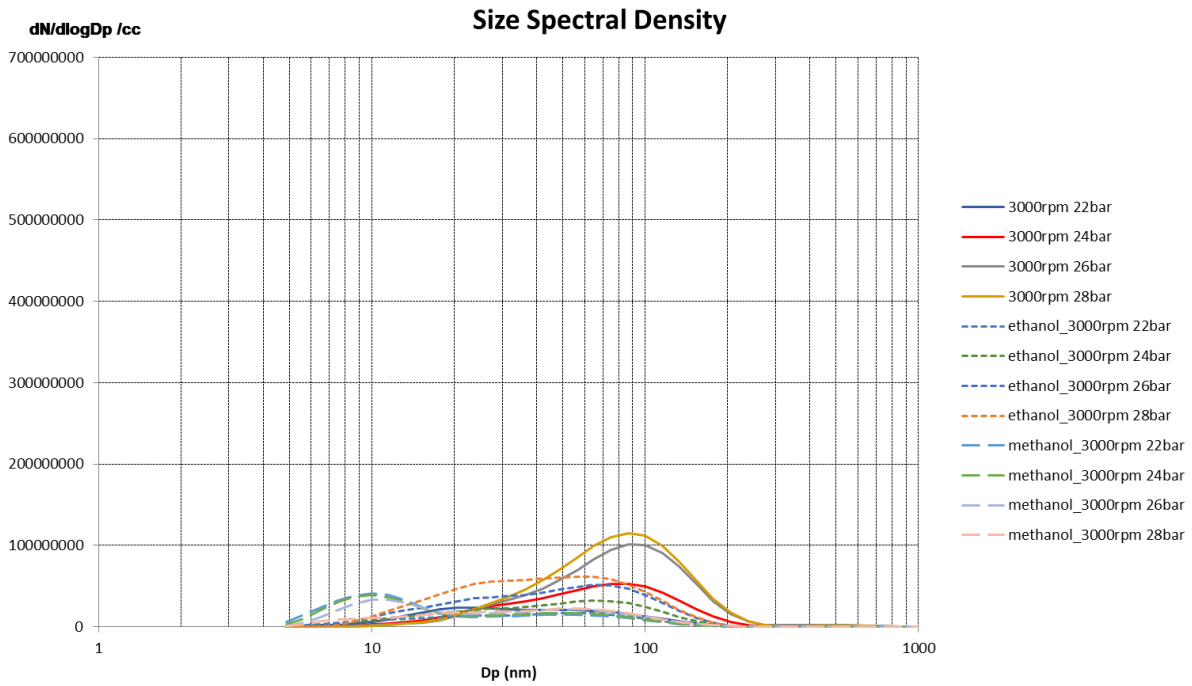

Figure 4-16 20-28bar IMEP size spectral density

The size spectral density of gasoline, ethanol and methanol from the load 22-28bar IMEP are shown in Figure 4-16. At high load, the particle released by gasoline mostly belongs to accumulation mode as a result of small particle sticking with each other. All ethanol's curves are also mano-peak and more than half particle's size is between 20-100nm. For methanol, the curves of its high load points are dual-peaks curves and most particle size is under 20nm by means of nucleation mode.

4.2.3 4000rpm Load Sweep

4000rpm load sweep for gasoline, ethanol and methanol were done from 3.1bar to 26.9bar IMEP to explore the difference between these three fuels at high speed. The maximum load is limited to 28bar IMEP by the knocking combustion of gasoline at high load, and unstable combustion of ethanol and methanol.

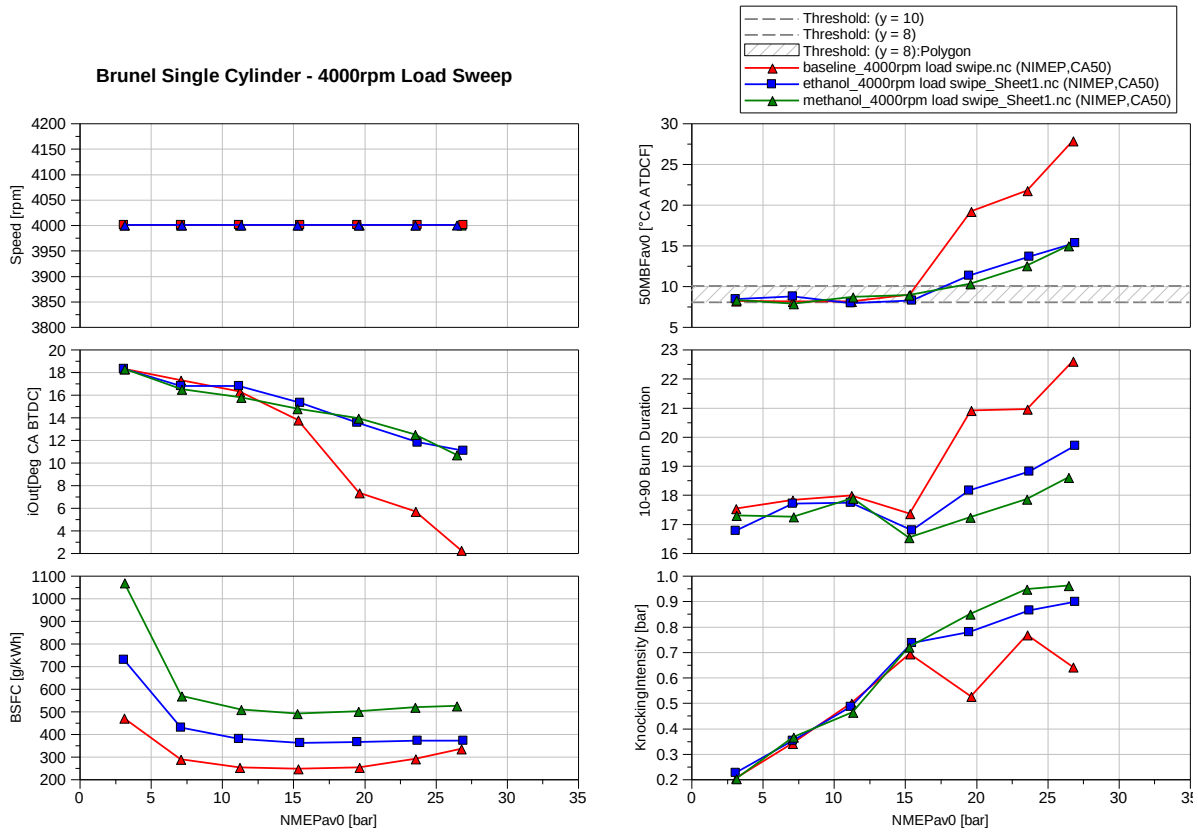

Figure 4-17 Combustion characteristic of 4000rpm load sweep

For 4000 rpm load sweep, all test points are running at the MBT spark timing if possible. The spark timing and CA50 are shown in Figure 4-17. The spark timing of gasoline is retarded from 18.3 Deg BTDC to 2.2 Deg BTDC with the load increases from 3.1bar to 26.9bar IMEP. The spark timings are similar for ethanol and methanol, they are retarded from 18.3Deg BTDC to 10.7 Deg BTDC. The CA50 of gasoline is retarded from 8.1 Deg ATDC to 27.8 Deg ATDC, while ethanol and methanol's CA50 are retarded from 8.2 Deg ATDC to 14.9 Deg ATDC. At 19.7bar and 23.6bar IMEP, ethanol's CA50 is slightly retarded than methanol since the spark timing of ethanol is retarded more as well as the laminar flame speed of ethanol is slower than methanol. Below 15.1bar IMEP all CA50 were kept at 8 Deg but after 15.1bar IMEP, the spark timing of gasoline is retarded because of knocking intensity (shown in Figure 4-17) is higher than 1 which is the maximum limit. For methanol and ethanol, their spark timings are retarded because the Pmax (peak in-cylinder pressure) limit of this engine is 120 bar and the Rmax (peak pressure rise rate) is 6bar/dCA. The knocking intensity of gasoline increases from 0.2bar to 0.69bar at 15.4bar IMEP then

is kept around 0.65bar. Ethanol and methanol's knocking intensity increases from 0.22bar to 0.89bar and 0.20bar to 0.96bar separately. The knocking intensities for ethanol and methanol are always under the limit of 1 even at highest load because their anti-knock characteristic is better than gasoline. At 11.2bar IMEP, methanol's spark timing is more retarded than gasoline and ethanol which cause methanol's knocking intensity at 11.2bar IMEP lower than the other fuels. The brake specific fuel consumption (BSFC) of the three different fuels could also be found in Figure 4-17. BSFC of gasoline decreases from 468g/kWh to 244g/kWh at 15.4bar, then increases to 333g/kWh at 26.9bar IMEP. With the load increases, ethanol's BSFC decreases from 727g/kWh to 359g/kWh at 15.4bar IMEP, and increases to 369g/kWh. Methanol's BSFC is similar to ethanol which decreases from 1068g/kWh to 489g/kWh at 15.4bar IMEP and increases to 523g/kWh at 26.9bar IMEP. The BSFC of different fuels have the same trend while the reason why the BSFC of methanol is higher than ethanol and gasoline is because the LHV (lower heating value) of methanol is the lowest of the three different fuels. The BSFC of gasoline increases after 19.7bar IMEP is because over-fuelling is introduced to decrease the exhaust gas temperature. For gasoline at 19.7bar, the spark timing could be advanced more since there is still some margine between its knocking intensity and the limit. The burn duration of gasoline increases from 17.5CAD to 22.6CAD with the load increase. The burn duration of alcohol fuel keeps around 17.3CAD from 3.1bar to 15.4bar IMEP, then ethanol increases to 19.7CAD at 26.9bar IMEP and methanol increases from 17.3CAD to 18.6CAD. The burn duration of methanol is shorter than ethanol with similar spark timing after 15.4bar IMEP since methanol's laminar flame speed is higher than ethanol. From 3.1bar to 15.4bar IMEP, the knocking intensity of these three fuels keeps increasing from 0.2bar to 0.72bar. After that, gasoline's knocking intensity keeps around 0.7bar because of retarding spark timing. Even the spark timing of ethanol and methanol are also retarded, their knocking intensity increases to 0.89bar and 0.96bar.

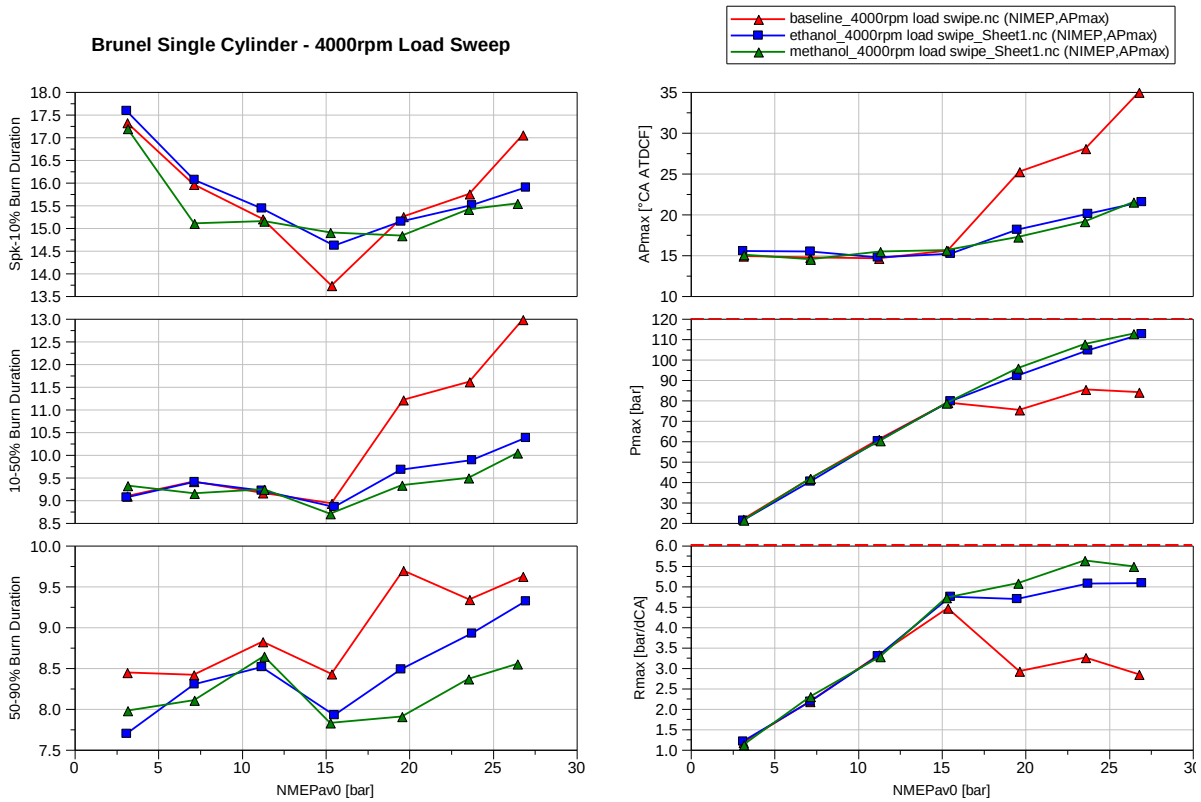

Figure 4-18 Combustion phasing, Pmax and Rmax

The combustion characteristics of the three fuels are shown in Figure 4-18. The 10% mass fraction burn of gasoline decreases from 17.5 CAD to 13.7 CAD at 15.4bar IMEP, then increases to 17 CAD at 26.9bar IMEP. That of ethanol decreases from 17.6 CAD to 14.6 CAD then increases to 15.9CAD, and methanol's CA10 decreases from 17.2CAD to 14.8CAD at 19.7bar IMEP then increases to 15.5CAD. Before 15.4bar IMEP, the CA10-50 keeps around 9CAD for these three different fuels. After that, CA10-50 of gasoline increases to 13CAD, and that of ethanol increases to 10.4CAD, methanol to 10CAD. The CA50-90 of gasoline keeps around 8.6CAD before 15.4bar IMEP, after that it increases to 9.7CAD and then keeps around that. The CA50-90 of ethanol increases from 7.7 CAD to 9.3 CAD, and that of methanol increases from 8.0 Cad to 8.5 CAD. At 11.2bar IMEP of methanol, the CA50-90 is slightly longer than other points since its spark timing is slightly retarded. Before 15.4bar IMEP, the CA10, CA10-50, and CA50-90 of them are similar since the spark timing is almost the same. After 15.1bar IMEP, as a result of knocking, gasoline needs to retard the spark timing more than alcohol fuel and got a longer combustion duration. As mentioned before, gasoline at 19.7bar IMEP is not at MBT which

causes the combustion phasing to be retarded. Because methanol's laminar flow rate is faster than ethanol and gasoline so that all the mass fraction burn of methanol is shorter than ethanol and gasoline. The AP_{max}(maximum in-cylinder pressure correspond to crank angle)can be found in Figure 4-18. The AP_{max} of gasoline is retarded from 14.8CAD ATDC to 34.9CAD ATDC. Because ethanol and methanol's spark timing aligns with each other, their AP_{max} also keeps the same which is retarded from 15.1CAD ATDC to 21.5CAD ATDC. The peak cylinder pressure (P_{max}) and peak pressure rise rate (R_{max}) are also shown in Figure 4-18. The P_{max} of gasoline increases from 21.6bar to 78.8bar IMEP at the load of 15.4bar IMEP, then the P_{max} keeps around that even with the load increase. The P_{max} of ethanol and methanol align with each other which increase from 21.3bar to 112.6bar IMEP. The R_{max} of gasoline increases from 1.2bar/dCA to 4.5bar/dCA at the load 15.4bar and R_{max} is kept around 3bar/dCA with the load increasing up to 26.9bar. For ethanol, its R_{max} increases from 1.2bar/dCA to 5.1bar/dCA while methanol's R_{max} increases from 1.1bar/dCA to 5.5bar/dCA. The limit of P_{max} is 120bar and the maximum R_{max} is 6bar/dCA so that even the knock intensity of ethanol and methanol is under the limit, their spark timing also needed to be retarded after 15.4bar IMEP. That's the reason why the combustion duration of ethanol and methanol are also increasing slowly after 15.4bar IMEP. After 15.4bar IMEP, the R_{max} of methanol is higher than ethanol since methanol's flame speed is faster than ethanol which causes the burn duration shorter than ethanol. Because the spark timing of gasoline is retarded more than ethanol and methanol, there is no need to pay attention to P_{max} and R_{max}.

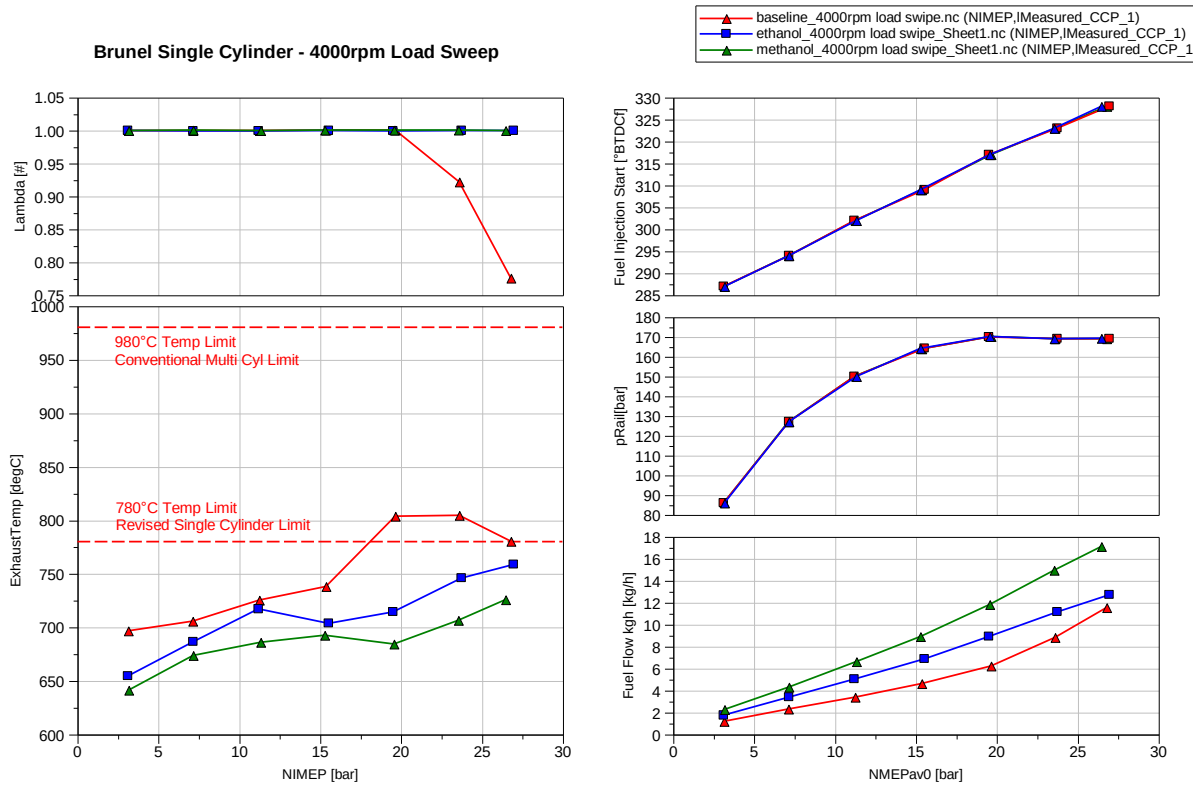

Figure 4-19 Lambda, TExh and injection parameters

The lambda and exhaust gas temperature of all test points are shown in Figure 4-19. The exhaust gas temperature of ethanol increases from 654°C to 759°C, and that of methanol increases from 641°C to 726°C with the load increasing from 3.1bar to 26.9bar IMEP. For ethanol and methanol, their lambda is kept at 1 since even if their combustion duration increase after 15.4bar IMEP, their exhaust temperature is still under the limit 780°C so over-fuelling is not needed. For gasoline, the spark timing was retarded more than alcohol fuel after 15.4bar IMEP because of knocking. After that, the exhaust temperature increases as a result of combustion duration increase and it reaches the limit at 23.6ba IMEP r. After 23.6bar IMEP, over-fuelling is introduced because of charge cooling effect can reduce the in-cylinder temperature. During testing, over-fuelling is achieved by decreasing lambda slowly as well as increasing the load step by step, at the same time, the exhaust gas temperature is also focused lower than 780°C. The lambda is 0.84 at 23.6bar IMEP and 0.78 at 27.9bar IMEP. The exhaust gas temperature of methanol is always lower than ethanol and gasoline because the lower heating value of methanol is the lowest of these fuels, more methanol is injected into cylinder and the charge cooling effect of

methanol is stronger than ethanol and gasoline which causes the lowest exhaust gas temperature. The injection timing and injection pressure are kept the same for different fuels as boundary conditions which are shown in Figure 4-19. The injection start is advanced from 287CAD BTDC to 328Deg BTDC, and rail pressure increases from 86bar to 169bar with load increases. The last diagram of Figure 4-19 shows the fuel flow rate of gasoline, ethanol and methanol. The fuel flow rate of gasoline increases from 1.18kg/h to 11.52kg/h. That of ethanol increases from 1.74kg/h to 12.71kg/h and methanol increases from 2.53kg/h to 17.12kg/h. Because the lower heating value of methanol is lower than ethanol and lower than gasoline, so the injection duration of methanol is the longest one of these fuels. As a result of this, the fuel consumption and fuel flow rate of methanol and ethanol are higher than gasoline at the same load. After 19.7bar IMEP, gasoline's fuel flow rate increases faster because of over-fuelling.

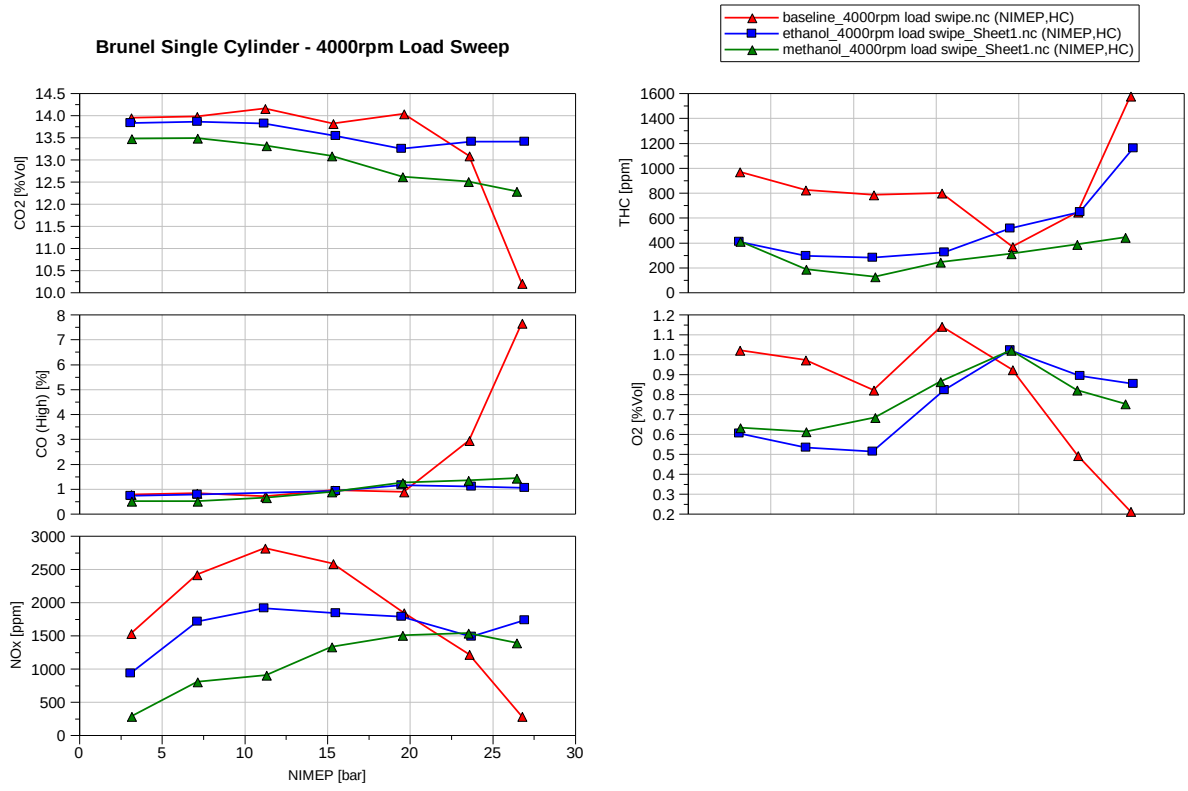

Figure 4-20 Emissions of 4000rpm load sweep

Most of the emissions data are shown in Figure 4-20. The CO_2 released by gasoline keeps around 14%vol from 3.1bar to 19.7bar IMEP, then it starts to reduce from 23.6bar to 26.9bar IMEP which contains CO_2 10.2%vol. The CO_2 produced by ethanol keeps around 13.5%vol during the load sweep. Methanol's CO_2 reduce slowly from 13.46%vol to 12.28%vol. The CO_2 gasoline decreases quickly from 19.7bar IMEP as a result of over-fuelling. The CO_2 produced by ethanol and methanol is lower than gasoline since alcohol fuel leads to lower specific CO_2 because of CO_2's energy-specific basis (g CO_2/MJ). The CO released by gasoline keeps around 0.85%vol from 3.1bar to 19.7bar IMEP, then it increases quickly to 7.63%vol at 26.9bar IMEP. The CO produced by ethanol and methanol increases slowly during this 4000rpm load sweep. Ethanol's CO increases from 0.70%vol to 1.03%vol while that of methanol increases from 0.49%vol to 1.41%vol. The amount of CO in the exhaust gas has the opposite trend with CO_2 and it's mainly affected by Lambda (shown in Figure 4-19). The amount of CO keeps stable for methanol and ethanol since all the combustion are stoichiometric. For gasoline, the content of CO is also similar to alcohol fuel before 19.7bar IMEP. After 19.7bar IMEP, the CO increase because over-fuelling is introduced. Additional, NO_x is also shown in Figure 4-20. The NO_x of gasoline increases from 1522ppm to 2811ppm at 11.2bar IMEP, then it decreases to 276ppm at 26.9bar IMEP. The NO_x produced by ethanol increased from 926ppm to 1901ppm at 23.6bar IMEP, and it keeps around 1700ppm at the rest of load. Methanol's NO_x increases from 280ppm to 1530ppm at 23.6bar then it decreases to 1382ppm at 26.9bar. The content of NO_x is affected by the peak in-cylinder pressure (shown in figure 4-18) because higher peak cylinder pressure results in higher peak burned gas temperature then causes higher NO_x. The NO_x of methanol and ethanol increases with the increase of peak cylinder pressure before 15.4bar IMEP. After that, the spark timing of them were retarded because the maximum in-cylinder pressure 120bar has achieved and the peak in-cylinder pressure was kept at 120bar so that the NO_x release by methanol and ethanol keeps stable after 15.4bar IMEP. For gasoline, the NO_x increases from 3.1bar to 15.4bar IMEP with the increase of peak in-cylinder pressure. Afterwards, to keep the knocking intensity under limit, the spark timing was retarded and the peak in-cylinder pressure keeps around 80bar so that the NO_x keeps stable between 15.1bar and 19.7bar IMEP. When achieving 23.6 bar, the lambda decreases, more fuel was injected and evaporation cause the in-cylinder temperature decrease then NO_x

decreases fast as a result of this. Overall, methanol's NO_x is the lowest of the three fuels since its exhaust gas temperature is lower than ethanol and gasoline as a result of more effective charge cooling effect.

THC is shown after NO_x in Figure 4-20. The THC released by gasoline decreases from 967ppm to 363ppm at 19.7bar IMEP because the in-cylinder thermal dynamic condition is better with the load increases so that the combustion is more sufficient with the unburn hydrocarbon decreases. After that, THC increases to 1572ppm at 26.9 bar IMEP because of over-fuelling, more fuel is injected into cylinder but not burned. THC has the same trend with the reference from MAHLE powertrain and the THC released by methanol and ethanol are lower than gasoline because of flame ionization detector (FID) which has been explained in the previous section. The O_2 released by gasoline keeps around 1%vol from 3.1bar to 19.7bar, then it drops to 0.21%vol because of over-fuelling. Ethanol's O_2 decreases from 0.6%vol to 0.51%vol from 3.1bar to 11.2bar IMEP, then it increases to 1.02%vol at 19.7bar IMEP and decreases to 0.85%vol at 26.9bar IMEP. The O_2 produced by methanol increases from 0.63%vol to 1.02%vol from 3.1bar to 19.7bar IMEP, and it reduces to 0.75%vol at 26.9bar IMEP.

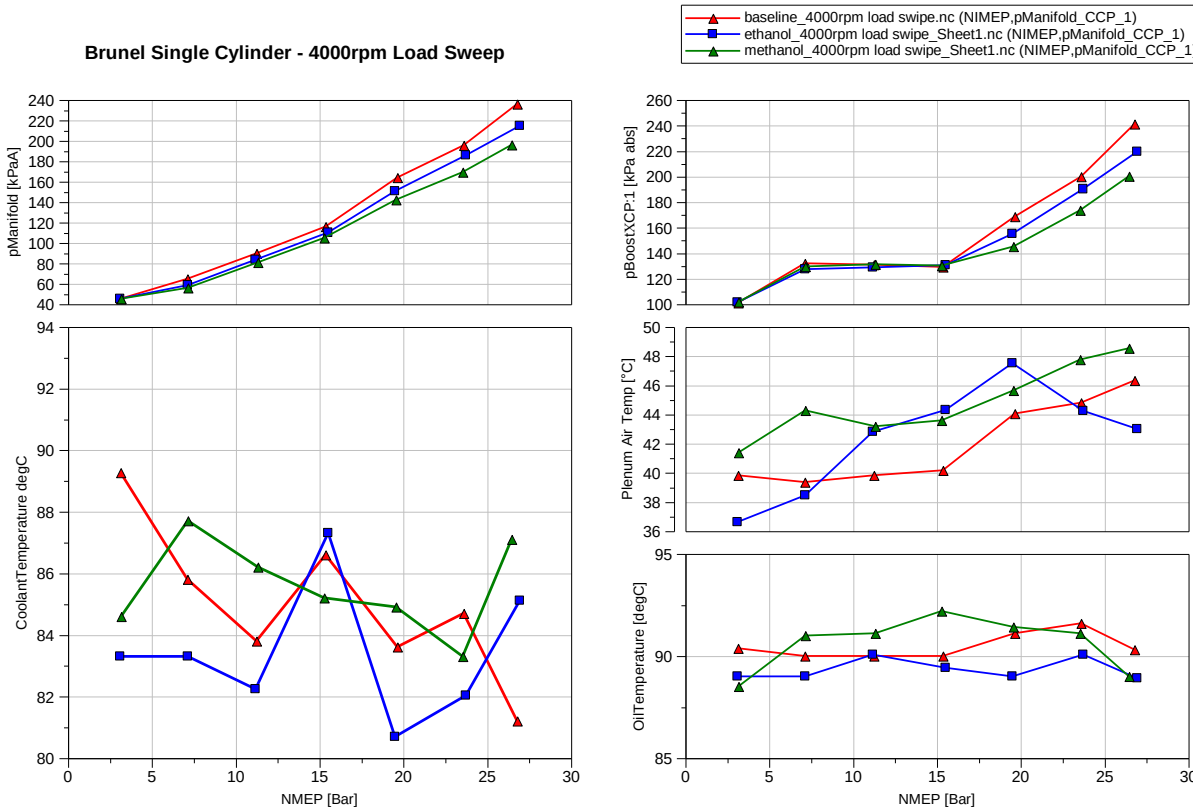

Figure 4-21 Engine conditioning temperature and pressure

Most boundary conditions of this test are shown in Figure 4-21. The manifold pressure is shown in the first diagram of Figure 4-21. The $P_{manifold}$ of gasoline, ethanol and methanol increase from 45kPa to 235.8kPa, 45kPa to 214.4kPa and 45kPa to 195.8kPa. The reason why gasoline's intake pressure is higher since its stoichiometric air-fuel ratio is higher than ethanol and methanol, to get the same power, more air is needed for gasoline. The coolant and oil temperature are kept around 90°C for all test points of this load sweep. The Intake air temperature are kept around 40°C. P_{boost} set point is also shown in figure 4-21. Before 15.4bar, the P_{boost} for these three fuels are the same, they are 100kPa at 3.1bar IMEP then increases to 130kPa from 7.1bar to 15.4bar IMEP. After 15.4bar IMEP, the P_{boost} of gasoline, ethanol and methanol are increased to 240.9kPa, 219.1kPa and 200.2kPa separately. The manifold pressure trends are similar with boost pressure and the reason why P_{boost} of gasoline is higher than ethanol and methanol is the same with intake manifold pressure. The intake air temperature is kept at 40°C all the time by an intake heater which located upstream of the plenum.

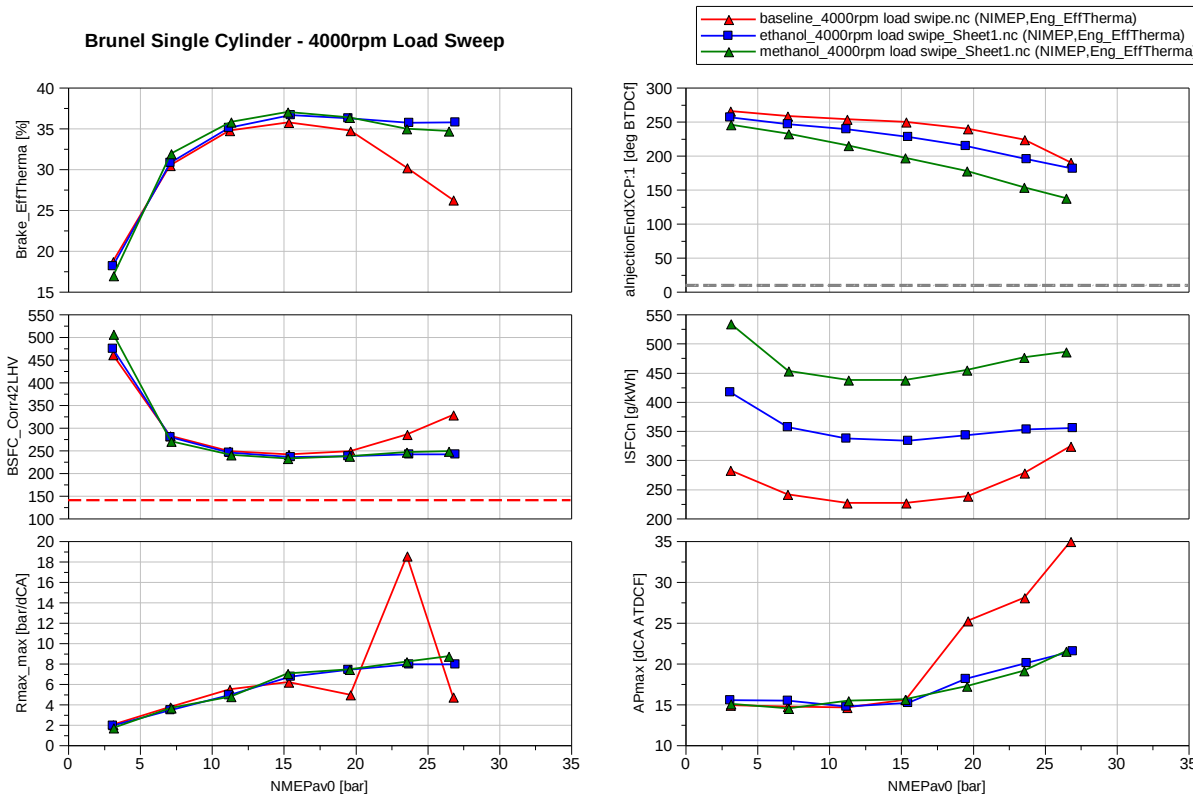

Figure 4-22 Combustion characteristics of 4000rpm load sweep

The brake thermal efficiency (BTE) and fuel consumption are shown in Figure 4-22. The BTE of gasoline increases from 18.6% to 35.7% at 15.4bar IMEP, then it decreases to 26.2%. The BTE of ethanol increases from 18.1% to 36.6% then it drops to 35.7% at 26.9bar. Methanol's BTE increases from 16.9% to 36.9% and it decreases to 34.6% with load increases to 26.9bar IMEP. Before 15.4bar IMEP, the BTE of the three fuels are similar. After that, the BTE of them decrease because the spark timing was retarded by the effect of knocking for gasoline and engine limit for alcohol fuels. The spark timing was more retarded for gasoline and its BTE decrease faster as a result of this. In order to compare the BSFC of the three different fuels, their original BSFC is timed by their LHV (lower heating value) then divided by 42. The BSFC corrected by 42 is shown after BTE. Gasoline's BSFC drops from 460.4g/kWh to 247.1g/kWh at 19.7bar, then it increases to 327.2g/kWh because of over-fuelling. That of ethanol and methanol are aligned with each other which drops from 473.5k/kWh to 234g/kWh and keeps around that for the rest of load. The

injection end timing is also shown in Figure 4-22. The injection end of gasoline, ethanol and methanol is retarded from 265CAD BTDC to 190CAD BTDC, 256CAD BTDC to 180CAD BTDC and 245 CAD BTDC to 137CAD BTDC separately. Because they have the same injection start timing, so that the injection duration of methanol is longer than ethanol and gasoline because the LHV (lower heating value) is lower.

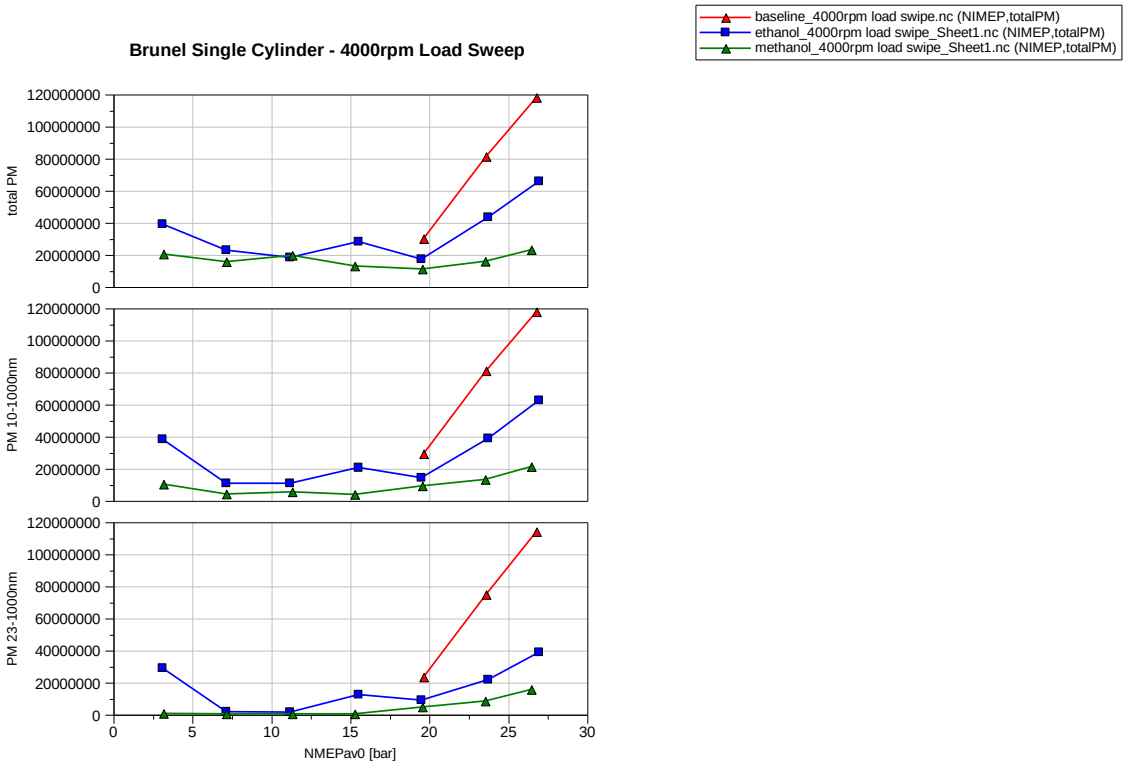

Figure 4-23 Particulate number of gasolines, ethanol and methanol

The particle numbers of gasoline, ethanol and methanol are shown in Figure 4-23 which includes total particle numbers, 10-1000 particle numbers as well as 23-1000nm particle numbers. Gasoline's PN data is only collected from 19.7bar to 26.9bar IMEP. The total particle number of gasoline is shown in the first diagram of figure4-23. It increases from 2.99e7 to 1.2e8 with the load increasing from 19.7bar to 26.9bar IMEP. The total PN released by ethanol reduces slowly from 3.81e7 to 1.72e7 at 19.7bar IMEP, it then increases to 6.25e7 at 26.9bar IMEP. The total number of particles produced by methanol keeps around 1.7e7 during the load

sweep. The second diagram of Figure 4-23 shows the number of particle which size between 10 to 1000nm. Gasoline PN 10-1000nm increases from 2.92e7 to 1.18e8. That of ethanol drops from 3.81e7 to 1.09e7 at 7.1bar, then it keeps around 1.5e7 from 11.2bar to 19.7bar IMEP. After that, it increases fast to 6.25e7 at 26.9bar IMEP. The PN 10-1000nm of methanol decreases slowly from 1.02e7 to 3.75e6 at 15.4bar then it increases gradually to 1.56e7 at 26.9bar. The last diagram of Figure 4-23 shows the number of particle size between 23-1000nm. Gasoline's PN 23-1000nm also increases from 2.33e7 to 1.14e8 quickly. The particle size from 23-1000nm released by ethanol decreases from 2.88e7 to 1.79e6 at 7.1bar IMEP, then it increases slowly to 3.87e7 at 26.9bar IMEP. Methanol's PN 23-1000nm reduces from 5.91e5 to 2.95e5 at 11.2bar. After that, it increases gradually from 4.82e5 to 1.56e7 at 26.9bar IMEP with the load increases. It's easy to find that there's a tiny difference between gasoline's PN with these three ranges which means that the most particles released by gasoline, their size is larger than 23nm. This could be verified by the spectral size density analysis afterwards. The reason why gasoline, ethanol and ethanol's PN increase from 19.7 to 26.9bar is because the injection timing is advanced as well as the rail pressure is high which causes fuel impingement on the piston and cylinder wall. What's more, the in-cylinder temperature increases which caused by the burn duration also has a negative effect on the PN number. Gasoline's total PN is higher than ethanol and methanol from 19.7bar to 26.9bar IMEP because of over-fuelling, the rich mixture leads to the sharp increase of PN. Both ethanol and methanol's total PN drops with the load increases from 3.1bar to 7.1bar IMEP because the spark timing is retarded, more sufficient time for air-fuel mixing. What's more, the injection is advanced from 287CA BTDC to 294CA BTDC which also gives more time for air-fuel mixing.

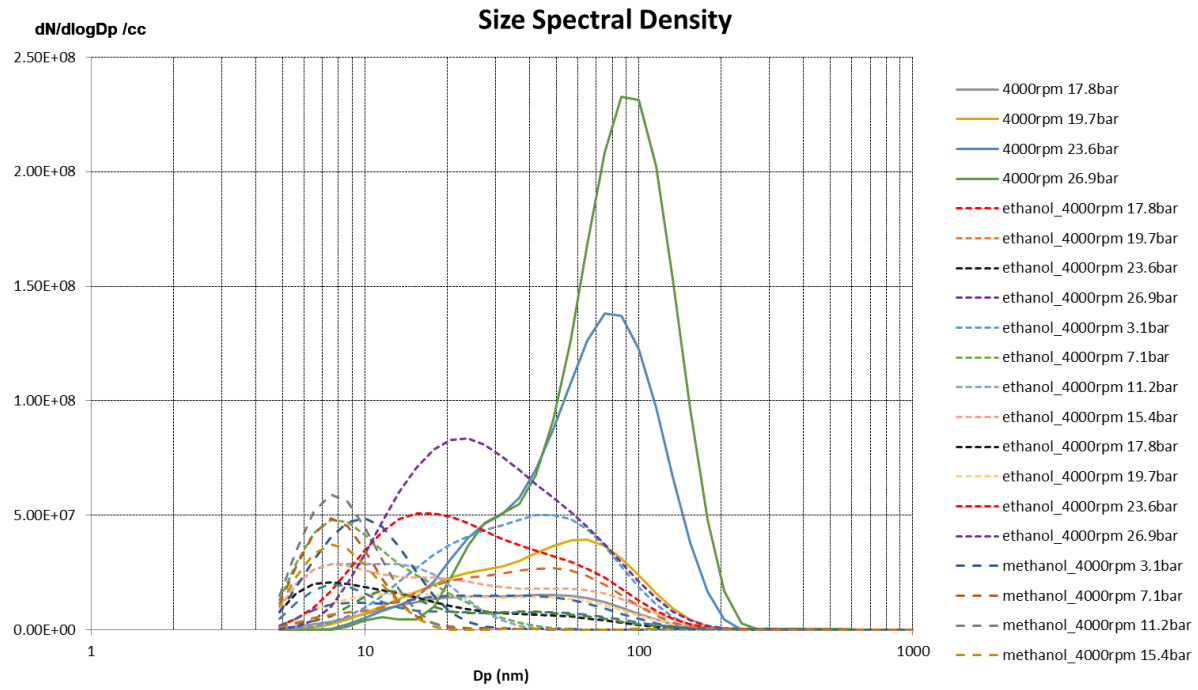

Figure 4-24 Size spectral density of 4000rpm load sweep

The particle size distribution of 4000rpm load sweep is shown in Figure 4-24. The particle size curves of gasoline are all mano-peak curves and their size is between 50 to 100nm so most particle released by gasoline is accumulation mode. As a result of over-fuelling, the THC produced by gasoline increases at 23.6bar and 26.9bar IMEP. The THC is oxidation into soot particle in nucleation mode and then stick together to form bigger size particle. That's the reason why the particle numbers and size increase sharply after over-fuelling. Most particle released by ethanol, its size is between 10 to 100nm so that it contains both nucleation mode and accumulation mode. All methanol's particle size is around 10nm so that no particle of accumulation mode is released by methanol.

4.3 Summary

For the 2000rpm load sweep, ethanol and methanol exhibited similar combustion characteristics to E10 gasoline when the load is limited to 11bar IMEP. Even ethanol and methanol's burn speed are faster than gasoline, but it doesn't reflect clearly on

combustion phasing and burn duration. There's a reduction of CO_2 released by ethanol and methanol on the energy-specific basis. What's more, the THCs released by ethanol and methanol are also lower than gasoline partially due to the ineffectiveness of FID in detecting the partially oxidised HCs.

For 3000rpm load sweep, the load ranges from 2bar to 28bar IMEP. Below 16bar IMEP, the indicated thermal efficiency of gasoline, ethanol and methanol are similar since all fuels' CA50 were controlled at 8 CAD ATDC at the MBT timing. Above 16bar IMEP, all these fuels' spark timings were retarded. For gasoline, its spark timing was retarded since knocking happened at higher load than 16bar IMEP. For alcohol fuels, the spark timings were limited by either or both peak in-cylinder pressure and pressure rise rate. But gasoline's spark timing needs to be retarded more than alcohol fuels to prevent knocking. As a result of this, ethanol and methanol can achieve higher thermal efficiency than gasoline at higher load operations. Methanol achieved the highest brake thermal efficiency 37.9% at 18bar IMEP and ethanol's highest BTE was 37.7% also at 18bar. Gasoline's best BTE was 36.5% at 10bar. For gasoline, over-fuelling was introduced at 26bar and 28bar IMEP to keep the exhaust gas temperature below 780°C. For ethanol and methanol, because their evaporation enthalpy is higher than gasoline which lead to lower in-cylinder temperature so that their exhaust gas temperature is under limit. As a result of this, over-fuelling is not required for ethanol and methanol. A reduction of NO_x emission was observed from ethanol and methanol engine operations. HC released by alcohol fuels are also lower than gasoline because of two reasons. The first one is FID which has mentioned before. Another is that, alcohol fuel evaporates faster than gasoline so that they got longer time to mix with air which can makes air-fuel mixture quality better than that of gasoline so that the amount of unburned hydrocarbon is less than gasoline. Across the 3000rpm load sweep, ethanol and methanol release less particulate emission compared with gasoline. There's up to 90% reduction of PN number by ethanol and methanol. What's more, the particle produced by ethanol and methanol whose size is also less than that of gasoline. The disadvantage of ethanol and methanol is that their lower heating values are lower than gasoline which cause longer injection duration and higher fuel consumption.

4000rpm load sweep's conclusion is similar to the 3000rpm load sweep.

5. Chapter Five: Effects of Injection Timing, Rail Pressure on Ethanol and Methanol Engine's Performance and Emissions

5.1 Introduction

This chapter focuses on the effects of injection timings and rail pressure on the fuel efficiency, combustion characteristics, emissions as well as particle numbers from the single cylinder spark ignition engine operated with ethanol or methanol. The baseline results are obtained for E10 Euro 6 gasoline. Two groups of fuel matrix tests which are 2000rpm 4.6bar IMEP and 3000rpm 16bar IMEP were selected to investigate the difference between alcohol fuels and gasoline. These two groups of tests cover medium-speed medium load and high-speed high load. By adjusting the injection timing and rail pressure, the best fuelling strategies for each fuel can be found. Also, injection timing and rail pressure have a big effect on particle number and particle size which will also be explained in this chapter. At 2000rpm 4bar IMEP, there is no knocking combustion since the load is low. At 3000rpm 16bar IMEP, as mentioned in chapter 4, gasoline's knocking intensity is high and the spark timing needs to be retarded but the 50% mass fraction of burn (CA50) of methanol and ethanol can be controlled at 8 Deg $ATDC_f$.

5.2 Experimental Setup and Test Conditions

All the testing work were carried out on the same single-cylinder direct injection engine. Two groups of fuel matrix tests which are 2000rpm 4.6bar IMEP and 3000rpm 16bar IMEP and the details of these fuel matrix test points are shown in Table 5.1.

Table 5-1 Fuel matrix test point

Speed & Load	IMOP (ATDC)	EMOP (BTDC)	SOI (CAD BTDCf)	Rail Pressure (bar)	Spark timing	Lambda
2000rpm 4.6bar IMEP	100	100	[275,300,325,350]	[50,100,150,200]	DBL	1
3000rpm 16bar IMEP	82	100			DBL	1

For each group of testing, the IMOP and EMOP are the same and the injection timing is adjusted from 275 Deg $BTDC_f$ to 350 Deg $BTDC_f$ with a gap of 25 Deg, and the rail pressure is adjusted from 50 bar to 200 bar with a gap of 50bar so that there are 16 test points in each group of testing.

5.3 Results and Discussion

5.3.1 2000rpm 4bar IMEP Fuel Matrix Analysis

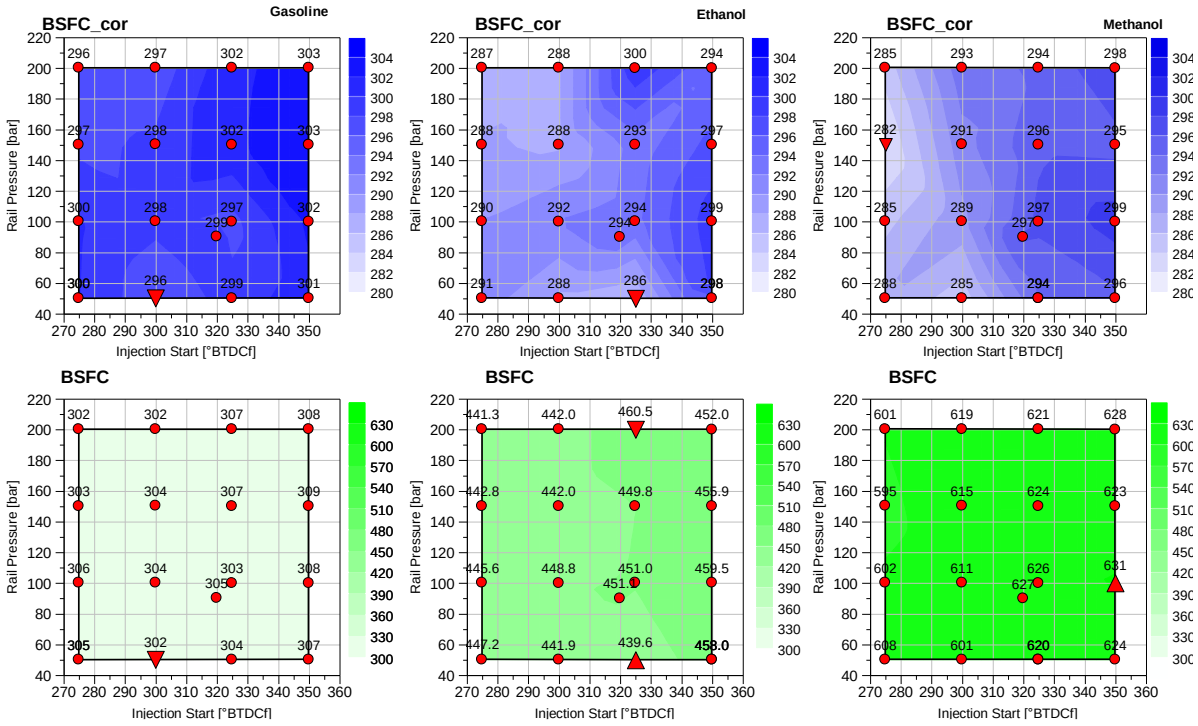

Figure 5-1 BSFC of different inject timing and rail pressure

The sequence of the fuel are gasoline, ethanol and methanol from left to right, and each column shows the same fuel in all the diagrams in this chapter.

The 3 diagrams on the top of Figure 5-1 shows the brake fuel consumption corrected by 42 of gasoline, ethanol and methanol. The X-axis shows the injection start timing and Y-axis shows the rail pressure (injection pressure). It's much clear to find the difference between these three different fuels by correcting their BSFC by a specific value since they have different lower heating values. The actual BSFC times the lower heating value of each fuel than divided by 42 is the value of BSFC_Cor. The lowest BSFC_cor point of gasoline is at the injection timing 300CA BTDC and rail pressure 50bar, and its BSFC_cor is 296.4g/kWh. Keep rail pressure the same, and the BSFC_cor decreases with the injection timing is advanced from 275CA BTDC to

300CA BTDC since there is more sufficient time for air-fuel mixing. After that, the BSFC_cor increases with the injection timing advanced to 350CA BTDC since the injection timing is too early and the piston is very close to the injector then causing wall-wetting on the piston so that the BSFC_cor increases. At the late injection points of injection timing at 275CA BTDC, the BSFC_cor decreases with the rail pressure since higher injection pressure can decrease the size of fuel droplets hence the evaporation of fuel is better, then it can give a positive effect on the air-fuel mixing. What's more, higher rail pressure also advances the end ofinjection which can give more time for air-fuel mixing before the spark ignition. The maximum BSFC_cor for gasoline is 303.1g/kWh which occurs at injection start 350CA BTDC, rail pressure 150bar. At the points which injection timing is 350CA BTDC, their BSFC gets worse as the rail pressure increases since early injection and high rail pressure will cause fuel impingement on the top of the piston hence pool fire. Ethanol's average BSFC_cor is lower than gasoline since its boiling point is lower than gasoline. The minimum BSFC_cor point of ethanol of 286.1g/kWh happens at the injection timing 325CA BTDC, rail pressure of 50bar. This is because the lower heating value of ethanol is lower than gasoline, to get the same power, more fuel is injected into cylinder so that the injection end timing of ethanol is more retarded than gasoline. As a result of this, ethanol's best BSFC_cor point's injection time is more advanced than gasoline to get more sufficient time for air-fuel mixing. The high BSFC_cor regions happen at early injection& high rail pressure region and the maximum BSFC_cor occurs at injection timing 325CA BTDC, rail pressure 200bar which value is 299.7g/kWh. Methanol's BSFC_cor is shown in the last column of Figure 5-1. It's easy to find that methanol has the lowest average BSFC_cor of these three fuels since it has the highest evaporation enthalpy thus the fuel-power transfer rate is the highest. Methanol's lowest BSFC_cor is at injection start 275CA BTDC, rail pressure 150bar which value is 281.9g/kWh. The maximum BSFC_cor happens at 350CA BTDC, rail pressure 100bar and its value is 298.9g/kWh. High BSFC_cor region also occurs at injection early points by the reason of fuel impingement on the top of the piston. At the same injection timing and rail pressure, methanol has lower BSFC_cor than ethanol and gasoline because it got the highest evaporation enthalpy so its air-fuel mixture is the best. Compare with gasoline's best BSFC_cor, ethanol's best BSFC_cor is reduced by 3.5% and that of methanol is reduced by 4.8%.

The second column of Figure 5-1 shows the brake specific fuel consumption (BSFC) of gasoline, ethanol and methanol. The highest and lowest points of BSFC are the same as BSFC_cor. The lowest BSFC of gasoline is 301.8g/kWh and the highest is 308.6g/kWh. The best BSFC of ethanol is 439.6g/kWh while the worst point's value is 460.5g/kWh. Methanol's minimum BSFC is 594.9g/kWh and its maximum BSFC is 630.9g/kWh. Methanol gets the highest average BSFC because its lower heating value is lower than ethanol and gasoline so that more methanol is injected into the cylinder to get the same power as ethanol and gasoline.

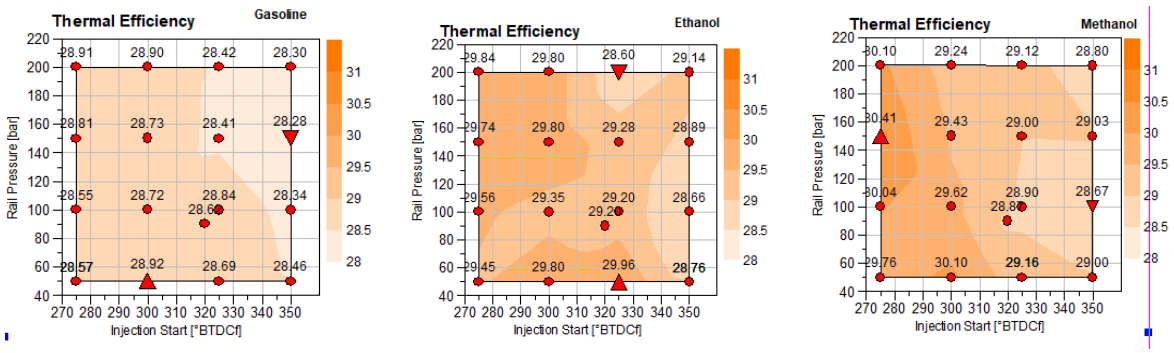

Figure 5-2 Brake Thermal Efficiency of gasoline, ethanol and methanol

The brake thermal efficiency (BTE) of these fuels are shown in Figure 5-2. The maximum BTE of gasoline is 28.92% which happens with the start of injection at 300CA BTDC, rail pressure of 50bar while the minimum BTE of gasoline is 28.28%. The best BTE of ethanol is 29.96% with an injection timing at 325CA BTDC and rail pressure at 50bar. At injection start timing 275CA BTDC and rail pressure 150bar, methanol gets its highest BTE of 30.41%. Compared with gasoline's best BTE, ethanol's best BTE improved by 3.6% and that of methanol improved by 5.2%. The difference between the best and worst BTE of gasoline, ethanol and methanol are 0.64%, 1.36% and 1.74% which means that injection timing and rail pressure have more effect on methanol than ethanol and gasoline.

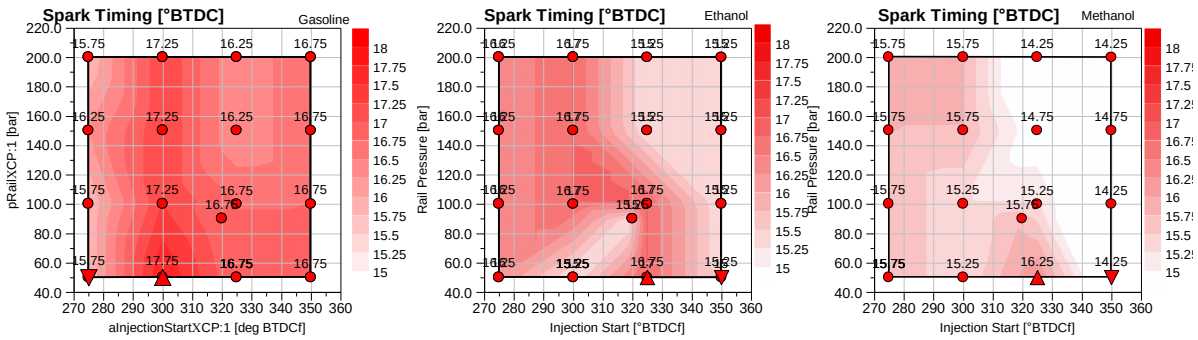

Figure 5-3 Spark Timing of gasoline, ethanol and methanol

The spark timing of gasoline is shown in the first diagram of Figure 5-3. The spark timing of gasoline is between 15.75CA BTDC and 17.75CA BTDC. The most advanced spark timing occurred when the injection starts 300CA BTDC and rail pressure at 50bar while the most retarded one happened at the injection timing 275CA BTDC, rail pressure 50bar. The reason why late injection and low rail pressure point got the most retarded spark timing is because the last injection causes there is insufficient time for air-fuel mixing. What's more, low injection pressure increases the droplet's size hence give negative effect on air-fuel mixing. At the other rail pressure, with the injection timing advanced from 275CA BTDC to 350CA BTDC, the spark timing was advanced from 16CA BTDC to more than 17CA BTDC since there is more time for air-fuel mixing.

Ethanol's spark timing is slightly retarded than gasoline when the CA50 is controlled at 8CA ATDC because ethanol's laminar flame speed is faster than gasoline. Also, at the same rail pressure, ethanol's injection duration is longer than gasoline since ethanol's lower heating value is lower than gasoline, and more fuel was injected into cylinder. The injection end timing of ethanol is also more retarded than gasoline, this is another reason why ethanol's spark timing is more retarded. The most retarded spark timing of ethanol is 15.25CA BTDC which happened at the test points whose injection timing is 350CA BTDC and 325CA BTDC, rail pressure at 100& 150bar. The most advanced spark timing is 16.75CA BTDC which occurred at some points whose injection timing are 300CA BTDC and 325CA BTDC. But only the point with injection timing 300CA BTDC and rail pressure 100bar gets the CA50 (shown in Figure 5-4) at 8CAD ATDC, the other points' spark timings are slightly retarded.

Methanol got the most retarded average spark timing since it has the fastest laminar flame speed of the three fuels. What's more, methanol got the longest injection duration of these three fuels so that more time is required for air-fuel mixing, and the fuel quantity is larger also causes the mixing time longer. The most advanced spark timing is 16.25CA BTDC which happened at injection timing 325CA BTDC and rail pressure 50bar and the most retarded spark timing of 14.25CA BTDC occurred at the early injection region.

In theory, keeping injection timing constant, increase rail pressure will cause the injection end timing advanced thus the spark timing is advanced. Also, the fuel's droplet becomes smaller which can enhance the quality of air-fuel mixture as a result of increasing rail pressure. But by looking through the spark timing of gasoline, ethanol and methanol, increasing rail pressure has a limit effect on spark timing. Even at earler and later injections, the spark timing remains the same as the rail pressure is changed.

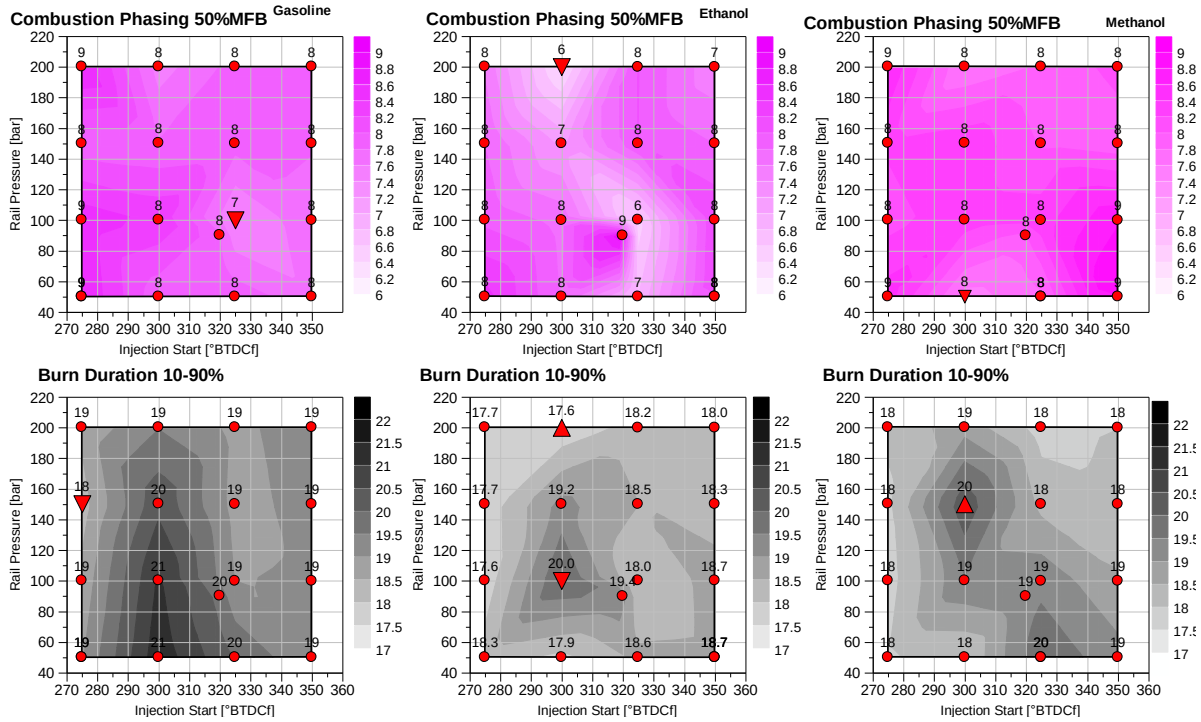

Figure 5-4 Mass fraction burn (MFB) and burn duration of gasoline, ethanol and methanol

On the first column of Figure 5-4, it shows the combustion phasing of all test points. All the test points at 2000rpm fuel matrix testing were run at by means of CA50 at 8 crank angle degree $ATDC_f$. Gasoline and methanol's CA50 were controlled better than ethanol, most of their test points' CA50 are around 8CAD ATDC. For ethanol, at injection timing 275CA BTDC rail pressure 200bar and injection start 300CA BTDC rail pressure 100bar, their spark timings still has some space to be retarded to get better fuel economies.

The burn duration of these three different fuels are shown in the second column of Figure 5-4. Gasoline has the burn duration from 18.2CAD to 21.3CAD. The shortest burn duration happened at the injection timing 275CA BTDC and rail pressure at 150bar while the longest burn duration happened at injection timing 300CA BTDC and rail pressure at 50bar. Ethanol's burn duration is between 17.6CAD to 20.0CAD. At the injection timing of 300CA BTDC, the minimum burn duration is achieved with a rail pressure at 200bar and the maximum point's rail pressure is 100bar. The minimum burn duration of methanol is 17.7CAD which happened at 275CA BTDC rail pressure 100bar while the maximum is 20.38CAD which occurred with the injection timing 300CA BTDC and rail pressure 150bar. Alcohol fuels got shorter average burn duration than gasoline since their laminar flame speed are faster than gasoline.

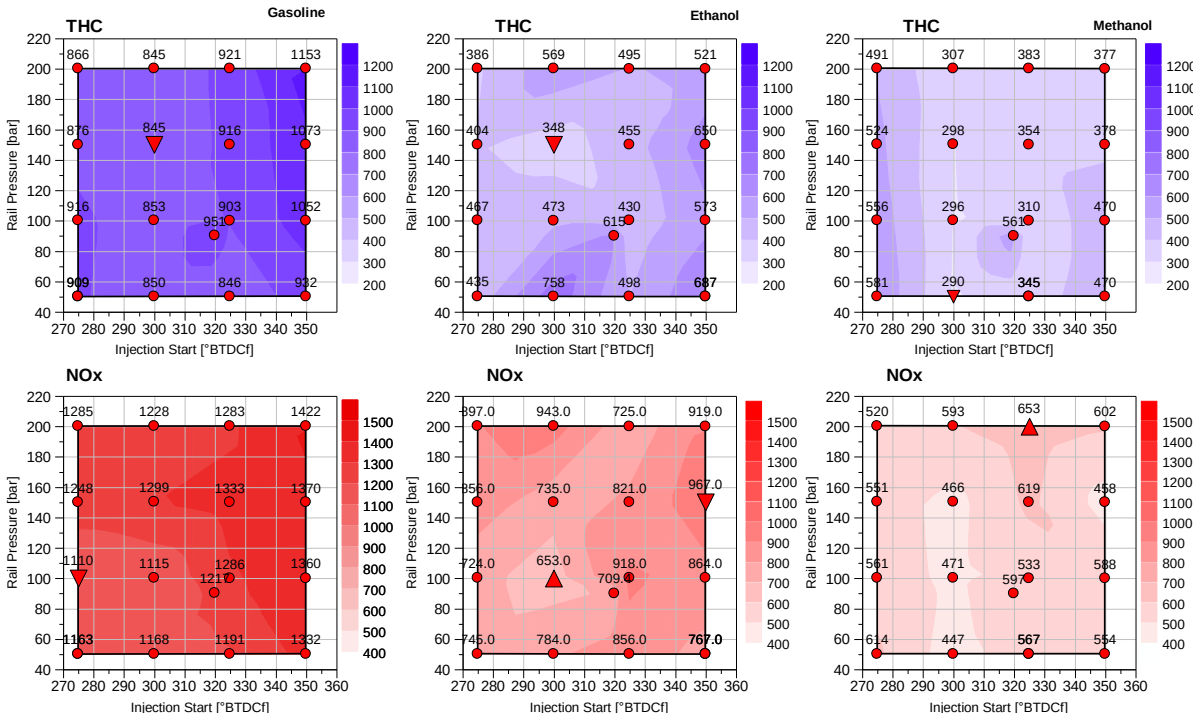

Figure 5-5 THC and NOx emission of fuel matrix

The THC released by gasoline, ethanol and methanol are shown in the first column of Figure 5-5. The THC produced by gasoline has the minimum value of 845ppm with the injection timing 300CA BTDC and rail pressure 150bar, the maximum THC 1153ppm happened at injection start 350CA BTDC and rail pressure 200bar. With earlier injection, the THC increased from 932ppm to 1153ppm with the rail pressure increased from 50bar to 200bar since the top of piston is close to the injector, and increased rail pressure will lead fuel propagate further thus more fuel will impingement on the piston. with the later injection, the THC decreased from 909ppm to 866ppm with the rail pressure increasing from 50bar to 200bar. This is because fuel droplet's size decreases with the rail pressure. At the same rail pressure, both early and late injections got higher THC than the other two injection timings since the injection timing between early and late have the advantage not only avoiding fuel impingement on the piston but also having enough timing for air-fuel mixing.

Ethanol got its lowest THC of 348ppm at injection timing 300CA BTDC, rail pressure 150bar. The maximum THC of 758ppm during the ethanol operation occurs with the injection timing 300CA BTDC and rail pressure 50bar. At the same injection timing, ethanol's THC decreased with the increases of rail pressure since higher rail

pressure can improve the quality of the air-fuel mixture. What's more, it is easier for ethanol to evaporate in the combustion chamber so that less fuel impingement on the top of the piston at high rail pressure conditions. The THC produced by methanol reaches the minimum of 290ppm with an injection timing 300CA BTDC and rail pressure 50bar and the maximum 581ppm happens at injection start 275CA BTDC and rail pressure 50bar. The average THC released by methanol is lower than ethanol and gasoline since its lowest boiling point. What's more, considering that the flame ionization detector (FID) is relatively insensitive to alcohol fuels, the effect on HC emissions is less clear. HC emissions trends for alcohol fuel blends are well documented to be misinterpreted when measured using conventional FIDs when oxygenates are present in the exhaust stream. Compare with gasoline, the lowest THC produced by ethanol decreases by 58.8% and methanol reduced by 65.7%.

The NO_x released by these three fuels are shown in the second column of Figure 5-5. Gasoline has its lowest NO_x at injection timing 275CA BTDC rail pressure 100bar which value is 1110ppm. The highest THC produced by gasoline located at injection start at 350CA BTDC and rail pressure 200bar and its value is 1422ppm. The NO_x released by ethanol has the highest value 967ppm with the start of injection at 350CA BTDC and the lowest NO_x 653ppm at injection timing 300CA BTDC and rail pressure 100bar. Methanol's NO_x reaches its highest NO_x emission of 653ppm when the injection timing is 325CA BTDC and the rail pressure 200bar whilst the lowest NO_x happened at injection start 300CA BTDC and rail pressure 50bar.

At the same fuel quantity, methanol's evaporation enthalpy is higher than ethanol and that of gasoline so more heat is absorbed by the alcohol fuel's evaporation than gasoline thus gasoline's exhaust gas temperature is higher than ethanol and methanol. What's more, because methanol's lower heating value is lower than ethanol and gasoline, more methanol was injected into the cylinder so that charge cooling effect is more obvious which will lower the exhaust gas temperature thus lowering the NO_x in the exhaust gas. Compare with gasoline, the lowest NO_x produced by ethanol decreases by 41.2% and methanol reduced by 58.7%.

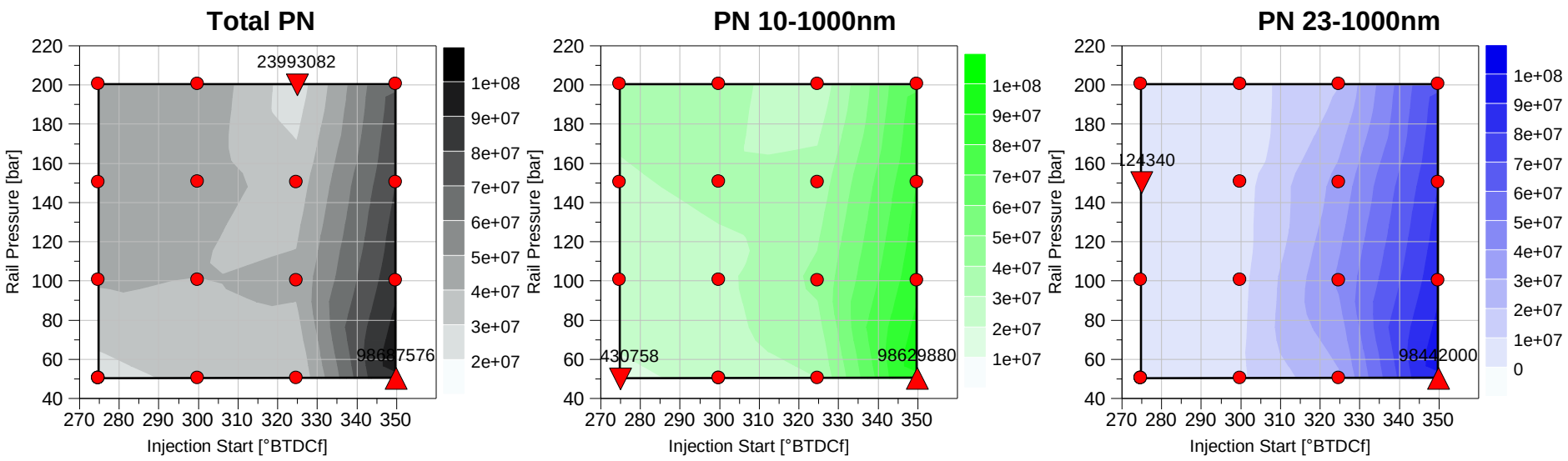

Figure 5-6 Particle numbers released by gasoline of different regulations

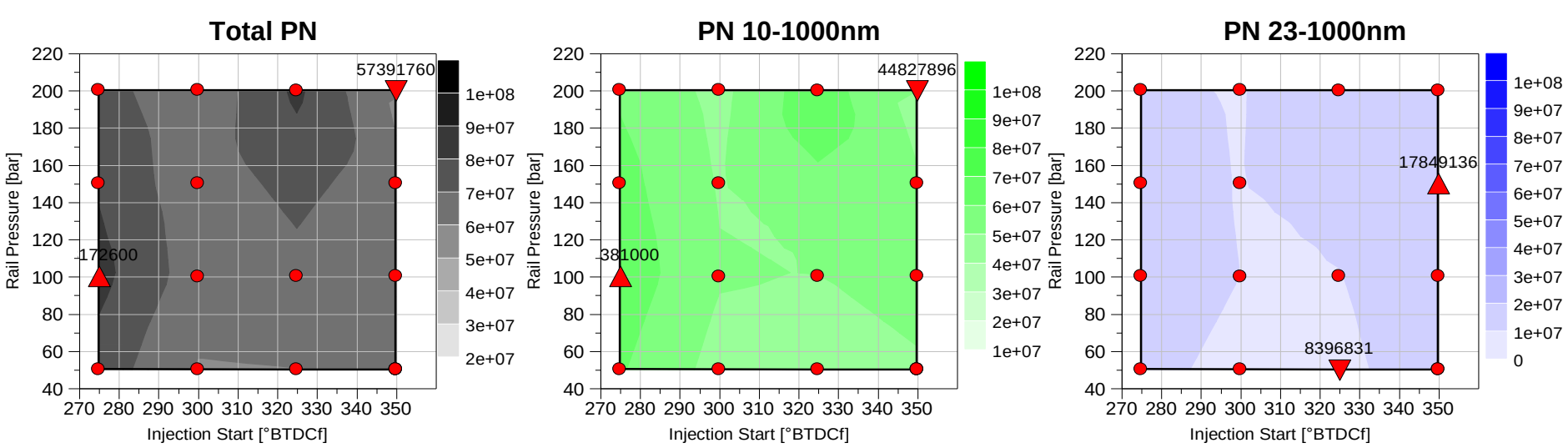

Figure 5-7 Particle numbers released by ethanol of different regulations

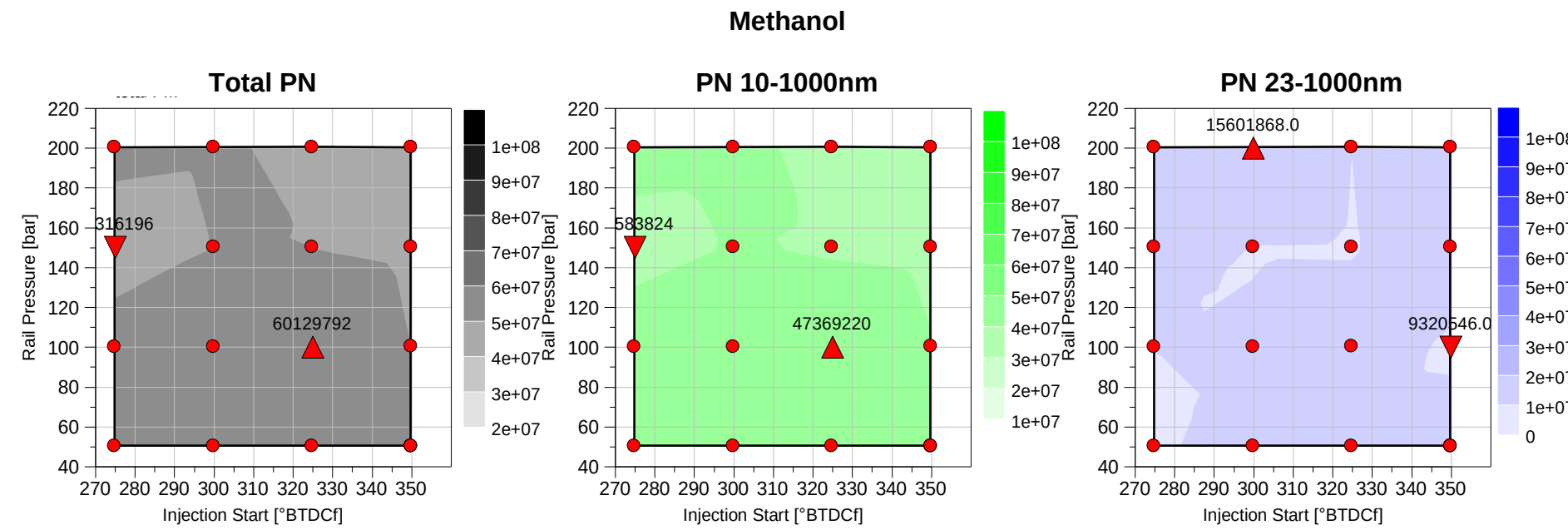

Figure 5-8 Particle numbers released by methanol of different regulation

The total PN produced by gasoline is shown in the first diagram of Figure 5-6. The lowest total PN achieved by gasoline is 2.4e7 which happened at injection start 325CA BTDC and rail pressure 200bar. The maximum total PN of gasoline occurred at injection timing 350CA BTDC and rail pressure 50bar and its value is 9.87e7. This is because early injection causes fuel impingement on the top of the piston. What's more, low rail pressure has a negative effect on air-fuel mixing thus more fuel impingement so that the total PN is high at this engine operation. In addition, low rail pressure will cause the injection duration longer which has negative effect on particle numbers. The second diagram shows the PN 10-1000nm which is the regulation of ERUO 5. PN 10-1000nm of gasoline got the lowest value 1.74e7 at injection timing 275CA BTDC and rail pressure 50bar while the highest value is 9.86e7 which located at injection start 350CA BTDC and rail pressure 50bar. Particle numbers of 23-1000nm is the regulation of EURO6. PN 23-1000 of gasoline has the lowest value 5.12e6 at injection start 275CA BTDC and rail pressure 150bar, and the highest PN 23-1000nm occurred at the same point with total PN and PN 10-1000 which value is 9.84e7.

Total PN produced by ethanol is shown in the first diagram of Figure 5-7. The lowest total PN achieved by ethanol is 5.74e7 which happened at injection start 350CA BTDC and rail pressure 200bar. The maximum total PN of gasoline occurred at injection timing 275CA BTDC and rail pressure 100bar and its value is 8.32e7. The second diagram shows the PN 10-1000nm. The maximum and minimum values of PN 10-1000nm have the same location with total PN whose values are 6.64e7 and 4.48e7. PN 23-1000 of ethanol has the lowest value 8.40e6 at injection start 325CA BTDC and rail pressure 50bar, and the highest PN 23-1000nm occurred at injection timing 350CA BTDC and rail pressure 150bar which value is 1.78e7. For ethanol, the best efficiency point (shown in figure 5-2) matches with the lowest PN size 23-1000nm.

Total PN produced by methanol is shown in the first diagram of figure 5-8. The lowest total PN achieved by methanol is 4.13e7 which happened at injection start 275CA BTDC rail pressure 150bar. The maximum total PN of methanol occurred at injection timing 325CA BTDC rail pressure 100bar and its value is 6.01e7. PN 10-1000nm of methanol got the lowest value 3.56e7 at injection timing 275CA BTDC rail

pressure 150bar while the highest value is 4.74e7 which is located at injection start 325CA BTDC rail pressure 100bar. PN 23-1000 of methanol has the lowest value 9.32e6 at injection start 325CA BTDC rail pressure 100bar, and the highest PN 23-1000nm occurred at injection timing 300CA BTDC and rail pressure 200bar which value is 1.56e7.

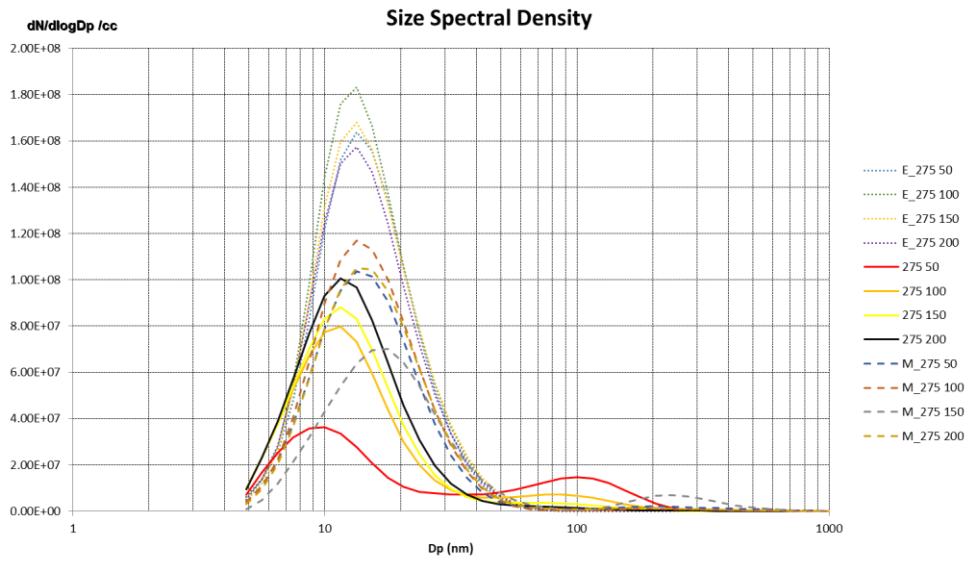

Figure 5-9 Size spectral density of gasoline ethanol and methanol injection start at 275CA BTDC

All the points' size spectral density which injection start at 275CA BTDC are shown in Figure 5-9. Apart from gasoline rail pressure at 50bar& 100bar and methanol injection pressure at 150bar, other curves have a single peak between 10 to 40nm, which mean that those particles are in nucleation mode. At gasoline rail pressure at 50bar& 100bar and methanol injection pressure at 150bar, the particle size distributions are characterised by dual-peak curves, most of particles are formed by nucleation mode with sizes between 5nm and 30nm, but there are also some particles fomed by the accumulation mode in the range of 100nm.

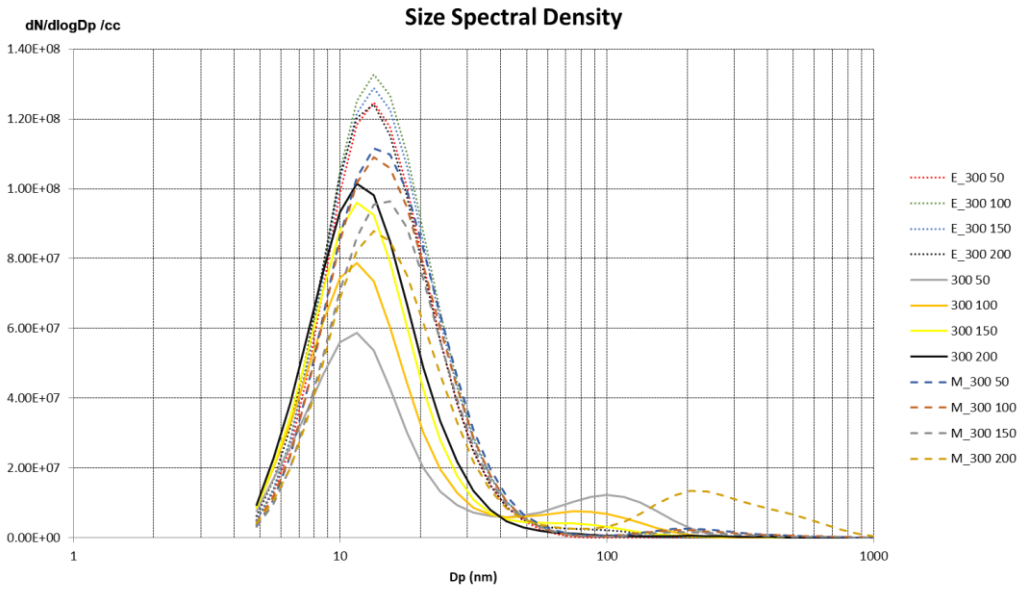

Figure 5-10 Size spectral density of gasoline ethanol and methanol injection start at 300CA BTDC

The size spectral density of the points with an injection timing of 300CAD BTDC are shown in Figure 5-10. Most of the particle's size is between 10 to 100nm by means of nucleation mode. Only the test point fueled by methanol which rail pressure is 200bar has some particles in accumulation mode. It is clear that ethanol release more smaller particles than methanol and gasoline at injection timing 300CAD BTDC.

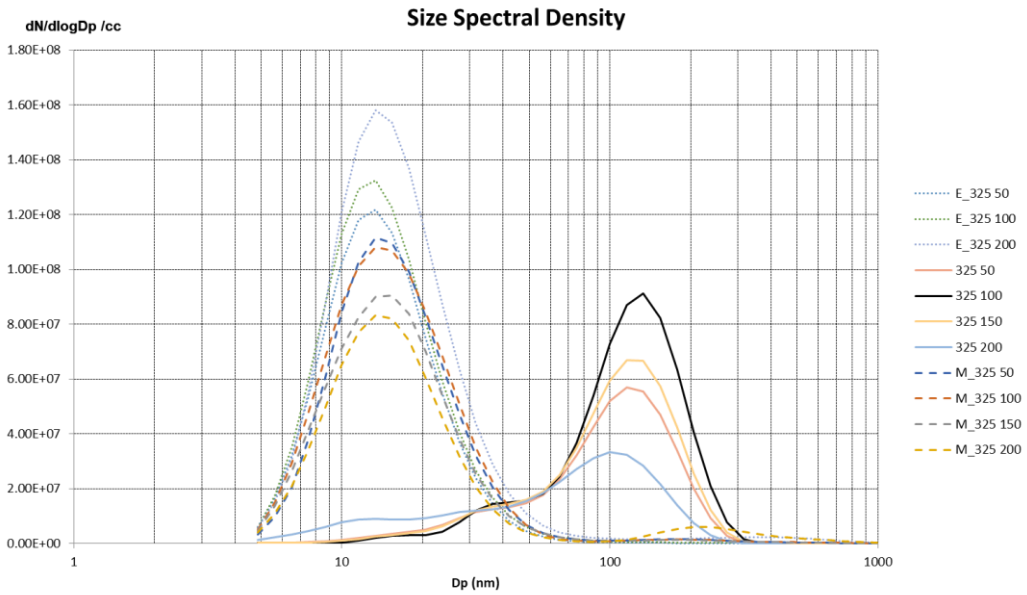

Figure 5-11 Size spectral density of gasoline ethanol and methanol injection start at 325CA BTDC

The size spectral density of the points which injection timing is 325CAD BTDC are shown in Figure 5-11. All the particles produced by ethanol and methanol whose size is less than 100nm are belong to nucleation mode. Also, with the increase of rail pressure, ethanol and methanol's PN decrease since higher injection pressure result in small fuel droplets which has positive effect on air-fuel mixing. Most particles released by gasoline are in accumulation mode.

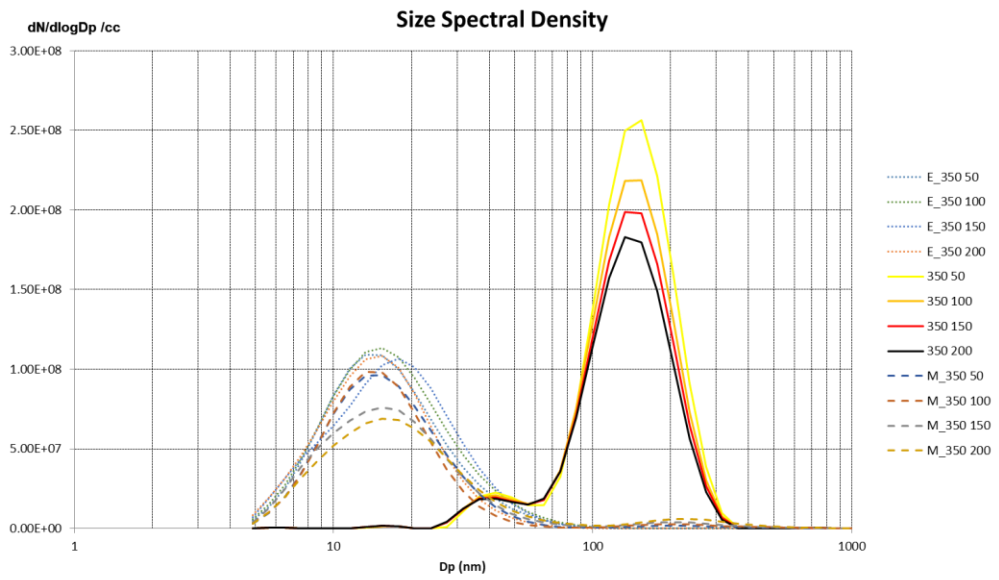

Figure 5-12 Size spectral density of gasoline ethanol and methanol injection start at 350CA BTDC

All the points' size spectral density with injection start at 350CA BTDC are shown in Figure 5-12. Ethanol and methanol's PN curves are mano-peak curves, and most of particle produced by them are smaller than 100nm so they are nucleation mode particles. Most particles released by gasoline their size is larger than 100nm by means of accumulation mode. What's more, at this injection timing, gasoline produces more particles than ethanol and methanol since this injection timing is too early and gasoline cannot evaporate as fast as alcohol fuel. As a result of this, some fuel impingement on the top of piston which causes big amount of particle emissions.

5.3.2 3000rpm 16bar IMEP Fuel Matrix Analysis

Compared with fuel matrix testing at 2000rpm 4.6bar IMEP, the 3000rpm 16bar IMEP testing is more critical since the speed is higher which causes a shorter time for air-fuel mixing and the load is higher will cause the fuel quantity injected into cylinder more than 2000rpm so that charge cooling effect play a more important during testing, there are more difference between gasoline, ethanol and methanol on fuel efficiency and emissions. On the other hand, more fuel means that the injection

duration is longer than 2000rpm 4.6bar IMEP so the injection end timing of ethanol and methanol are more retarded hence there is less time for air-fuel mixing. What's more, gasoline starts to knocking from 16bar IMEP according to the data from 3000rpm load sweep in the last chapter.

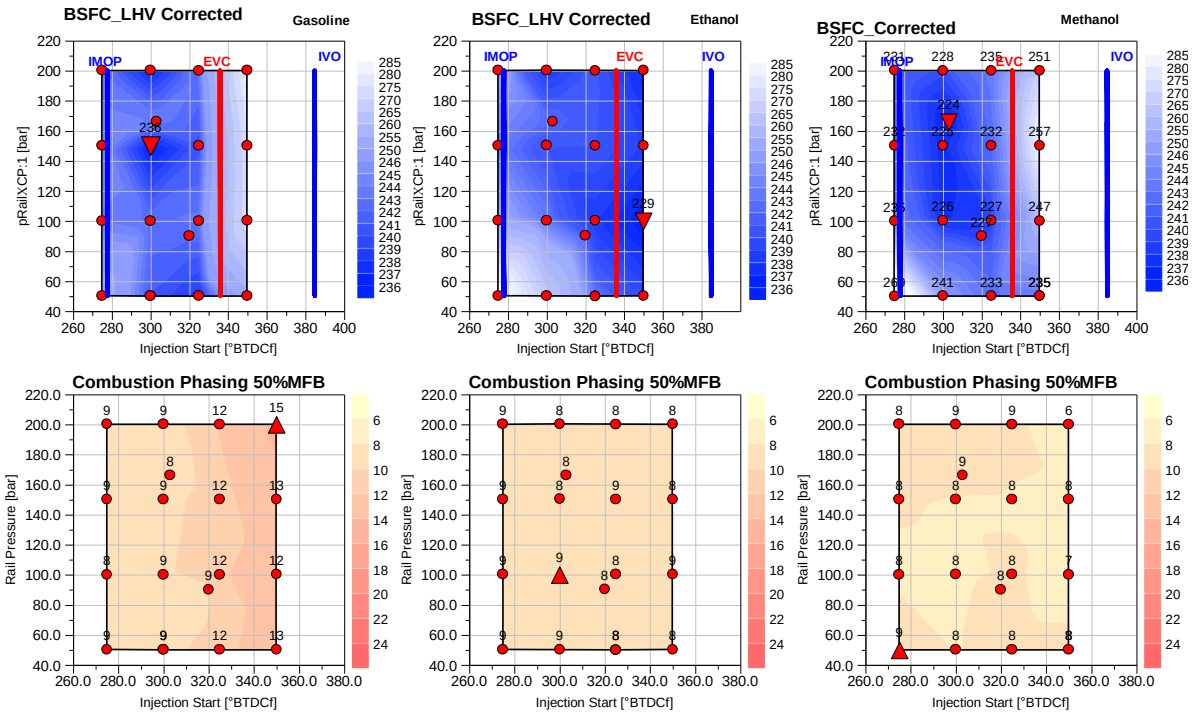

Figure 5-13 BSFC_cor and CA50 of gasoline, ethanol and methanol

The BSFC corrected by 42 of different fuels are shown in the first column of Figure 5-13. Gasoline's BSFC_cor is shown in the first diagram. The highest BSFC_cor of gasoline is 281g/kWh which happened at injection timing 350CA BTDC rail pressure 200bar, and the best BSFC point occurred at injection timing 300CA BTDC rail pressure 150bar which value is 236g/kWh. The best BSFC point occurred at a medium injection high rail pressure since the injection started not too early and too late so that less fuel would impingement on the cylinder wall and top of the piston. In addition, higher rail pressure will promote gasoline evaporation hence reducing impingement so that the BSFC_cor decreases. At late injection points which injection timing is 275 and 300CA BTDC, the BSFC_cor decreases with the increase of rail pressure since higher rail pressure can increase the penetration of fuel droplets in

cylinder. Also, high rail pressure has a positive effect on air-fuel mixing by promoting evaporating. Last but not the least, the injection duration is very long at low rail pressure so there is no sufficient time for air-fuel mixing. At the injection timing 325 and 350CA BTDC, the BSFC_cor increases with the increase of rail pressure since the piston is close to the top dead centre, increase rail pressure causes fuel impingement on the top of the piston hence pool fire. Another reason for the high BSFC_cor at early injection is because of knocking. Because early injection timing will result in air-fuel mixture staying in a high temperature and pressure environment for a long time which can lead to auto-ignition and knocking combustion. The 50% mass fraction burnt is shown in the second column of Figure 5-13. The CA50 becomes more retarded with the earlier injection. At the same rail pressure, with the advance of injection timing, BSFC_cor decrease firstly then increase. This is because earlier injectioin is more likely to cause fuel impingement on the piston top while late injection causes fuel impingement on cylinder wall.

The BSFC_cor of ethanol is shown in the second diagram of Figure 5-13. Compared with gasoline, ethanol has better anti-knock characteristics so that all the points were run at the MBT timing. The best BSFC_cor 229g/kWh happened at injection timing 350CA BTDC and rail pressure 100bar, and the worst BSFC_cor 261g/kWh occurred at injection timing 275CA BTDC and rail pressure 50bar. Compared with gasoline, ethanol's lower heating value is lower so that ethanol's injection duration is longer than gasoline at the same rail pressure. At the point injection start 275CA BTDC and rail pressure 50bar, ethanol got the shortest air-fuel mixing time since the injection is too late and injection duration is too long so that the BSFC_cor at this point is higher. In addition, the penetration of fuel is not further at low rail pressure which causes wall wetting hence pool fire. At early injection points (injection start 350CA BTDC), there is more time for air-fuel mixing. What's more, even the piston is very close to TDC at early injection points, but it's easier for ethanol to evaporate than gasoline so that less fuel impingement on the top of piston. At the same rail pressure, the BSFC_cor decreases with the advance of injection timing since there's more time for air-fuel mixing. Compared with gasoline, the lowest BSFC_cor of ethanol is reduced by 18.5%.

Methanol's BSFC_cor is shown in the third diagram of Figure 5-13. The best BSFC_cor 224g/kWh occurs at the reference point when the injection timing is 303CA BTDC and rail pressure at 166bar. This point's injection strategies were taken from 16bar IMEP 3000rpm load sweep. Beyond this reference point, the best BSFC_cor 225g/kWh happens at injection timing 300CA BTDC and rail pressure 100bar, similar to the reference point.The worst BSFC_cor is 269g/kWh which happened at injection timing 275BTDC and rail pressure 50bar. Because methanol has the lowest lower heating value of these three fuels, it has the longest injection duration and most retarded injection end timing. There is not only no enough time for air-fuel mixing but also fuel droplets penetration not further and results in fuel impingement on the cylinder wall hence pool fire. With retarded injection timings at 275 and 300CA BTDC, the BSFC_cor decreases with the increase of rail pressure since high rail pressure decreases the size of fuel droplets and makes the air-fuel mixture better. Moreover, because the injection timing is retarded, high rail pressure makes fuel penetrate further into cylinder and less fuel will impingement on the top of piston since the injection timing is late, the piston is far away from the top dead centre. At injection timing 350CA BTDC, the BSFC_cor increases with the rail pressure. That's because methanol has the longest injection duration compared with gasoline and ethanol at the same rail pressure, more fuel was injected into cylinder and some of them impinge on the piston. Compared with gasoline, the lowest BSFC_cor of methanol has reduced by 20.3%.

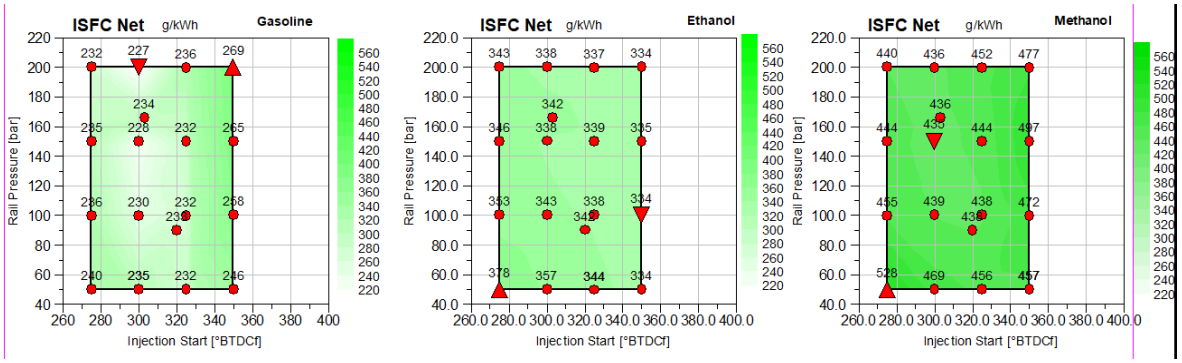

Figure 5-14 Indicate specific fuel consumption of gasoline, ethanol and methanol

The indicate specific fuel consumption (ISFC) of these three fuels are shown in Figure 5-14. The analysis of ISFC is similar to BSFC_cor. Because methanol's lower heating value is the highest while that of gasoline is the lowest so that methanol has the highest average ISFC since more fuel is needed to get the same power as ethanol and gasoline.

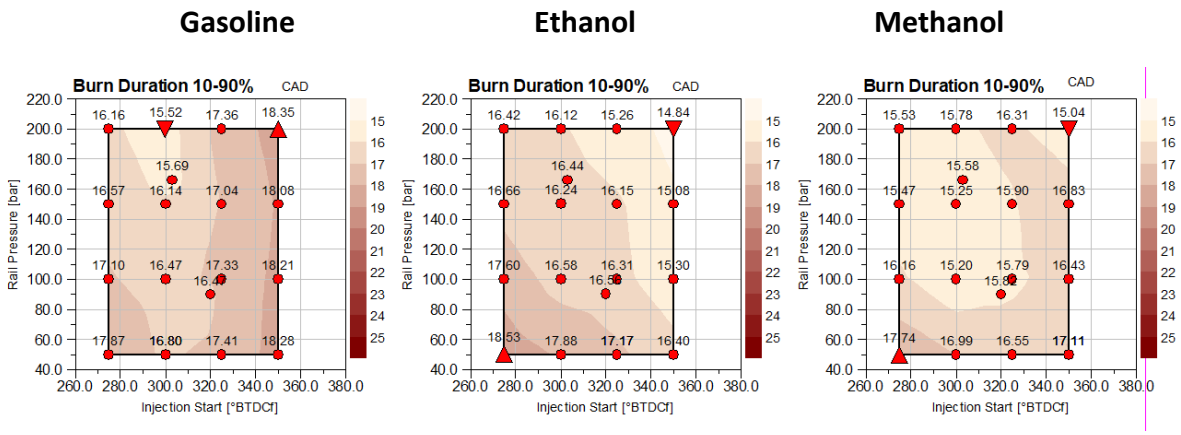

Figure 5-15 Burn duration of gasoline, ethanol and methanol

The burn duration of gasoline is shown in the first diagram of Figure 5-15. Gasoline has its shortest burn duration 15.52CAD with the start of fuel injection at 300CA BTDC and rail pressure at 200bar, and the longest burn duration 18.35CAD at injection start at 350CA BTDC and rail pressure at 200bar. The shortest and longest burn duration occurred at the same positions with the best and worst ISFC of gasoline. At injection timing 300CA BTDC and rail pressure of 200bar, the injection starts neither too early nor too late so that there is minimum fuel impingement on the piston and cylinder wall. Also, high rail pressure decreases the size of fuel droplets. At injection timing 300CA BTDC rail pressure 200bar, the air-fuel mixture quality is the best among all gasoline's fuel strategies so that all the heat can be released in the shortest time for the best fuel efficiency.

The longest burn duration point occurs with the most retarded combustion phasing. At late injection points (injection timing 275 and 300CA BTDC), the burn duration decreases with the increase of rail pressure since the air-fuel mixture quality increase. After that, all points whose injection timing before 325CA BTDC (including

325CA BTDC) have their burn duration longer than 17CAD since injection timing is advanced and pre-ignition caused knocking at these control strategies.

Ethanol got its shortest burn duration 14.84CAD at injection timing 350CA BTDC and rail pressure 200bar, and its longest burn duration 18.53CAD at injection timing 275CA BTDC and rail pressure 50bar. At early injection and low rail pressure condition, because of ethanol's lower LHV, the injection duration is longer than gasoline so that there's no sufficient time for air-fuel mixing properly, and that's why ethanol got its worst in-cylinder combustion result. At early injection high rail pressure points, ethanol got its shortest combustion duration since there is sufficient time for air-fuel mixing properly and high rail pressure reduce the size of fuel droplets which can also improve air-fuel mixture quality. The laminar flow speed of ethanol is faster than gasoline so that the average burn duration of fuel matrix testing is shorter than gasoline.

Methanol got its shortest and longest combustion duration at the same fuel injection timing and pressure as ethanol and the reasons why those points got the shortest and longest burn duration are also similar to methanol. But methanol has the fastest laminar flow rate of these three fuels so that methanol got the shortest average combustion duration. The shortest combustion duration point could burn even faster since its CA50 is at 6CAD ATDC, if the ignition timing is slightly retarded, the heat could release in a shorter time.

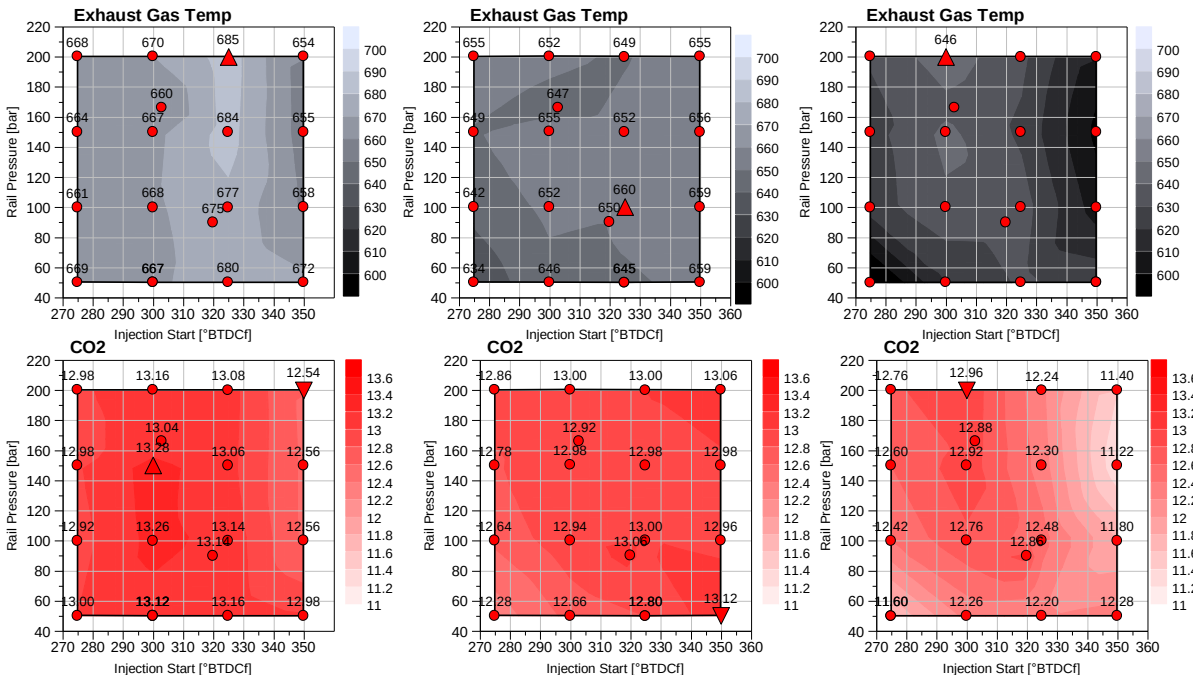

Figure 5-16 Exhaust gas temperature and CO2

The exhaust gas temperature is shown in the first column of Figure 5-16. Exhaust gas temperature can reflect the in-cylinder combustion temperature. The highest exhaust gas temperature 685°C of gasoline happened at injection timing 325CA BTDC and rail pressure 200bar which value is. The lowest exhaust gas temperature 654°C occurred at injection timing 350CA BTDC and rail pressure 200bar. The highest point got the longest combustion duration since its spark timing was retarded to avoid knocking. The lowest point even got a longer duration but its injection timing is between the intake valve open (IVO) and exhaust valve close (EVC), some fuel droplet was absorbed into the exhaust manifold so that lean combustion happened at that moment, and the in-cylinder temperature is lower than stoichiometric combustion. That's why this point got the lowest exhaust gas temperature even though its combustion duration is longer than that of the highest point.

Ethanol's got its highest exhaust gas temperature 660°C at injection timing 325CA BTDC and rail pressure 100bar, while the lowest exhaust temperature 634°C is at injection timing 275CA BTDC and rail pressure 50bar. Ethanol's average exhaust gas temperature is lower than gasoline since the enthalpy of evaporation is higher than gasoline and more heat is absorbed during the evaporation process compare

with the same quantity of gasoline. What's more, more ethanol is injected into cylinder and more heat is absorbed then causing lower in-cylinder temperature and thus lower exhaust gas temperature.

Methanol got its highest exhaust gas temperature 646°C at injection timing 300CA BTDC and rail pressure200bar, and its lowest exhaust gas temperature 583°C happened at injection timing 275CA BTDC rail pressure 50bar. Methanol got the lowest average exhaust gas temperature since it has the highest enthalpy of evaporation.

The CO_2 released by gasoline is shown in the second column of Figure 5-16. The highest CO_2 of gasoline happened at injection timing 300CA BTDC rail pressure 150bar which value is 13.26% vol. The lowest CO_2 produced by gasoline 12.54% vol located at injection timing 350CA BTDC rail pressure 200bar. The lowest CO_2 happened at early injection high rail pressure point is because this injection timing is between the intake valve open and the exhaust valve close, some fuel is absorbed in the exhaust pipe and an lean combustion is formed as a result of this. What's more, increases lambda will cause a decrease in CO_2 content in the exhaust gas. That's why the CO_2 released by early injection points are lower than at other points. At injection timing 350CA BTDC, CO_2 decreases with the increase of rail pressure. This is because the injection duration is shorter with the increase of rail pressure then more fuel is absorbed into the exhaust pipe at higher injection pressure, there's still some time for fuel injection after EVC at low injection pressure points so that the lambda at high rail pressure is greater than low rail pressure so that CO_2 decreases.

The CO_2 released by ethanol has the greatest value of 13.12%vol at injection timing 350CA BTDC and rail pressure 50bar, and the minimum CO_2 happened at injection timing 275CA BTDC and rail pressure 50bar which value is 12.28%vol. The average CO_2 released by ethanol is lower than gasoline since ethanol leads to lower specific CO_2 because of CO_2's energy-specific basis (g CO_2/MJ). Compared with gasoline, the lowest CO_2 released by ethanol has dropped by 2.07%.

The CO_2 released by methanol has the greatest value of 12.96%vol at injection timing 300CA BTDC and rail pressure 2000bar, and the minimum CO_2 occurred at injection timing 350CA BTDC rail pressure 150bar which value is 11.22%vol. The

average CO_2 released by methanol is lower than gasoline and ethanol since methanol leads to 7% lower specific CO_2 emissions compared to gasoline. Compared with gasoline, the lowest CO_2 released by methanol has dropped by 10.5%.

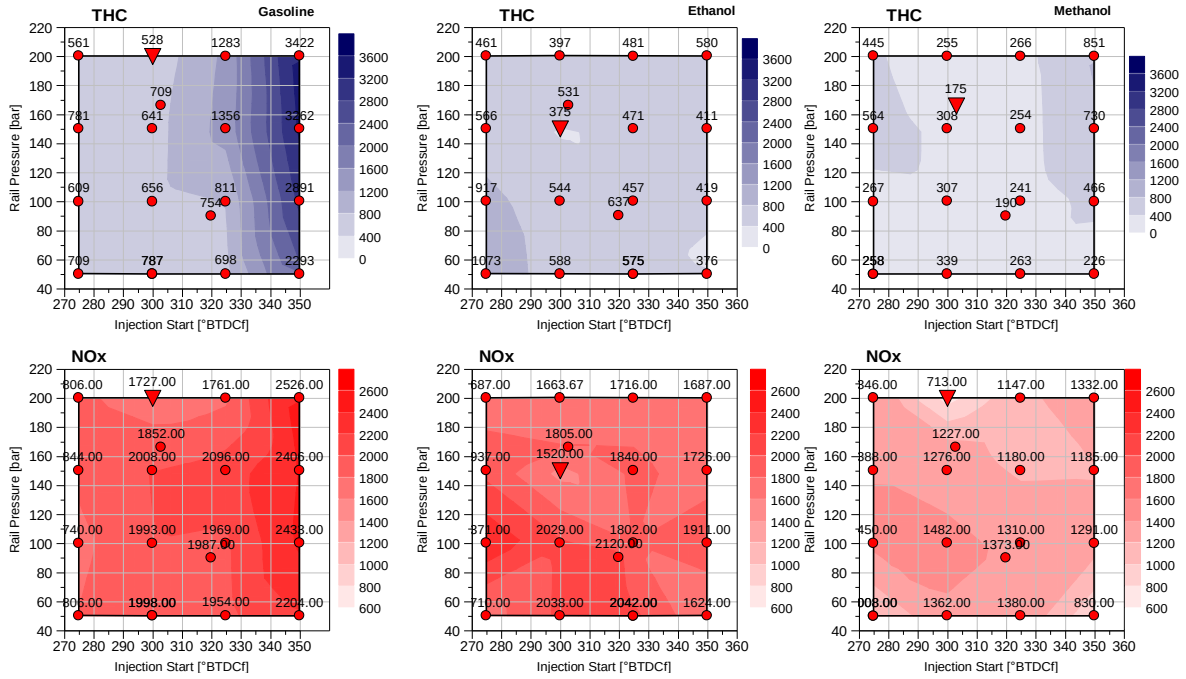

Figure 5-17 THC and NOx released by gasoline, ethanol and methanol

The THC released by gasoline is shown in the first diagram of Figure 5-17. Gasoline got its lowest THC at injection timing 300CA BTDC and rail pressure 200bar which value is 528ppm. The highest THC produced by gasoline is 3422ppm. The reason why THC is high at injection early region is because at early injection timing the distance between injector and piston is very short which causes a big amount of unburned fuel impingement on the top of the piston. At injection start at 325CA BTDC and 350CA BTDC, with the increase of rail pressure THC also increase since fuel droplets penetrate further at high rail pressure, but the piston is close to the injector at this stage so that THC increases. At injection starts at 275CA BTDC and 300CA BTDC, THC decreases with the increase of rail pressure since the piston is far from the injector at this region, increase rail pressure causes the size of fuel

droplets smaller hence better to evaporate so that fewer fuel droplets impingement on the cylinder wall and THC drops as a result of this.

The THC produced by ethanol is shown in the second diagram of Figure 5-17. The maximum THC 1073ppm released by ethanol happened at injection start 275CA BTDC and rail pressure 50bar, and the lowest THC is 375ppm which occurred at injection timing 300CA BTDC rail and pressure 150bar. Because ethanol's lower heating value is lower than gasoline, ethanol got more retarded injection end timing at late injection low rail pressure point. As a result of this, a big amount of unburned ethanol impingement on the cylinder wall which causes high THC. At injection timing 275, 300 and 325CA BTDC, THC decreases with the increase of rail pressure since the fuel droplets' size is smaller at high rail pressure, and it's easier for smaller droplets to evaporate. At injection timing 350CA BTDC, THC increases with the increase of rail pressure since the piston is close to the injector at early injection points, high rail pressure causes ethanol impingement on the top of the piston which results in high THC. From the 3D legend, it is clear that the average THC produced by ethanol is lower than that of gasoline since ethanol is easier to evaporate so that less fuel impingement on the cylinder wall and piston. Compare with gasoline, the lowest THC released by ethanol dropped by 28.9%.

THC released by methanol is shown in the last diagram in column 1 of Figure 5-17. The highest THC happened at injection timing 350CA BTDC rail pressure 200bar which value is 851ppm. The lowest THC released by methanol is 175ppm occurred at injection start 303CA BTDC rail pressure 166bar which is the reference point (same injection strategy with 3000rpm 16bar during load sweep). There are two reasons why the highest THC happened at early injection high rail pressure points. The first is because fuel has further penetration at high rail pressure which causes a big amount of methanol impingement on the top of the piston. The second reason is that methanol's lowest LHV result in the longest injection duration which will also increase the fuel impingement on the piston when the piston is close to the injector. The first reason has more influence on the THC so that at injection starts 350CA BTDC, THC increases with the increase of rail pressure. Methanol got the lowest average THC during 3000rpm fuel matrix testing since it's the easiest to evaporate so that less fuel impingement on the piston and cylinder wall compared with ethanol

and gasoline. The lowest THC released by methanol has reduced by 66.9% compared with gasoline.

For gasoline, ethanol and methanol, the lowest THC all occurred at injection timing 300CA BTDC and rail pressure 150bar and 200bar since injection is not too early to have fuel impingement on the piston, and not too late to produce fuel impingement on the cylinder wall. What's more, high rail pressure has a good effect on promoting evaporate which can also decrease THC.

The NO_x released by gasoline, ethanol and methanol is shown in the second column of Figure 5-17. Gasoline has its highest NO_x of 2526ppm which happened at injection timing 350CA BTDC and rail pressure 200bar, and the lowest NO_x which occurred at injection timing 300CA BTDC and rail pressure 200bar. With the injection timing advanced from 300CA BTDC to 325CA BTDC, NO_x increases because the knocking happened from injection start 325CA BTDC hence their spark timings are retarded so that burn duration increases, and in-cylinder temperature increases which causes NO_x in the exhaust gas increase. The NO_x at injection timing 350Ca BTDC is higher than other injection timing is because this injection starts during the overlap (when both intake valve and exhaust valve open), some fuel is absorbed into the exhaust pipe then causes lean combustion so that the NO_x is high at this region. At injection start 350CA BTDC, the NO_x increases with the increase of rail pressure since more fuel is injected before the exhaust valve closed and lambda increases with the rail pressure hence NO_x increases.

The NO_x released by ethanol has the maximum value 2371ppm at injection timing 275CA BTDC rail pressure 100bar, and its lowest NO_x 1520ppm occurred at injection timing 300CA BTDC rail pressure 150bar. From figure's colour, it's clear that the average NO_x value is lower than that of gasoline since the in-cylinder temperature is lower. Ethanol has higher evaporation enthalpy, more heat is absorbed during the evaporation process compared with the same amount of gasoline. Also, because the lower heating value of ethanol is lower than gasoline, more fuel is injected into the cylinder to get the same power as gasoline so that the charge cooling effect is more effective than gasoline.

Methanol got its highest NO_x 1482ppm at injection timing 300CA BTDC rail pressure 100bar and the best NO_x point at injection timing 300CA BTDC rail pressure 200bar. Methanol releases the lowest NO_x of these three fuels since its best evaporation enthalpy and lowest lower heating value. Compared with gasoline, the lowest NO_x released by ethanol is reduced by 11.9% and 58.7% for that of methanol.

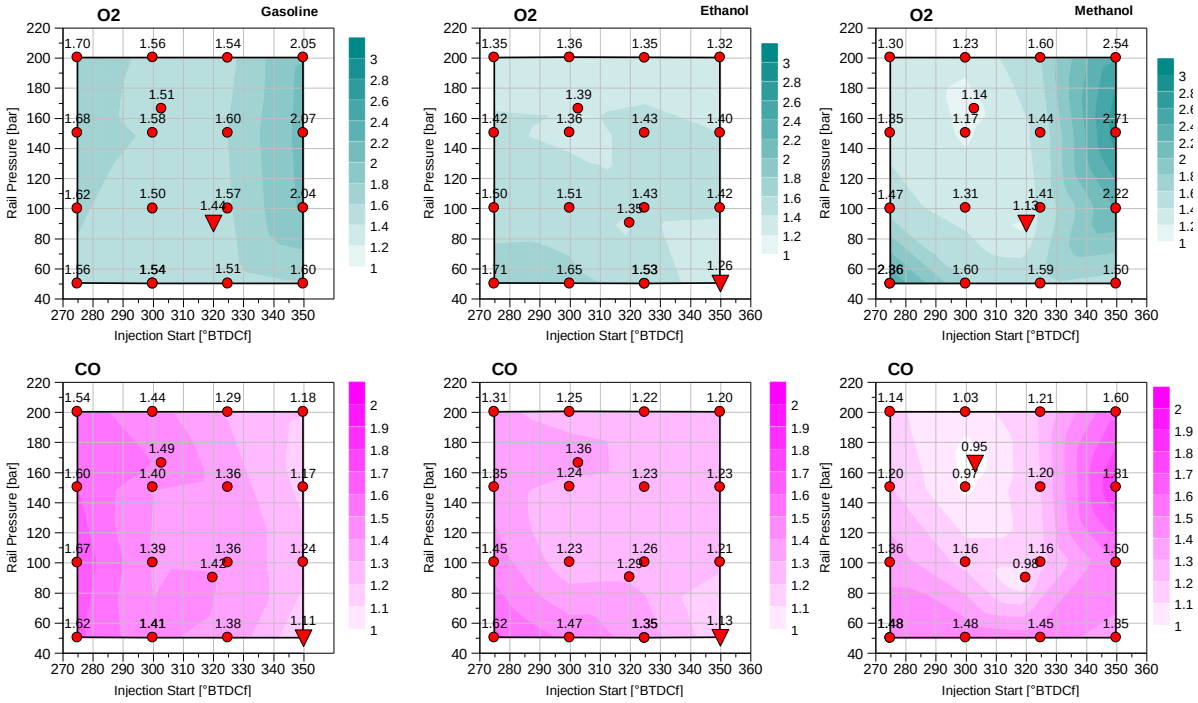

Figure 5-18 O2 and CO released by gasoline, ethanol and methanol

The O_2 data is shown in the first column of Figure 5-18. Gasoline got its highest O_2 2.07 Vol% at injection timing 350BTDC and rail pressure 150bar, and the lowest O_2 happened at injection timing 320CA BTDC and rail pressure 90bar which value is 1.44 Vol%. The point which got the lowest O_2 is another reference point which injection timing and rail pressure is the same as the idle mode. The O_2 data at injection start 350CA BTDC can also reflect that the in-cylinder combustion states are oxygen-rich since the O_2 released at this region is higher than that of other injection timings.

Ethanol has its highest O_2 1.71 vol% at injection timing 275CA BTDC and rail pressure 50bar since late injection timing and low rail pressure which causes long

injection duration result in fuel impingement so that this point is oxygen-rich. The lowest O_2 occurred at injection timing 350CA BTDC rail pressure 50bar which value is 1.26vol%.

The O_2 released by methanol has its highest value of 2.71vol% at injection timing 350CA BTDC and rail pressure 150bar. The lowest O_2 occurred at the same position as gasoline which value is 1.13vol%. There are two oxygen-rich regions during methanol's testing. The first one is at injection timing 275CA BTDC rail pressure 50bar since low injection pressure results in longer injection duration which causes big amount of fuel impingement on the cylinder wall, then there's excess oxygen. Another high oxygen region is at injection timing 350CA BTDC. There are two reasons why this region has excess oxygen. The first one is that this injection timing is between the intake valve open and exhaust valve close which causes fuel droplets absorbed into the exhaust pipe. The second reason is that at high rail pressure, fuel droplets have further penetration but the piston is very close to the injector at early injection so that fuel impingement on the top of piston so that there is excess oxygen.

The second column of Figure 5-18 shows the CO released by gasoline, ethanol and methanol. Gasoline has its highest CO at injection timing 275CA BTDC and rail pressure 100bar, while the lowest CO occurred at injection timing 350CA BTDC rail pressure 50bar which value is 1.11vol%. Ethanol has its best CO 1.13vol% produced at injection timing 350CA BTDC and rail pressure 50bar, and the worst CO 1.62vol% happened at injection timing 275CA BTDC rail pressure 50bar. The CO released by methanol has its lowest value 0.95vol% at injection timing 303CA BTDC and rail pressure 166bar. The highest CO released by methanol happened at injection timing 350CA BTDC and rail pressure 150bar which value is 1.81vol%.

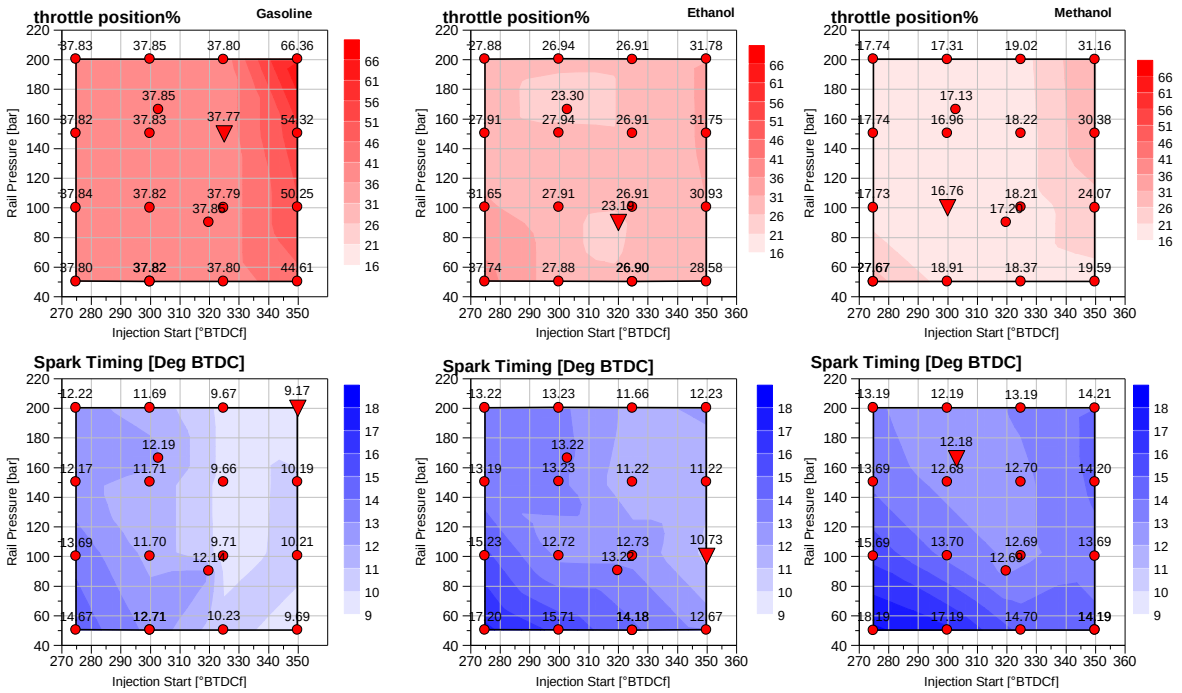

Figure 5-19 Throttle position and spark timing

The throttle position of gasoline, ethanol and methanol are shown in the first column of Figure 5-19. From the figure, it's easy to find that more throttle is opened for gasoline than ethanol and methanol since gasoline's stoichiometric air-fuel ratio (14.7:1) is higher than that of ethanol (9:1) and methanol (6.5:1) so that more air is needed to get stoichiometric combustion for gasoline. What's more, because ethanol and methanol have higher evaporation enthalpy as well as lower LHV so that the better charge cooling effect will result in lower intake air temperature so that methanol has the highest intake air density, and that of ethanol is also higher than gasoline. That's why gasoline's throttle position is more open than ethanol and methanol. For gasoline, the widest throttle open point is at injection timing 350CA BTDC and rail pressure 200bar. At injection timing 350CA BTDC, their throttle was open wider than other injection timings since engine has knocking at that injection timing so that their spark timing were retarded. Because these points were not running at MBT, more air and fuel are needed to get the same power as the other test points. Ethanol has its widest open throttle at injection timing 275CA BTDC and rail pressure 50bar since early injection cannot provide enough time for fuel evaporation. What's more, low injection pressure results in bigger fuel droplet size which also gives negative effect on evaporation. Combining the above reasons, the

charge cooling effect of this point is not good enough which decreases the intake air's density, and the throttle opens more as a result of this. Either advancing the injection timing or increasing rail pressure will reduce the throttle position which is also shown in Figure 5-19.

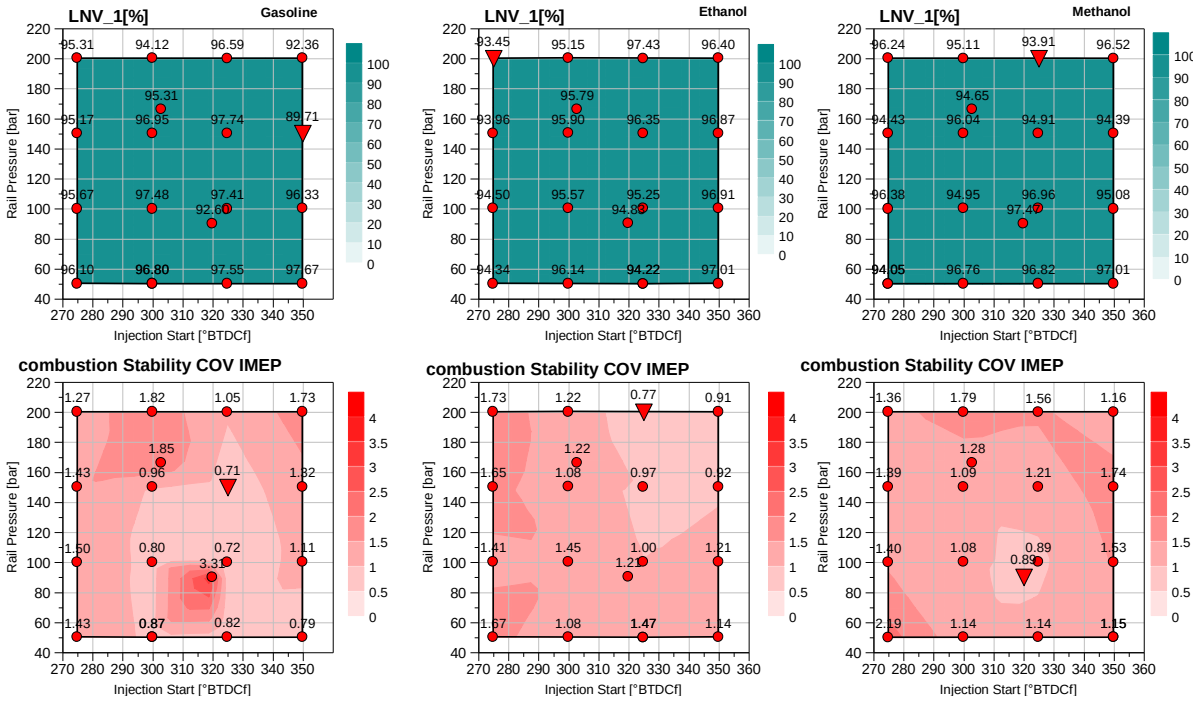

Figure 5-20 LNV and combustion stability of gasoline, ethanol and methanol

The LNV is a parameter which shows the trend to misfire and there is more chance to have misfire when LNV is lower than 90% so that the lowest valve of LNV is more focused. Gasoline got its lowest LNV at injection timing 350CA BTDC rail pressure 150bar which value is 89.71%, and it's more potential for this point to have misfire. Only this point has its LNV lower than 90% because injection timing is early, air-fuel mixture with high temperature and high pressure stay in the cylinder for a long time hence cause knocking, the spark timing of this point is needed to be slightly retarded. The lowest LNV for ethanol and methanol are 93.45% and 93.91%, both of them is greater than 90% so there's a small chance for ethanol and methanol to have misfire.

The combustion stability is shown in the second column of Figure 5-20. Only one point fuelled by gasoline with injection timing 320CA BTDC and rail pressure 90bar has its Coefficient of Variation (COV) IMEP greater than 3 as a result of knocking, the spark timing of this point should be slightly retarded to reduce COV IMEP less than 3.

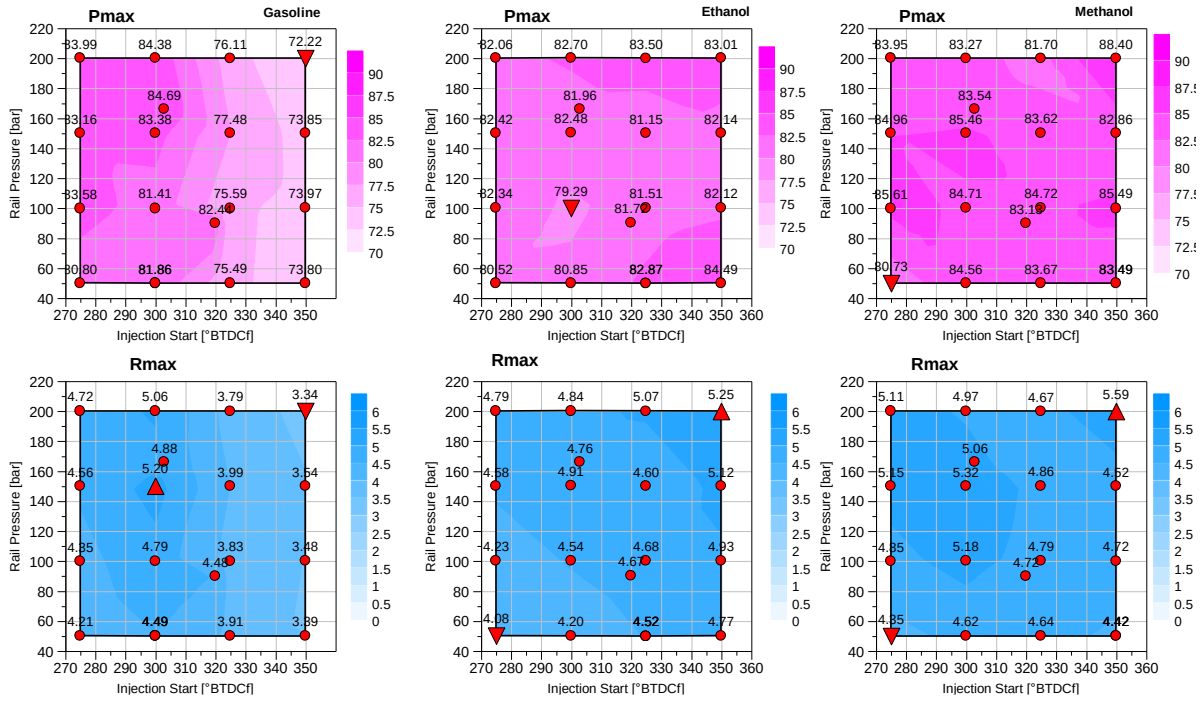

Figure 5-21 Peak in-cylinder pressure and maximum pressure rise rate

The peak in-cylinder pressure and the maximum pressure rise rate of gasoline, ethanol and methanol opearations are shown in Figure 5-21. Gasoline has its lowest P_{max} at injection timing 350CAD BTDC rail pressure 200bar since its combustion phasing is retarded as a result of knocking. Because of ethanol and methanol's anti-knock characteristic, their combustion phasing are more advanced than gasoline so their average P_{max} are higher than that of gasoline. The R_{max} of ethanol and methanol are also higher than gasoline and the description is the same with P_{max}.

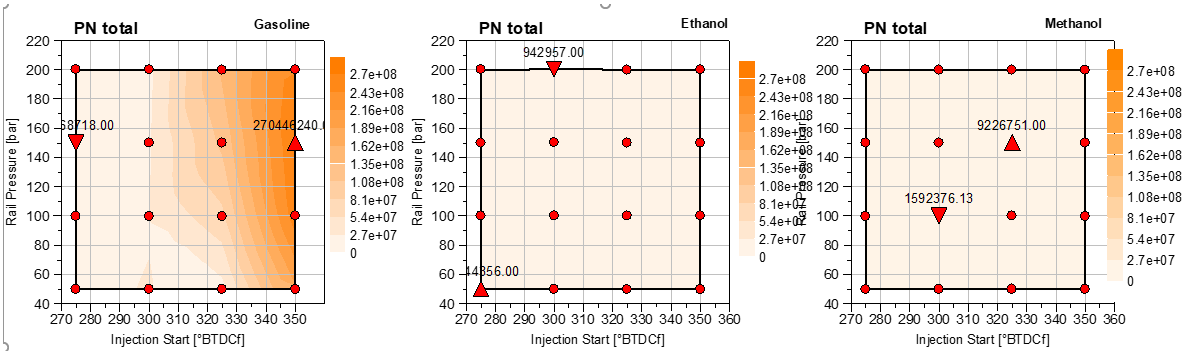

Figure 5-22 Total particle number of gasolines, ethanol and methanol

The total particle number of gasoline and alcohol fuel are shown in Figure 5-22. Gasoline got its lowest PN at injection timing 275CAD BTDC and rail pressure 150bar which value is 1.36e7. The highest PN released by gasoline is at injection timing 350CAD BTDC rail pressure 150bar, and the maximum PN is 2.7e8. For gasoline, with the advance of injection timing, the total PN increase because of early injection causes fuel impingement on the cylinder wall. What's more, with the increase of rail pressure, particles produced by gasoline increase since fuel propagates further into the cylinder which causes fuel impingement on the top of the piston hence the particle emission increase. Ethanol has its lowest PN at injection timing 300CAD BTDC rail pressure 200bar which value is 9.4e5, and its highest PN at injection timing 275CAD BTDC and rail pressure 50bar. There are two reasons why the late injection and low injection pressure have the highest PN. The first one is that ethanol's injection timing is longer than gasoline so its injection end timing is more retarded than gasoline, resulting in less timing for air-fuel mixing. The second reason is that lower rail pressure causes larger fuel droplets which has negative effect on air-fuel mixing.

5.4 Summary

In this chapter, a series of fuel injection parameter characteristic matrix testing was carried out for all three fuels in order to evaluate the effect of injection strategies on the combustion characteristic, efficiency and emissions. The experiment was

separated into two groups, the first one was running at 2000rpm 4.6bar IMEP, and the second one was running at 3000rpm 16bar IMEP. All the tests were running at stoichiometric and the 50% mass fraction burn is controlled at MBT except knocking.

The injection parameter was found has little impact on the combustion and emission at the 2000rpm 4.6bar IMEP operation, and combustion characteristic and combustion efficiency are similar between gasoline, ethanol and methanol. Ethanol and methanol's combustion efficiency is slightly higher because of their slightly faster flame speed. THC released by alcohol fuel is lower than gasoline since alcohol fuel's better evaporation character and FID. What's more, NO_x produced by ethanol and methanol is also lower since more heat is absorbed during evaporation. The particulate emission of alcohol fuels is also lower. For ethanol, the best efficiency point matches the lowest PN size 23-1000nm, and methanol's best efficiency condition also has the lowest total PN and PN 10-1000nm.

At the 3000rpm 16bar IMEP fuel operation, there are more differences between alcohol fuel and gasoline. Because ethanol and methanol's higher RON values, they don't have knocking combustion. But alcohol fuel's LHV is lower than gasoline, so their injection durations are longer than gasoline hence there's less time for air-fuel mixing. Therefore, ethanol and methanol have their lowest combustion efficiency at injection timing 275CAD BTDC and rail pressure 50bar because air fuel does not mix properly. But ethanol and methanol's peak efficiency area are still larger than gasoline. Alcohol fuel still produces fewer emissions than gasoline during the 3000rpm 16bar IMEP fuel matrix testing.

6. Chapter Six: Analysis of the Spark Retard Capability of Alcohol Fuels for Fast Catalyst Light-off

6.1 Introduction

Nowadays, most modern ICE vehicle calibrations utilise a catalyst light off strategy to be able to conform to modern legislative drive cycle regulations. The final study on the alcohol fuels was a lower temperature spark retard sweep under steady state conditions. This test is aimed to find the most retarded spark timing and the maximum exhaust gas temperature during the spark sweep for the catalyst light off.

6.2 Experimental Set-up

The engine was operated at 1500rpm 2bar IMEP with the coolant temperature, oil temperature as well as intake temperature kept below 40°C, as shown in Table 6.1. As the spark timing is retarded, combustion becomes more unstable. The test was continued until the coefficient of variation (COV) IMEP achieved 15% then stopped.

Table 6-1 Fuel matrix test point

Speed& load	IMOP	EMOP	SOI (CAD BTDCf)	Rail Pressure(bar)	Spark timing	Lambda	Coolant temperature	Oil temperature
1500rpm 2bar	120	110	320	60	DBL	1	40°C	40°C

6.3 Result and discussion

The IMEP standard deviation which can reflect the combustion stability is shown in Figure 6-1a. Gasoline's IMEP_SD increases from 0.02bar to 0.30bar with the spark timing retarded. That of ethanol increases from 0.03bar to 0.24bar and methanol's IMEP_SD increases from 0.02bar to 0.19bar as the spark timing is retarded. Ethanol's stability is slightly worse than gasoline when the combustion phasing CA50, is retarded from 8CAD ATDC to 15CAD ATDC. After that, ethanol performed better during the rest of the test. Methanol has the best combustion stability at all test points.

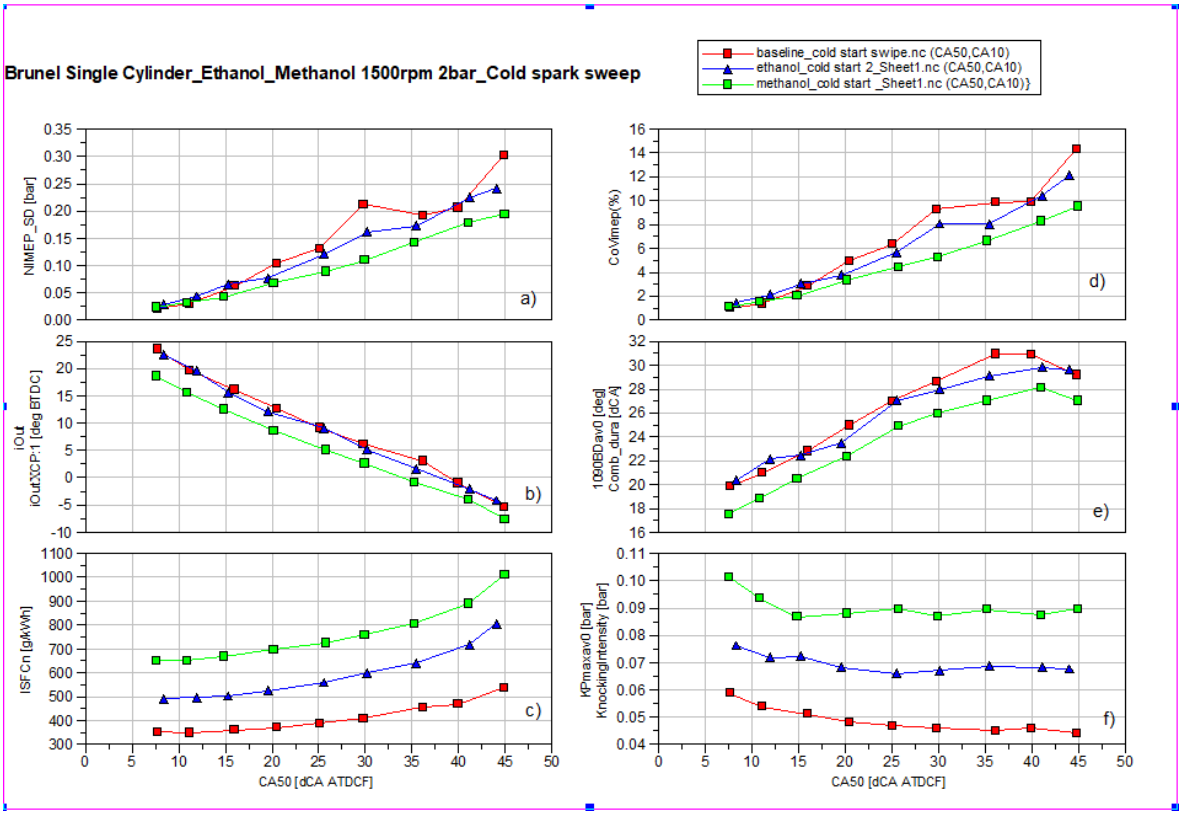

Figure 6-1 Combustion characteristic of cold spark sweep

The spark timing is shown in Figure 6-1b. The spark timings of gasoline and ethanol are retarded from 23.6CA BTDC to 5.4CA ATDC with the CA50 retarded from 8CAD ATDC to 45CAD ATDC. The spark timing of ethanol can be more retarded than

gasoline since the laminar flame speed of ethanol is faster than gasoline. Thus to achieve the same CA50, ethanol can be ignited later than gasoline. Methanol's spark timing is retarded from 18.5CAD BTDC to 7.6CAD ATDC during the spark timing sweep. The spark timing of methanol can be more retarded than ethanol and gasoline since methanol has the fastest laminar flame speed.

The indicated specific fuel consumption is shown in Figure 6-1c. The ISFC of gasoline, ethanol and methanol increase from 350.3g/kWh to 537.5g/kWh, 490.8g/kWh to 803.6g/kWh and 651.5g/kWh to 1010.1kWh with the same trend since the combustion efficiency becomes lower with the retarded CA50. Coefficient of variation (COV) IMEP (shown in Figure 6-1d) is another parameter which can reflect combustion stability. For this test, COV IMEP was limited under 15% to confirm engine stability. At CA50 8CAD ATDC, all these fuels have very good combustion stability with cold coolant and oil. At the end of the test, the COV IMEP of gasoline, ethanol and methanol are 14.3%, 12.1% and 9.7%. It seems there is still some margin for ethanol and methanol's spark timing to be retarded more, but misfire and partial burn occurred when their CA50 were retarded to 50CAD ATDC.

The burn duration is shown in Figure 6-1e. The burn duration of gasoline increases from 19.8CAD to 30.9CAD. Ethanol's burn duration is shorter than gasoline which increases from 20.3CAD to 29.8 CAD since it has a faster laminar flame speed. At CA50 11CAD ATDC, ethanol has a longer burn duration than gasoline since its CA50 is more retarded. Methanol has the fastest laminar flame speed of these fuels so that its burn duration is always shorter than ethanol and gasoline which increases from 17.5CAD to 28.1CAD at CA50 40CAD ATDC. The knocking intensity (KI) of gasoline, ethanol and methanol are shown in Figure 6-1f. All KI values of these fuels are under 1 which means there's no knocking happened during testing.

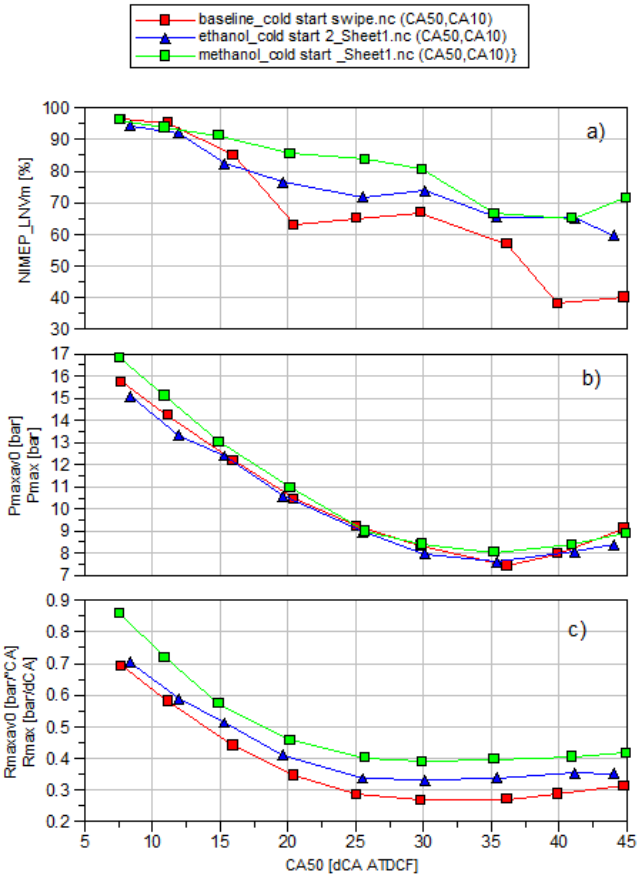

Figure 6-2 NV, maximum in-cylinder pressure and maximum pressure rise rate

The lowest normalized value (LNV) is a parameter which can reflect the trend to misfire which is shown in Figure 6-2a. Gasoline and methanol have their LNV higher than 90% before CA50 11CAD ATDC, after this point their LNV decreases to 84.8%, 86.3% which means there is more chance to misfire. Methanol has its LNV higher than 90% before and includes CA50 15CA ATDC whose value is 91.0%. Gasoline and methanol have their lowest LNV at CA50 40CAD ATDC whose values are 40.1% and 71.5%, while ethanol has its lowest LNV at CA50 45CAD ATDC whose value is 59.4%. Methanol has the lowest chance to misfire with the spark timing retarded, and it's more potential for gasoline has misfire after CA50 20CAD ATDC. The maximum in-cylinder pressure and maximum pressure rise rate are shown in Figure 6-2b and Figure 6-2c. After CA50 15CA ATDC, these fuels' Pmax curves almost align with each other, from CA50 8 to 15CAD ATDC, methanol has higher Pmax since it has the most retarded spark timing which is most close to the top dead

centre. The Rmax of ethanol decreases from 0.70bar/dCA to 0.35bar/dCA, and there's a small difference between these fuels.

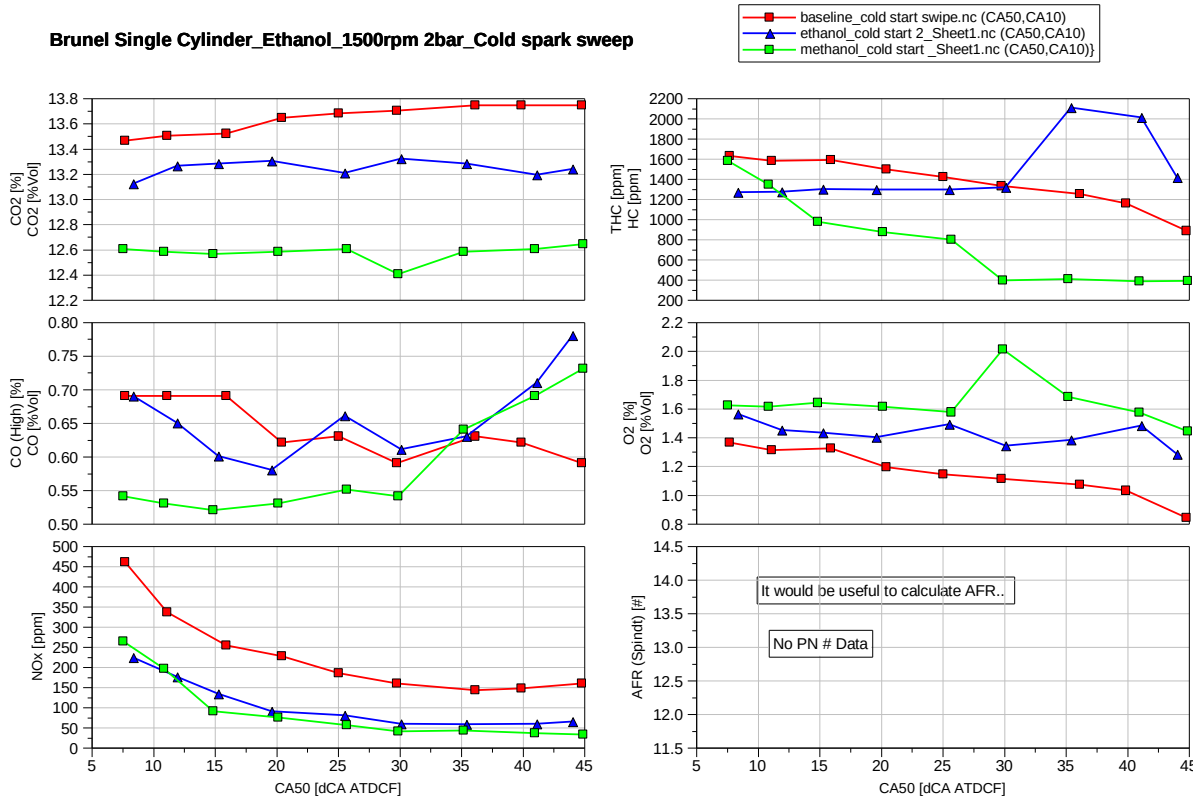

Figure 6-3 Emissions released by gasoline, ethanol and methanol

The gaseous emissions are shown in Figure 6-3. The CO_2 released by gasoline increased slowly from 13.46%vol to 13.72%vol with the spark timing retarded. The CO_2 released by ethanol keeps around 13.3%vol, and that of methanol keeps around 12.6%vol. The CO released by gasoline reduces slowly from 0.69%vol to 0.59%vol. Ethanol's CO decreases from 0.69%vol to 0.6%vol with the CA50 retarded from 8CAD ATDC to 20CAD ATDC. After that, it increases to 0.78%vol at CA50 45CAD ATDC. The CO produced by methanol keeps around 0.5%vol from CA50 8CAD ATDC to 30CAD ATDC, then increases to 0.73%vol at CA50 CAD ATDC. The reason why CO of ethanol and methanol increase is because of incomplete combustion as a result of poor atomisation of alcohol fuels under low temperature. The NO_x released by gasoline dropped from 460ppm to 158ppm with the CA50 retarded from 8CAD ATDC to 45CAD ATDC. The NO_x released by ethanol and

methanol are aligned with each other which is reduced from 245ppm to 50ppm. With the retarded of spark timing, all fuels' NO_x decreases since in-cylinder thermal dynamic environment not good when the spark timing is very retarded. With the same amount of gasoline, ethanol and methanol, ethanol and methanol's evaporation enthalpy are higher than gasoline, and the charge cooling effect of ethanol and methanol are better than gasoline which decreases the peak in-cylinder temperature. What's more, alcohol fuels' lower heating value are lower than gasoline so that their charge cooling effect is more effective than gasoline then their in-cylinder temperature are lower than gasoline. As a result of this, ethanol and methanol produce less NO_x but more CO emissions than gasoline. The THC released by gasoline reduced from 1624ppm to 882ppm with the retarded of spark timing. Ethanol's THC keeps around 1280ppm from CA50 8CAD ATDC to 30CAD ATDC. After that, at late spark timing points, its THC increases to 2102ppm because of incomplete combustion and poor air-fuel mixing. The THC released by methanol drops from 1576ppm to 390ppm at CA50 30CAD ATDC and it keeps stable after that. The THC of methanol at a low level at late combustion phasing is because methanol's O/C ratio is the highest of these three fuels. In general, the oxidation and evaporation of HC is promoted by higher in-cylinder temperature as a result of retarded spark timing.

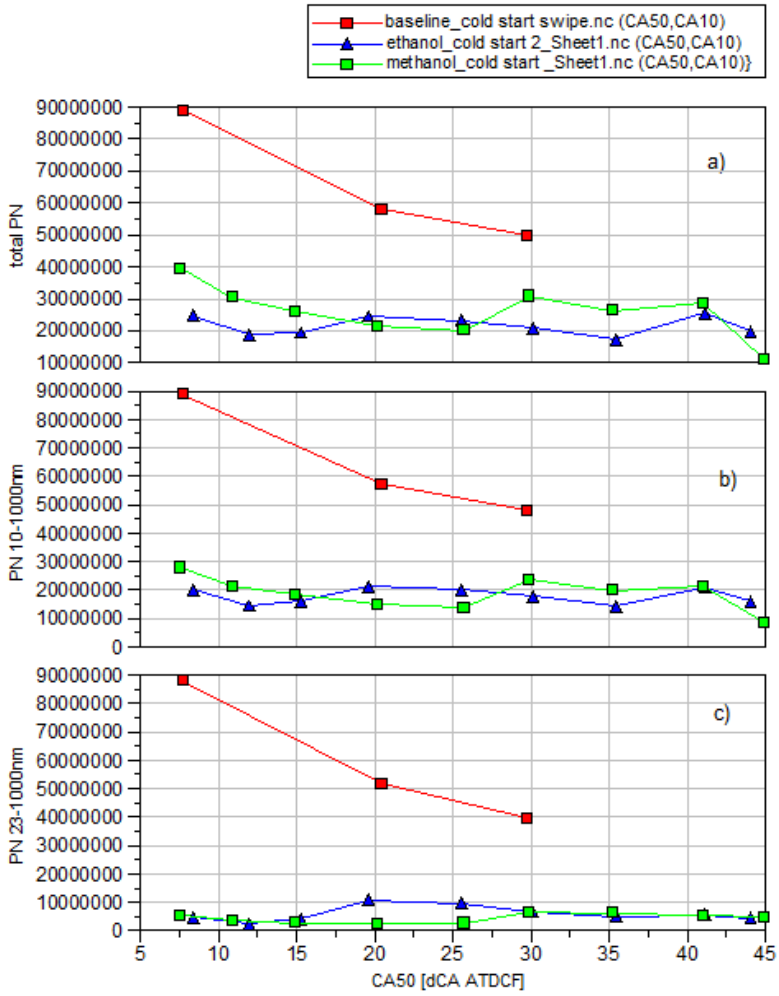

Figure 6-4 Particle numbers data of gasoline, ethanol and methanol

The three different size ranges of particle numbers are shown in Figure 6-4. Because of equipment's issue, only part of gasoline's data was collected. PN 10-1000nm is the regulation of EURO 5, and PN 23-1000nm is the regulation of EURO 6. The total PN is shown in Figure 6-4 a), the total PN of gasoline reduces from 8.9e7 to 4.9e7 with the CA50 retarded from 8CAD ATDC to 30CAD ATDC. The particle released by ethanol which numbers are around 2e7 during the cold start spark timing sweep. Methanol's total PN decreases from 3.9e7 to 2.0e7 at CA50 25CAD ATDC. After that, it increases and stays around 2.8e7 from CA50 30CAD ATDC to 40CAD ATDC, then it drops to 1.1e7 at CA50 45CAD ATDC. PN 10-1000nm is shown in figure6-4 b). Gasoline's PN 10-1000nm reduces from 8.8e7 to 4.8e7 during testing. The PN 10-1000nm of ethanol and methanol are around 2e7. PN 23-1000nm of gasoline drops from 8.8e7 to 3.9e7, that of ethanol and methanol keeps around 5e6 during

the whole testing. There is little difference between the PN of each size group of gasoline which mean that most particle released by gasoline whose size is larger than 23nm, and there are some small particles released by ethanol and methanol.

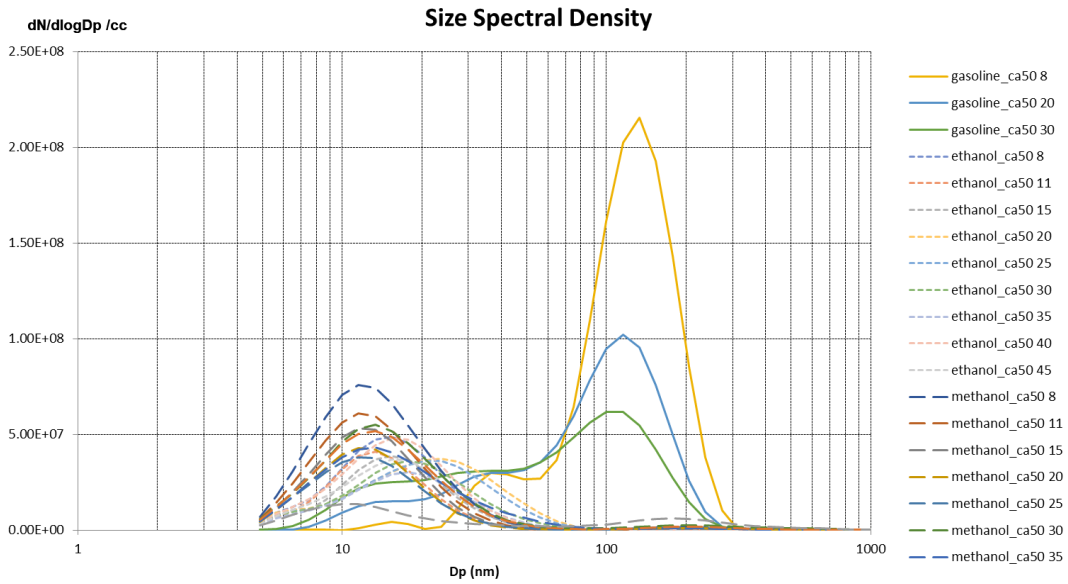

Figure 6-5 Size spectral density of gasoline, ethanol and methanol

Figure 6-5 shows the particle size distribution of these three fuels. The total PN released by gasoline is greater than methanol and ethanol. Most particles released by gasoline whose size is greater than 100nm by means of accumulation mode. With the spark timing retarded, the particulate in nucleation mode increase but there's a decrease in accumulation mode. The particulate emission produced by methanol is more than that of ethanol.

6.4 Summary

These tests were undertaken to assess whether alcohol fuels are able to perform as good as gasoline under catalyst light-off conditions. The result shows that both ethanol and methanol could operate with more retarded spark timings to increase the exhaust gas temperature for catalyst-light-off. What's more, the particle emissions released by alcohol fuels are lower and smaller.

7. Chapter Seven: Conclusion

7.1 Introduction

In this experimental study, the performance, efficiency and emissions of a direct injection spark ignition engine operating with ethanol and methanol have been measured and analysed, and then compared with EU6 E10 gasoline (RON 95). The testing was carried out on a single cylinder highly downsized spark ignition engine with no hardware change for different fuels.

Three series of testing were performed, including load sweeps at three engine speeds, fuel injection strategy matrix and cold spark sweep for methanol, ethanol and baseline gasoline fuel. Combustion characteristics and emissions, particle numbers and particle size spectral density results, are analysed and discussed.

The Load sweep testing (2000rpm & 3000rpm & 4000rpm) aims to have general understanding of the effect on engine performance, efficiency and emissions by ethanol and methanol at different speeds and loads. In particular, the potential benefits of a spark ignition engine operating with methanol or ethanol at high load conditions were assessed because of their higher-Octane number, charging cooling effect and faster laminar flame speeds.

In the second series of testing, the injection timing and injection pressure sweep is used to find the optimal injection timing and pressure which has the best fuel efficiency and the point which get the lowest emission. (2000rpm 4.6bar IMEP & 3000rpm 16bar IMEP)

Finally, a cold start spark timing sweep testing was carried out to identify the capability of alcohol fuels for fast catalyst light off through retarded spark timings.

7.2 Conclusions

7.2.1 Engine Performance, Combustion and Emissions of Alcohol Fuels

For the 2000rpm experiment, ethanol and methanol performed similarly to the E10 gasoline in terms of efficiency, combustion characteristics and emissions, because the engine was operated at part load conditions limited to 11bar IMEP. Although ethanol and methanol's burn speed are faster than gasoline, the combustion durations are similar for all three fuels when the spark timings were set to MBT. There's a reduction of CO_2 released by ethanol and methanol. What's more, the THC released by ethanol and methanol is also lower than gasoline, which is due to the lower FID response to partially oxidised alcohols).

For the 3000rpm load sweep, the load range was extended and varied from 2bar to 28bar IMEP. Below 16bar IMEP, the indicated thermal efficiency of gasoline, ethanol and methanol are similar since all fuels' CA50 were controlled at 8 CAD ATDC when the MBT spark timing was applied. At loads higher than 16bar IMEP, spark timings were retarded due to different reasons for gasoline and alcohol fuels. For gasoline, its spark timing was retarded to avoid knocking combustion. For alcohol fuels, the most advanced spark timings were limited by the maximum peak in-cylinder pressure 120bar and the maximum rate of the pressure rise of 6 bar/CAD at 16bar IMEP. Gasoline's spark timing had to be retarded more than alcohol fuels to prevent knocking at all higher load operations. As a result of this, ethanol and methanol led to higher thermal efficiency than gasoline at high loads. Methanol achieved the highest brake thermal efficiency 37.9% at 18bar IMEP, and ethanol's highest BTE was 37.7% at 18bar IMEP as well. Gasoline's best BTE was 36.5% happened at 10bar IMEP.

For gasoline, over-fuelling was introduced at 26bar IMEP and 28bar IMEP in order to keep the exhaust gas temperature below the limit of 780 Deg C. Because of their higher enthalpy of evaporation enthalpy, ethanol and methanol combustion took place at lower temperature so that their exhaust gas temperature was always below the limit. As a result of this, over-fuelling was not required for ethanol and methanol.

The lower combustion temperature also led to lower NO_x emissions released by ethanol and methanol.

At 3000rpm, HC released by alcohol fuels are also lower than gasoline because of two reasons. The first one is the lower response of FID to the partially oxidised alcohol fuels and the other alcohol fuels evaporates faster than gasoline when the engine is hot so that they can make the air-fuel mixture quality better. In particular, ethanol and methanol engine operations produced significantly less particles than gasoline. There's up to 90% reduction of PN number by ethanol and methanol. What's more, the particles produced by ethanol and methanol are of smaller sizes than that of gasoline, but smaller size particle has more effect on human's health. The disadvantage of ethanol and methanol is that their lower heating value are lower than gasoline which causes longer injection duration and higher fuel consumption.

The results obtained during the 4000rpm engine experiments are similar to those of the 3000rpm load sweep.

7.2.2 Effect of fuel injection timing and pressure

The fuel injection strategy studies were carried at two operating conditions: low load operation at 2000rpm 4bar IMEP and high load operation at 3000rpm 16bar IMEP. The results demonstrated combustion characteristic and engine efficiency of all three fuels were little affected by the injection timing at 2000rpm 4bar IMEP.

Ethanol and methanol's combustion efficiency is slightly higher than gasoline. THC released by alcohol fuel is lower than gasoline since alcohol fuel's better evaporation character and lower FID response to the partially oxided alcohol fuels. NO_x produced by ethanol and methanol is also lower due to their lower combustion temperature. The particulate emission of alcohol fuels is much lower than gasoline. For ethanol, the best efficiency point matches the lowest PN size 23-1000nm, and methanol's best efficiency condition also has the lowest total PN and PN 10-1000nm.

At 3000rpm 16bar IMEP, gasoline engine operation was limited by the knocking combustion with earlier injection timings but engine operations with both ethanol and methanol were free from knocking combustion. But alcohol fuel's LHVs are lower than gasoline so their injection durations are longer. As a result of this, ethanol and methanol have their lowest combustion efficiency with later injection timing 275CAD BTDC and at rail pressure 50bar because of poorer atomisation at lower injection pressure. But, ethanol and methanol's peak efficiency area are still larger than gasoline. Alcohol fuels produce less emissions than gasoline for the same reason as the operation at 2000rpm 4.6bar IMEP.

7.2.3 Cold Start Spark Timing Sweep

For the cold start spark timing sweep, the result shows that both ethanol and methanol could operate with more retarded spark timings than gasoline to enable by faster catalyst-light-off. What's more, the particulate emissions released by alcohol fuels are much less and of smaller sizes.

7.3 Recommendations for Future Work

In order to facilitate future research works to be carried out on the single cylinder engine, it would be desirable to update the intake air pressure control system to enable more stable supply of compressed air to the engine. An automatic coolant& oil temperature control system is preferred for high-load engine testing in place of the manual control system in use to minimise the risk during high-speed & load testing.

After the completion of the current study, a number of areas has been identified which would need to be investigated further, including

1) How to improve the cold start operation of ethanol and methanol spark ignition engine (e.g. by injector heater& intake air heater)

2) Effects of alcohol on non-regulated emissions from alcohol, such as aldehydes.
3) In this study, the maximum thermal efficiencies of ethanol and methanol engine operations are limited by the engine's mechanical design (Pmax 120bar, Rmax 6bar/CA). It would be useful to repeat the studies in an engine with higher Pmax and Rmax limit to achieve higher engine thermal efficiency.
4) Higher compression ratio and higher dilution tolerance could be introduced to increase the engine's thermal efficiency further.

Reference

[1] Smil V. The two prime movers of globalization: history and impact of diesel engines and gas turbines. Journal of global history 2007;2(3):373-394.

[2] Cairns A, Stansfield P, Fraser N, Blaxill H, Gold M, Rogerson J, Goodfellow C. A Study of Gasoline-Alcohol Blended Fuels in an Advanced Turbocharged DISI Engine. SAE International Journal of Fuels and Lubricants 2009;2(1):41-57.

[3] Larsson T, Mahendar SK, Christiansen-Erlandsson A, Olofsson U. The effect of pure oxygenated biofuels on efficiency and emissions in a gasoline optimised disi engine. Energies (Basel) 2021;14(13):3908.

[4] Martins FP, Lacava PT, De Andrade CR, Garzuzi S. Alternative Fuels: A Review about Anhydrous and Hydrous Ethanol Properties. SAE technical paper series 2016;127082(October).

[5] Michael S, Timothy B, Ingemar D, Bengt J. CI Methanol and Ethanol combustion using ignition improver. SAE Technical Papers 2019(December).

[6] Sarathy SM, Oßwald P, Hansen N, Kohse-Höinghaus K. Alcohol combustion chemistry. Progress in energy and combustion science 2014;44:40-102.

[7] Dan Gearino. California Just Banned Gas-Powered Cars. Here's Everything You Need to Know. 2022;2022(September 1,).

[8] Hu T, Wei Y, Liu S, Zhou L. Improvement of Spark-Ignition (SI) Engine Combustion and Emission during Cold Start, Fueled with Methanol/Gasoline Blends. Energy Fuels 2007;21(1):171-175.

[9] Miller P, Solomon M. A brief history of technology-forcing motor vehicle regulations. EM (Pittsburgh, Pa.) 2009:8.

[10] Delphi Technologies P. Delphi-worldwide-emissions-standards-passenger-cars-light-duty-2017-2018. 2017.

[11] DieselNet. EU Emission Standards for Passenger Cars. 2017.

[12] New York Auto Show Receives Global Recognition from International Organization of Motor Vehicle Manufacturers. PR newswire 2008.

[13] SMMT. New Car CO2 Report 2017 - The 16th Edition. 2017.

[14] Z. Yang, A. Bandivadekar. 2017 Global update: Light-duty vehicle greenhouse gas and fuel economy standards. 2017.

[15] WardsAuto. 2016 WardsAuto Survey | DuPont Automotive | DuPont USA. 2016.

[16] Handbook of Air Pollution from Internal Combustion Engines: Pollutant Formation and Control. Mechanical Engineering 1998;120(7):90.

[17] Harrington JA, Shishu RC. A single-cylinder engine study of the effects of fuel type, fuel stoichiometry, and hydrogen-to-carbon ratio on CO, NO, and HC exhaust emissions. SAE technical paper series 1973.

[18] Shimotani K, Oikawa K, Horada O, Kagawa Y. Characteristics of gasoline in-cylinder direct injection engine. JSAE Rev 1996;17(3):267-272.

[19] Bowman CT. Kinetics of pollutant formation and destruction in combustion. Progress in energy and combustion science 1975;1(1):33-45.

[20] Johnson GL, Caretto LS, Starkman ES. The kinetics of CO oxidation in reciprocating engines. 1970.

[21] Zhao F, Lai M, Harrington DL. The spray characteristics of automotive port fuel injection-a critical reviews. SAE technical paper series 1995.

[22] Daniel WA. Flame quenching at the walls of an internal combustion engine. Symposium, International, on Combustion 1957;6(1):886-894.

[23] Wentworth JT. The piston crevice volume effect on exhaust hydrocarbon emission. Combustion Sci Technol 1971;4(1):97-100.

[24] Stone R. Introduction to internal combustion engines. 2012.

[25] Lavole GA, Heywood JB, Keck JC. Experimental and theoretical study of nitric oxide formation in internal combustion engines. Combustion Sci Technol 1970;1(4):313-326.

[26] Zeldovich YA, Frank-Kamenetskii D, Sadovnikov P. Oxidation of nitrogen in combustion. 1947.

[27] Komiyama K, Heywood JB. Predicting NOx emissions and effects of exhaust gas recirculation in spark-ignition engines. SAE technical paper series 1973.

[28] Kummer JT. Catalysts for automobile emission control. Progress in energy and combustion science 1980;6(2):177-199.

[29] Heywood JB. Internal combustion engine fundamentals. 1988.

[30] Taylor CF. Internal Combustion Engine in Theory and Practice: Combustion, Fuels, Materials, Design. 1985;2.

[31] Zhao H. Advanced direct injection combustion engine technologies and development: Volume 1, Gasoline and gas engines. 2010.

[32] Reif K, Dietsche K, Robert Bosch GmbH, STAR Deutschland GmbH. Automotive handbook. 2014.

[33] Weberbauer F, Rauscher M, Kulzer A, Knopf M, Bargende M. Generally applicate split of losses for new combustion concepts. MTZ worldwide 2005;66(2):17-19.

[34] International Comparison of Light-Duty Vehicle Fuel Economy 2005-2015. 2017;2017.

[35] Van Basshuysen R, Spicher U. Gasoline engine with direct injection: processes, systems, development, potential : with 399 figures. 2009.

[36] Inoue T, Matsushita S, Nakanishi K, Okano H. Toyota lean combustion system - The third generation system. SAE technical paper series 1993.

[37] Kühn M, Abthoff J, Kemmler R, Kaiser T. Influence of the inlet port and combustion chamber configuration on the lean-burn behaviour of a spark-ignition gasoline engine. SAE technical paper series 1996.

[38] Borges LH, Hollnagel C, Muraro W. Development of a mercedes-benz natural gas engine M 366 LAG, with a lean burn combustion system. SAE technical paper series 1996.

[39] Zhao F, Lai M-, Harrington DL. Automotive spark-ignited direct-injection gasoline engines. Progress in energy and combustion science 1999;25(5):437-562.

[40] Zhao H. Advanced direct injection combustion engine technologies and development: Gasoline and gas engines. 2009:9.

[41] Krebs R, Pott E, Kreuzer TP, Göbel U, Glück K. Exhaust gas aftertreatment of volkswagen FSI fuel stratified injection engines. SAE technical paper series 2002.

[42] Rohr F, Peter SD, Lox E, Kögel M, Müller W, Sassi A, Rigaudeau C, Juste L, Belot G, Gélin P, Primet M. The impact of sulfur poisoning on NOx-storage catalysts in gasoline applications. SAE technical paper series 2005.

[43] Merdes N, Enderle C, Vent G, Weller R. The New Turbocharged Four-Cylinder Gasoline Engine by Mercedes-Benz. MTZ worldwide 2011;72(12):16-23.

[44] Zhao H. HCCI and CAI engines for the automotive industry. 2007.

[45] Chen T, Xie H, Li L, Zhang L, Wang X, Zhao H. Methods to achieve HCCI/CAI combustion at idle operation in a 4VVAS gasoline engine. Appl Energy 2014;116:41-51.

[46] Yamasaki Y, Umahashi S, Uesugi Y, Ma Q, Kaneko S, Hikita T, Mizuno S, Tsumura Y, Hashiguchi T. Development of Dynamic Models for an HCCI Engine with Exhaust Gas Rebreathing System. 2015.

[47] Konigstein A, Grebe UD, Wu K, Larsson P. Differentiated analysis of downsizing concepts. MTZ. Motortechnische Zeitschrift 2008;69(6).

[48] M. Kratzsch, M. Günther. Knocking in Gasoline Engines. DCM Druck Center Meckenheim GmbH 2013.

[49] Low Speed Pre-ignition (LSPI), Oxidation and Wear. Lubrizol360 2017.

[50] Sroka ZJ. Work Cycle of Internal Combustion Engine Due to Rightsizing. 2021:Ch. 1.

[51] W. Hannibal. Variable Valve Timing Systems on Modern Spark Ignition Engines. 2009.

[52] Potul S, Nachnolkar R, Bhave S. Analysis Of Change In Intake Manifold Length And Development Of Variable Intake System.

[53] Moriya Y, Watanabe A, Uda H, Kawamura H, Yoshioka M, Adachi M. A newly developed intelligent variable valve timing system-continuously controlled cam phasing as applied to a new 3 liter inline 6 engine. SAE technical paper series 1996.

[54] Leone TG, Christenson EJ, Stein RA. Comparison of variable camshaft timing strategies at part load. SAE technical paper series 1996.

[55] Tuttle JH. Controlling Engine Load by Means of Late Intake-Valve Closing. SAE transactions 1980;89:2429-2441.

[56] Hentschel W, Block B, Hovestadt T, Meyer H, Ohmstede G, Richter V, Stiebels B, Winkler A. Optical diagnostics and CFD-simulations to support the combustion process development of the Volkswagen FSI® direct-injection gasoline engine. SAE technical paper series 2001.

[57] Szengel R, Middendorf H, Voeltz S, Laumann A, Tilchner L, Theobald J, Etzrodt T, Krebs R. The TSI engine with 90 kW: Extension of the economical petrol engine series by Volkswagen. MTZ worldwide 2007;68(7-8):8-11.

[58] Roberts M. Benefits and Challenges of Variable Compression Ratio (VCR). 2003.

[59] Hoppe F, Thewes M, Baumgarten H, Dohmen J. Water injection for gasoline engines: Potentials, challenges, and solutions. International journal of engine research 2016;17(1):86-96.

[60] hakariya M, Toda T, Sakai M. The New Toyota Inline 4-Cylinder 2.5L Gasoline Engine. 2017.

[61] J. Atkinson. Gas Engine. 1886(USA Patent 336505).

[62] J. Atkinson. Gas Engine. 1887(USA Patent 367496).

[63] Ting DS, Checkel MD. The effects of turbulence of spark-ignited, ultra lean, premixed methane-air flame growth in a combustion chamber. SAE technical paper series 1995.

[64] Kato T, Saeki K, Nishide H, Yamada T. Development of CNG fueled engine with lean burn for small size commercial van. JSAE Rev 2001;22(3):365-368.

[65] Surisetty VR, Dalai AK, Kozinski J. Alcohols as alternative fuels: An overview. Applied Catalysis A: General 2011;404(1-2):1-11.

[66] Siwale L, Kristóf L, Bereczky A, Mbarawa M, Kolesnikov A. Performance, combustion and emission characteristics of n-butanol additive in methanol–gasoline blend fired in a naturally-aspirated spark ignition engine. Fuel Process Technol 2014;118:318-326.

[67] Ramadhas AS. Alternative fuels for transportation. 2011.

[68] Reed TB, Lerner RM. Methanol: A Versatile Fuel for Immediate Use. Science 1973;182(4119):1299-1304.

[69] He B, Jian-Xin Wang, Hao J, Yan X, Xiao J. A study on emission characteristics of an EFI engine with ethanol blended gasoline fuels. Atmos Environ 2003;37(7):949-957.

[70] Hu T, Wei Y, Liu S, Zhou L. Improvement of Spark-Ignition (SI) Engine Combustion and Emission during Cold Start, Fueled with Methanol/Gasoline Blends. Energy Fuels 2007;21(1):171-175.

[71] Kim S, Dale BE. Environmental aspects of ethanol derived from no-tilled corn grain: nonrenewable energy consumption and greenhouse gas emissions. Biomass Bioenergy 2005;28(5):475-489.

[72] Kim S, Dale BE. Environmental aspects of ethanol derived from no-tilled corn grain: nonrenewable energy consumption and greenhouse gas emissions. Biomass Bioenergy 2005;28(5):475-489.

[73] Solomon BD, Barnes JR, Halvorsen KE. Grain and cellulosic ethanol: History, economics, and energy policy. Biomass Bioenergy 2007;31(6):416-425.

[74] Awad OI, Mamat R, Ali OM, Sidik NAC, Yusaf T, Kadirgama K, Kettner M. Alcohol and ether as alternative fuels in spark ignition engine: A review. Renewable & sustainable energy reviews 2018;82:2586-2605.

[75] Thomas V, Kwong A. Ethanol as a lead replacement: phasing out leaded gasoline in Africa. Energy Policy 2001;29(13):1133-1143.

[76] Jeuland N, Montagne X, Gautrot X. Potentiality of Ethanol As a Fuel for Dedicated Engine. Oil & gas science and technology 2004;59(6):559-570.

[77] Yüksel F, Yüksel B. The use of ethanol–gasoline blend as a fuel in an SI engine. Renewable Energy 2004;29(7):1181-1191.

[78] Mills JE. THE INTERNAL HEAT OF VAPORIZATION. J Am Chem Soc 1909;31(10):1099-1130.

[79] Koç M, Sekmen Y, Topgül T, Yücesu HS. The effects of ethanol–unleaded gasoline blends on engine performance and exhaust emissions in a spark-ignition engine. Renewable Energy 2009;34(10):2101-2106.

[80] Milpied J, Jeuland N, Plassat G, Guichaous S, Dioc N, Marchal A, Schmelzle P. Impact of Fuel Properties on the Performances and Knock Behaviour of a Downsized Turbocharged DI SI Engine – Focus on Octane Numbers and Latent Heat of Vaporization. SAE International Journal of Fuels and Lubricants 2009;2(1):118-126.

[81] Munack A. Book Reviews: Biodiesel - The Comprehensive Handbook. Edited by Martin Mittelbach, Claudia Remschmidt. CLEAN - Soil, Air, Water 2007;35(1):14.

[82] Daniel R, Tian G, Xu H, Wyszynski ML, Wu X, Huang Z. Effect of spark timing and load on a DISI engine fuelled with 2,5-dimethylfuran. Fuel 2011;90(2):449-458.

[83] Demirbas A. Combustion characteristics of different biomass fuels. Progress in Energy and Combustion Science 2004;30(2):219-230.

[84] Alternative Fuels Data Center. Biobutanol. ;2022(October 17,).

[85] Rask KN. Clean air and renewable fuels: the market for fuel ethanol in the US from 1984 to 1993. Energy Econ 1998;20(3):325-345.

[86] El-Emam SH, Desoky AA. A study on the combustion of alternative fuels in spark-ignition engines. Int J Hydrogen Energy 1985;10(7):497-504.

[87] Pourkhesalian AM, Shamekhi AH, Salimi F. Alternative fuel and gasoline in an SI engine: A comparative study of performance and emissions characteristics. Fuel 2010;89(5):1056-1063.

[88] Nakata K, Utsumi S, Ota A, Kawatake K, Kawai T, Tsunooka T. The effect of ethanol fuel on a spark ignition engine. SAE technical paper series 2006.

[89] Mahendar SK, Venkataraman V, Erlandsson AC. The Impact of Miller Valve Timing on Combustion and Charging Performance of an Ethanol- and Methanol-Fueled Heavy-Duty Spark Ignition Engine. SAE International journal of engines 2021;14(5):733-748.

[90] Çelik MB, Özdalyan B, Alkan F. The use of pure methanol as fuel at high compression ratio in a single cylinder gasoline engine. Fuel (Guildford) 2011;90(4):1591-1598.

[91] Vancoillie J, Demuynck J, Sileghem L, Van De Ginste M, Verhelst S, Brabant L, Van Hoorebeke L. The potential of methanol as a fuel for flex-fuel and dedicated spark-ignition engines. Appl Energy 2013;102:140-149.

[92] Pannone GM, Johnson RT. Methanol as a fuel for a lean turbocharged spark ignition engine. SAE transactions 1989:243-253.

[93] VANCOILLIE J, DEMUYNCK J, SILEGHEM L, VAN DE GINSTE M, VERHELST S, BRABANT L, VAN HOOREBEKE L. The potential of methanol as a fuel for flex-fuel and dedicated spark-ignition engines : Advances in sustainable biofuel production and use. Applied energy 2013;102:140-149.

[94] Dhaliwal B, Yi N, Checkel D. Emissions Effects of Alternative Fuels in Light-Duty and Heavy-Duty Vehicles. 2000.

[95] Kabasin D, Hoyer K, Kazour J, Lamers R, Hurter T. Heated Injectors for Ethanol Cold Starts. SAE International Journal of Fuels and Lubricants 2009;2(1):172-179.

[96] Golzari R, Li Y, Zhao H. Impact of Port Fuel Injection and In-Cylinder Fuel Injection Strategies on Gasoline Engine Emissions and Fuel Economy. SAE technical paper series 2016;2016-.

[97] Hancock D, Fraser N, Jeremy M, Sykes R, Blaxill H. A new 3 cylinder 1.2l advanced downsizing technology demonstrator engine. SAE technical paper series 2008.

[98] Bassett M, Hall J, Hibberd B, Borman S, Reader S, Gray K, Richards B. Heavily Downsized Gasoline Demonstrator. SAE International Journal of Engines 2016;9(2):729-738.

[99] Hall J, Bassett M, Hibberd B, Streng S. Heavily Downsized Demonstrator Engine Optimised for CNG Operation. SAE International Journal of Engines 2016;9(4):2250-2261.

[100] Bassett M, Hall J, Cains T, Underwood M, Wall R, Richards BG. Dynamic Downsizing Gasoline Demonstrator. SAE International Journal of Engines 2017;10(3):884-891.

[101] Bassett M, Vogler C, Hall J, Taylor J, Cooper A, Reader S, Gray K, Wall R. Analysis of the Hardware Requirements for a Heavily Downsized Gasoline Engine Capable of Whole Map Lambda 1 Operation. SAE technical paper series 2018;2018-.

[102] Lumsden G, OudeNijeweme D, Fraser N, Blaxill H. Development of a Turbocharged Direct Injection Downsizing Demonstrator Engine. SAE International Journal of Engines 2009;2(1):1420-1432.

[103] Zhang Y. Experimental investigation of CAI combustion in a two-stroke poppet valve DI engine. 2015.

[104] Zhao H, Ladommatos N. Engine combustion instrumentation and diagnostics. 2001.

[105] Coates BP. Investigation of engine design parameters on the efficiency and performance of the high specific power downsized SI engine. 2012.

[106] Zhao H, Ladommatos N. Engine combustion instrumentation and diagnostics. 2001.

[107] Randolph AL. Methods of processing cylinder-pressure transducer signals to maximize data accuracy. SAE technical paper series 1990.

[108] De Melo, Tadeu Cavalcante Cordeiro, De Brito, Marcos Fernando Mendes, MacHado GB, Paiva CEF. Procedure for uncertainty of measurement determination of spark ignition engine emission tests. SAE technical paper series 2012.

[109] Raza M, Chen L, Leach F, Ding S. A Review of particulate number (PN) emissions from gasoline direct injection (gdi) engines and their control techniques. Energies (Basel) 2018;11(6):1417.

[110] Yanju W, Shenghua L, Hongsong L, Rui Y, Jie L, Ying W. Effects of Methanol/Gasoline Blends on a Spark Ignition Engine Performance and Emissions. Energy Fuels 2008;22(2):1254-1259.

[111] Qin J, Li X, Pei Y. Effects of Combustion Parameters and Lubricating Oil on Particulate Matter Emissions from a Turbo-Charged GDI Engine Fueled with Methanol/Gasoline Blends. 2014.